

1985

# Pulsed Amperometric Detection: a method for detecting amines in liquid chromatography

John A. Polta  
*Iowa State University*

Follow this and additional works at: <https://lib.dr.iastate.edu/rtd>

 Part of the [Analytical Chemistry Commons](#)

## Recommended Citation

Polta, John A., "Pulsed Amperometric Detection: a method for detecting amines in liquid chromatography" (1985). *Retrospective Theses and Dissertations*. 7880.  
<https://lib.dr.iastate.edu/rtd/7880>

This Dissertation is brought to you for free and open access by the Iowa State University Capstones, Theses and Dissertations at Iowa State University Digital Repository. It has been accepted for inclusion in Retrospective Theses and Dissertations by an authorized administrator of Iowa State University Digital Repository. For more information, please contact [digirep@iastate.edu](mailto:digirep@iastate.edu).

## INFORMATION TO USERS

This reproduction was made from a copy of a document sent to us for microfilming. While the most advanced technology has been used to photograph and reproduce this document, the quality of the reproduction is heavily dependent upon the quality of the material submitted.

The following explanation of techniques is provided to help clarify markings or notations which may appear on this reproduction.

1. The sign or "target" for pages apparently lacking from the document photographed is "Missing Page(s)". If it was possible to obtain the missing page(s) or section, they are spliced into the film along with adjacent pages. This may have necessitated cutting through an image and duplicating adjacent pages to assure complete continuity.
2. When an image on the film is obliterated with a round black mark, it is an indication of either blurred copy because of movement during exposure, duplicate copy, or copyrighted materials that should not have been filmed. For blurred pages, a good image of the page can be found in the adjacent frame. If copyrighted materials were deleted, a target note will appear listing the pages in the adjacent frame.
3. When a map, drawing or chart, etc., is part of the material being photographed, a definite method of "sectioning" the material has been followed. It is customary to begin filming at the upper left hand corner of a large sheet and to continue from left to right in equal sections with small overlaps. If necessary, sectioning is continued again—beginning below the first row and continuing on until complete.
4. For illustrations that cannot be satisfactorily reproduced by xerographic means, photographic prints can be purchased at additional cost and inserted into your xerographic copy. These prints are available upon request from the Dissertations Customer Services Department.
5. Some pages in any document may have indistinct print. In all cases the best available copy has been filmed.

**University  
Microfilms  
International**

300 N. Zeeb Road  
Ann Arbor, MI 48106

8514432

**Polta, John A.**

**PULSED AMPEROMETRIC DETECTION: A METHOD FOR DETECTING  
AMINES IN LIQUID CHROMATOGRAPHY**

*Iowa State University*

**PH.D. 1985**

**University  
Microfilms  
International**

300 N. Zeeb Road, Ann Arbor, MI 48106

**PLEASE NOTE:**

In all cases this material has been filmed in the best possible way from the available copy. Problems encountered with this document have been identified here with a check mark .

1. Glossy photographs or pages \_\_\_\_\_
2. Colored illustrations, paper or print \_\_\_\_\_
3. Photographs with dark background \_\_\_\_\_
4. Illustrations are poor copy \_\_\_\_\_
5. Pages with black marks, not original copy \_\_\_\_\_
6. Print shows through as there is text on both sides of page \_\_\_\_\_
7. Indistinct, broken or small print on several pages
8. Print exceeds margin requirements \_\_\_\_\_
9. Tightly bound copy with print lost in spine \_\_\_\_\_
10. Computer printout pages with indistinct print \_\_\_\_\_
11. Page(s) \_\_\_\_\_ lacking when material received, and not available from school or author.
12. Page(s) \_\_\_\_\_ seem to be missing in numbering only as text follows.
13. Two pages numbered \_\_\_\_\_. Text follows.
14. Curling and wrinkled pages \_\_\_\_\_
15. Dissertation contains pages with print at a slant, filmed as received \_\_\_\_\_
16. Other \_\_\_\_\_  
\_\_\_\_\_  
\_\_\_\_\_

University  
Microfilms  
International

Pulsed Amperometric Detection:  
A method for detecting amines in  
liquid chromatography

by

John A. Polta

A Dissertation Submitted to the  
Graduate Faculty in Partial Fulfillment of the  
Requirements for the Degree of  
DOCTOR OF PHILOSOPHY

Department: Chemistry  
Major: Analytical Chemistry

Approved:

Signature was redacted for privacy.

In Charge of Major Work

Signature was redacted for privacy.

For the Major Department

Signature was redacted for privacy.

For the Graduate College

Iowa State University  
Ames, Iowa

1985

## TABLE OF CONTENTS

I.	INTRODUCTION	1
II.	LITERATURE REVIEW	5
A.	Adsorption at Pt Electrodes	5
1.	Methods of determining surface coverage	5
a.	Electroactive adsorbates	5
b.	Nonelectroactive adsorbates	6
c.	Radioactive tracers	8
2.	Effects of adsorption on PtOH/PtO formation	9
B.	Methods for Determination of Amino Acids	10
1.	Wet chemical analysis	10
2.	Chromatographic separations of amino acids with spectrophotometric detection	11
a.	Underivatized methods	11
b.	Pre-derivatized methods	16
3.	Chromatographic separations of amino acids with electrochemical detection	17
a.	Detection of derivatized amino acids	17
b.	Direct detection of underivatized amino acids	18
C.	Aminoglycoside Determinations	21
1.	Nonchromatographic techniques	21
a.	Microbiological assay	22
b.	Radioenzymatic assay	22
c.	Radioimmuno assay	23
2.	Chromatographic techniques	23
III.	EXPERIMENTAL	25
A.	Electrodes and Rotators	25
B.	Potentiostats	25

1.	Interface/Potentiostat	32
a.	GPIO	35
b.	Digital-to-analog conversion	38
c.	Analog-to-digital conversion	38
d.	Control amplifier and current-to-voltage converter	43
e.	Triangular waveform generator	43
f.	Pulsed signal sampling circuit	43
C.	Flow-Injection Apparatus	51
D.	Liquid Chromatography	54
E.	Chemicals	54
IV.	ELECTROCHEMICAL SURVEY OF SELECTED COMPOUNDS	55
A.	Introduction	55
B.	Carboxylic Acids	56
C.	Amines	56
V.	THE EFFECT OF pH ON PULSED AMPEROMETRIC DETECTION AT PLATINUM ELECTRODES	61
VI.	PULSED AMPEROMETRIC DETECTION OF ELECTRO- INACTIVE ADSORBATES AT PLATINUM ELECTRODES	68
A.	Introduction	68
B.	Competitive Adsorption	69
C.	Current Responses in the Presence of an Adsorbing Species	72
D.	Determination of Surface Coverage	84
E.	Adsorption Isotherm	85
VII.	THE DIRECT ELECTROCHEMICAL DETECTION OF AMINO ACIDS AT A PLATINUM ELECTRODE IN AN ALKALINE EFFLUENT	96
A.	Cyclic Voltammetry	96
B.	Triple-step Waveform	99
C.	Flow-Injection Analysis	106

D. Calibration	112
E. Liquid Chromatography	117
VIII. LIQUID CHROMATOGRAPHIC SEPARATION OF AMINOGLYCOSIDES WITH PULSED AMPEROMETRIC DETECTION	124
A. Introduction	124
B. Cyclic Voltammetry	127
C. Triple-step Waveforms	130
D. Chromatography	131
E. Calibration	139
IX. SUMMARY	147
X. FUTURE RESEARCH	150
XI. BIBLIOGRAPHY	152
XII. ACKNOWLEDGEMENTS	162



## LIST OF FIGURES

Figure III-1.	Pt wire-tip flow-through cell	26
Figure III-2.	Dionex flow-through cell	28
Figure III-3.	Simple Pt wire-tip flow through cell	30
Figure III-4.	Block diagram of the interface /potentiostat	33
Figure III-5.	GPIO handshake timing diagram	36
Figure III-6.	Digital-to-analog converter	39
Figure III-7.	Analog-to-digital converter	41
Figure III-8.	Potentiostatic control diagram	44
Figure III-9.	Triangular waveform generator	46
Figure III-10.	Pulsed signal sampling circuit	49
Figure III-11.	Pulsed signal sampling circuit timing diagram	52
Figure V-1.	Detection peaks for injection of alkaline solutions in 0.251 M NaOH	63
Figure V-2.	Calibration curves for alkaline (A) and acidic (B) samples	65
Figure VI-1.	Current-potential curves for $\text{CN}^-$ at a Pt RDE in 0.25 M NaOH	70
Figure VI-2.	Current-time curves for $\text{Cl}^-$ and $\text{CN}^-$ at Pt	74
Figure VI-3.	Pulsed amperometric detection of $\text{CN}^-$ in 0.25 M NaOH	76
Figure VI-4.	Current-voltage curves for $\text{Cl}^-$ at a Pt RDE in 0.5 M $\text{H}_2\text{SO}_4$	79
Figure VI-5.	The indirect ("negative") detection of $\text{Cl}^-$ in 0.5 M $\text{H}_2\text{SO}_4$	81
Figure VI-6.	Plots of $\theta_{\text{ad}}$ vs. $t_{\text{d}}$ for $\text{Cl}^-$ in 0.5 M $\text{H}_2\text{SO}_4$	86

Figure VI-7.	Plot of $\log[\theta_{ad}/(1-\theta_{ad})]$ <u>vs.</u> $\log [Cl^-]$	89
Figure VI-8.	Calibration curves for the direct ("positive") detection of $Cl^-$ in 0.5 M $H_2SO_4$	93
Figure VII-1.	Current-potential curves for glycine by cyclic, linear-scan voltammetry at a Pt RDE	97
Figure VII-2.	Current-time curves for glycine at a Pt RDE	103
Figure VII-3.	Peaks obtained for glycine over a short time span by flow-injection with PAD	107
Figure VII-4.	Peaks obtained for glycine over a long time span by flow-injection with PAD	109
Figure VII-5.	Calibration curves ( $i_{peak}$ <u>vs.</u> $C_b$ ) for glycine by flow-injection with PAD	113
Figure VII-6.	Calibration curve ( $1/i_{peak}$ <u>vs.</u> $1/C_b$ ) for glycine by flow- injection with PAD	115
Figure VII-7.	Chromatogram of selected amino acids using PAD	118
Figure VII-8.	Chromatogram of amino acids	120
Figure VIII-1.	Structure of nebramycin factors	125
Figure VIII-2.	Current-potential curves for tobra- mycin at a Pt RDE in 0.25 M NaOH	128
Figure VIII-3.	Chromatogram of a mixture of several nebramycin factors	132
Figure VIII-4.	Valving diagram	135
Figure VIII-5.	Effect of sample size in dual- column separations	137

Figure VIII-6.	Chromatogram of spiked blood serum	140
Figure VIII-7.	Chromatogram of fermentation broth	142
Figure VIII-8.	Chromatographic calibration curves	144

## LIST OF TABLES

Table IV-1.	Electroactivity of selected carboxylic acids at Pt	57
Table IV-2.	Electroactivity of selected aliphatic amines at Pt	59
Table IV-3.	Electroactivity of selected amines at Pt	60
Table VII-1.	Description of two triple-step potential waveforms for detection of amino acids at Pt electrodes in 0.25 M NaOH	100
Table VII-2.	Relative sensitivities of 20 amino acids normalized to glycine	111
Table VII-3.	Values of $k'$ for 14 amino acids	123
Table VIII-1.	Description of two triple-step potential waveforms for detection of aminoglycosides at Pt electrodes in 0.25 M NaOH	130

## I. INTRODUCTION

Few electrochemical techniques, with notable exceptions, are suitable for the anodic detection of organic compounds. Organic compounds tend to have strong chemical interactions with electrode surfaces. The total faradaic charge passed during the anodic reactions of organic compounds is generally observed to be controlled by the surface area of the electrode. Hence, the anodic reactions are described as being surface controlled. The organic compounds may simply adsorb to the electrode surface, or the electrode surface may catalyze the anodic reaction of the organic compounds, as in the case of the oxidation of simple alcohols at a Pt electrode (1,2). For the case of simple alcohols, the initial rate of surface catalyzed dehydrogenation is large. The oxidation rate drops sharply with time, as the carbonaceous dehydrogenated reaction products adsorb strongly to the electrode surface, eliminating active surface sites. Thus, the anodic current decays rapidly to zero.

The rate of anodic reactions catalyzed by specific, active electrode states will quickly drop if these surface sites are blocked or converted to inactive surface states. For example, the oxidation of As(III) is strongly electrocatalyzed by PtOH: as PtOH is converted to PtO, the extent of electrocatalysis drops significantly (3).

Again, the anodic current is initially large, but decays with time.

Alternate anodic and cathodic polarization of a noble-metal electrode surface will alternately form and remove surface oxide. For Pt, in the case of the oxidation of As(III), the repeated formation of PtO assures the presence of the active PtOH intermediate. In this manner, the activity of the electrode is continually maintained, hence the oxidation of As(III) proceeds at a large rate. It also has been shown that alternate anodic and cathodic polarizations of the electrode at potentials corresponding to the solvent decomposition limits will remove adsorbed carbonaceous material from the electrode and effectively clean the surface (4,5).

The ability to maintain surface activity by repeatedly regenerating PtOH, allows the anodic detection and quantitation of organic compounds which have reactions heretofore thought too hopelessly irreversible to be of use. Previous publications have demonstrated the application of anodic pulsed amperometric detection (PAD) for alcohols, polyalcohols and carbohydrates at Pt and Au electrodes (6-9). This dissertation describes the use of PAD for the quantitation of organic amines and amino acids at Pt. The PAD technique applies a triple-step potential waveform in which the analytical signal is measured within

a few milliseconds after application of the detection pulse. The potential is then usually pulsed to a large positive value, at which the electrode surface is oxidatively cleaned very rapidly of any remaining adsorbed analyte or reaction products; the subsequent application of a large negative potential pulse causes reduction of the electrode surface oxide and allows adsorption of analyte prior to the next detection cycle. The frequency of the waveform can be sufficiently high (ca. 1-2 Hz) to allow application of PAD to chromatographic and flow-injection systems.

Oxide-catalyzed reactions must satisfy two criteria for successful application to electrochemical detection: (1) The detection potential ( $E$ ) must be in the region of oxide formation; and (2)  $E$  must be greater than  $E_0$  for the oxidation of the analyte. The oxide-catalyzed reactions of amines meet the above stated criteria. However, the rate of PtO formation is potential dependent; hence, for large  $E$ , PtOH has a short lifetime because of the rapid conversion to PtO, and therefore the need arises to restore surface activity.

Factors affecting the oxide growth characteristics will affect the current response of the electrode. Hence, even electroinactive species with strong chemical interactions with Pt will alter the Pt oxide growth

characteristics, altering the analytical current. Strongly adsorbed electroinactive inorganic anions (e.g.  $\text{CN}^-$ ) are used as model compounds for PAD to study adsorption phenomenon at Pt. The responsiveness that PAD has for adsorbed compounds allows for the detection of virtually any nonelectroactive compound that will adsorb to Pt, in addition to electroactive compounds. Therefore, PAD is a general detector for adsorbates, whether electroactive or inactive. No selectivity is afforded by choice of detection potential; hence, the detector relies upon chromatographic separations to provide analytical resolution of mixtures.

The application of PAD to amino acids and aminoglycosides has a distinct advantage over standard spectrophotometric detectors in that post-column addition of reagent is not necessary if the required electrolyte is used as the chromatographic eluent. PAD sensitivity compares favorably with fluorescence detection of primary amines, and exceeds in sensitivity for detection of secondary amines (i.e. proline and hydroxy-proline).



## II. LITERATURE REVIEW

### A. Adsorption at Pt Electrodes

#### 1. Methods of determining surface coverage

a. Electroactive adsorbates      Surface coverages of adsorbed electroactive species on Pt can be determined from the anodic or cathodic charge passed until oxygen or hydrogen evolution potentials are reached, respectively, in the presence and absence of adsorbate. Charging of the electrode can be accomplished in a galvanostatic mode (i.e. passing a direct current until the appropriate potential is attained), or in a potentiodynamic mode (i.e. the electrode potential is linearly scanned between set limits while monitoring the current). The charging curve obtained in the absence of an adsorbate, is compared to the charging curve obtained in the presence of adsorbate after surface equilibrium has been established. The difference in charge that results from the oxidation or reduction of the adsorbate is used to estimate the amount of adsorbate present at the electrode surface (10). This technique, as first used by Shlygin and Manzhelei (11), requires that the electrode be washed with adsorbate-free electrolyte after being equilibrated in the adsorbate solution. In addition to this technique requiring a well characterized electrochemical process,

the washing step mandates that the adsorbate must have a negligible desorption rate. Some of the first adsorption studies of methanol were done by Pavela (12) using this technique.

Rapid potential sweep techniques (13,14) were developed to eliminate the need to replace the adsorbate solution with adsorbate-free electrolyte prior to surface charging. It has been shown that potential sweep rates greater than 200 V/s will virtually eliminate the contribution of diffusion of an adsorbate to the total charge (15). An assumption inherent in this technique is that the production of an oxide layer does not change in the presence of the adsorbed substance. Adsorbed methanol has been shown to alter the formation of PtO (16). To compensate for this effect, a current reversal method was developed by Brummer (17); Brummer and Ford (18). With this technique, a cathodic pulse is applied immediately following the rapid anodic potential sweep. In this manner, the amount of PtO formed on the anodic sweep is determined by the charge passed for PtO reduction after application of the cathodic pulse. Thus, the effect of the adsorbate on PtO formation is compensated.

b. Nonelectroactive adsorbates      The determination of nonelectroactive-adsorbate surface coverage by electrochemical means, must rely on an

indirect measurement. Adsorptional displacement (10) is one such indirect technique. The adsorptional displacement technique measures the surface equilibrium coverage of a nonelectroactive adsorbate through the observed decrease in the amount of adsorbed hydrogen from that normally adsorbed on the surface of the electrode in the absence of adsorbate. The reduction of adsorbed  $H^+$  during a cathodic potential step is assumed to form a complete monolayer of adsorbed H at the surface of Pt electrodes. The amount of charge required to form the monolayer ( $Q_H$ ) is determined by a rapid cathodic galvanostatic or potentiodynamic sweep in an adsorbate-free electrolyte. The adsorbate is introduced to the solution, and the surface coverage is allowed to reach equilibrium at a fixed potential out of the region that adsorbed  $H^+$  is reduced. The cathodic sweep is applied and the charge passed ( $Q_{H,ad}$ ) is a measure of the remaining free surface sites being covered by H. The adsorbate surface coverage ( $\theta$ ) is a ratio of

$Q_H - Q_{H,ad}$  to  $Q_H$ .

$$\theta = \frac{Q_H - Q_{H,ad}}{Q_H}$$

In order for this method to succeed, the adsorbate must not undergo reduction, nor desorb or adsorb further during the cathodic pulse. Adsorption of acetic acid

(19), methanol (20), alkenes (21), and nitriles (22) have been studied using the cathodic pulse technique. Gilman (23) expanded upon the cathodic pulse method by including a series of potential steps prior to the cathodic pulse to produce a reproducible state of the electrode surface on which the adsorbate was allowed to adsorb.

c. Radioactive tracers      Radioactive tracers play an important role in determination of surface coverages. Techniques based on measurement of radioactivity of a thin foil electrode have been suggested by Joliot (24), and implemented extensively (25-31). The thin foil method involves lowering a counter, covered by the thin foil electrode, into an electrolyte solution containing a labeled adsorbate. The background count is estimated by recording the count as a function of distance that the electrode is away from the solution. The count is then extrapolated to zero distance. The amount of adsorbate is calculated from the difference of the count of the electrode immersed in the adsorbate solution and the background count. This method is obviously limited to compounds containing radioactive atoms (e.g.  $C^{14}$  or  $S^{35}$ ). The accuracy of this method is best at low adsorbate concentrations. For adsorbate concentrations larger than  $10^{-3}$  M, the count due to the adsorbed

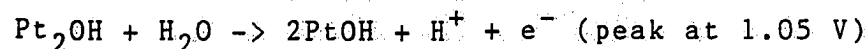
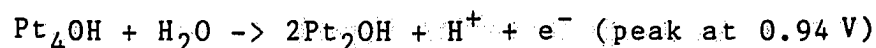
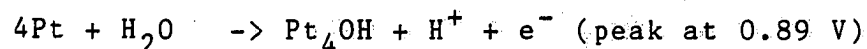
species becomes small with respect to the background count.

Gileadi et al. (32) points out the relative usefulness of both electrochemical and radiochemical techniques. Much information can be gained about an adsorbing species if a combination of the two types of techniques is used.

## 2. Effects of adsorption on PtOH/PtO formation

A complete review of the literature covering the oxidation of Pt was compiled by Cabelka (33). Specific literature will be reviewed here as it pertains to the affect of adsorbed substances upon the anodic formation of PtOH/PtO.

Angerstein-Kozłowska et al. (34) have shown that three discernible stages of Pt surface oxidation exist up to the formation of a monolayer of PtOH ( $E = 1.1$  V vs. NHE).



The I-E peaks for the three processes are not well resolved from voltammetric data. Only the first stage has been experimentally shown to be quasi-reversible. The following stages display more irreversibility which has

been thought to be consistent with place exchange mechanisms involving Pt atoms and the adsorbed OH species (35,36). The various states given for the products in these reactions should be interpreted as representing surface interaction stoichiometry of adsorbed  $\cdot\text{OH}$  rather than discrete oxidation states of the Pt atoms.

Competing adsorption will affect Pt oxide growth characteristics by affecting the initial quasi-reversible OH adsorption sites. Angerstein-Kozłowska *et al.* (37) have characterized the competitive adsorption effects as either "blocking effects" or "displacement effects." Blocking effects cause a reduction of the charge passed during the oxidation of the Pt surface because OH adsorption sites are occupied by competing adsorbates. Systems displaying displacement effects have the initial PtOH formation region delayed or shifted to potentials more positive, at which the deposited PtOH is again stable.

## B. Methods for Determination of Amino Acids

### 1. Wet chemical analysis

Analytical methods that are specific for particular amino acids exist, such as the Sakaguchi reaction for the determination of arginine (38), enzymatic decarboxylations (39), and microbiological assays (40,41). However, as in

the case of the analysis of protein hydrolysates, simultaneous determinations of many amino acids are desirable. Therefore, virtually all amino acid determinations rely on chromatographic separations. As this is the case, the phrase "classical determination" has come to describe the spectrophotometric detection of amino acids following chromatographic separation.

## 2. Chromatographic separations of amino acids with spectrophotometric detection

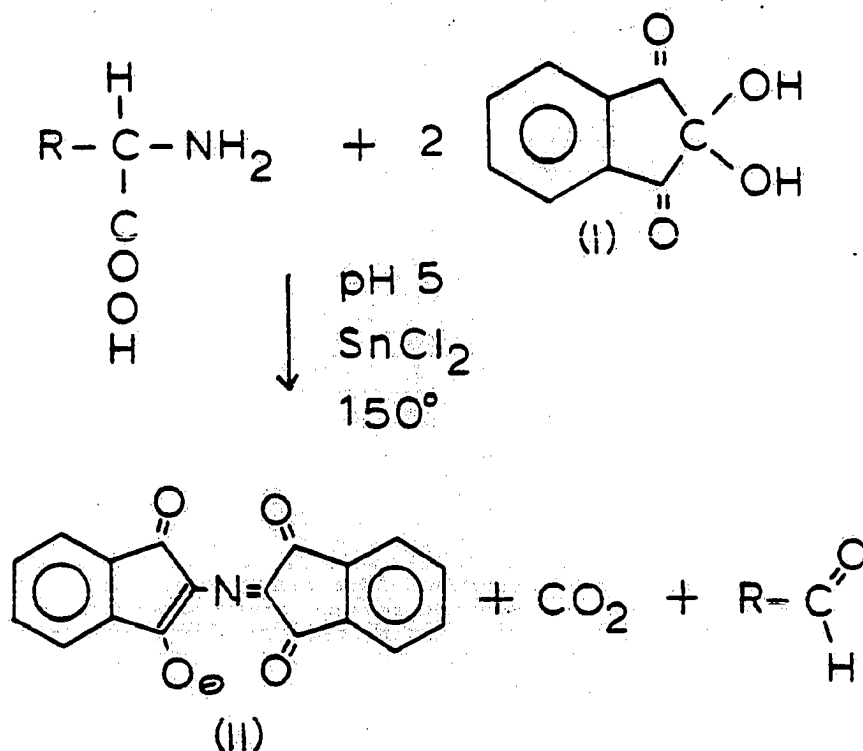
The original amino acid analyzer was developed by Spackman, Stein, and Moore (42). The analysis scheme consisted of a cation exchange separation with colorimetric detection using post-column addition of ninhydrin.

Of course, much improvement has been made in the area of chromatography since the first amino acid separation. Modern liquid chromatography of amino acids can be divided into two distinct categories: underivatized and pre-derivatized.

a. Underivatized methods The chromatography of underivatized amino acids generally rely on cation exchange chromatography with post-column addition of reagents to provide for spectrophotometric detection. Because of the varying acidity of the amino acids, the

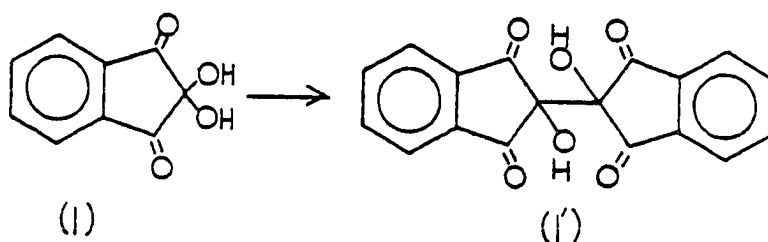
cation exchange separations require either an increase in eluent pH or ionic strength through the use of a step gradient or linear gradient. The most acidic of the acids elute first, the most basic elute last (43).

Since amino acids lack chromophores, chromatographic separations of underivatized amino acids must rely upon post-column derivatization to provide sensitive spectrophotometric detection. Post-column addition of ninhydrin reagent causes the formation of "Ruhemann's purple" (II) (44,45). The ninhydrin reagent contains ninhydrin (I), methyl cellosolve, and a reducing agent (usually stannous chloride) in a pH 5 buffer (acetate or citrate).





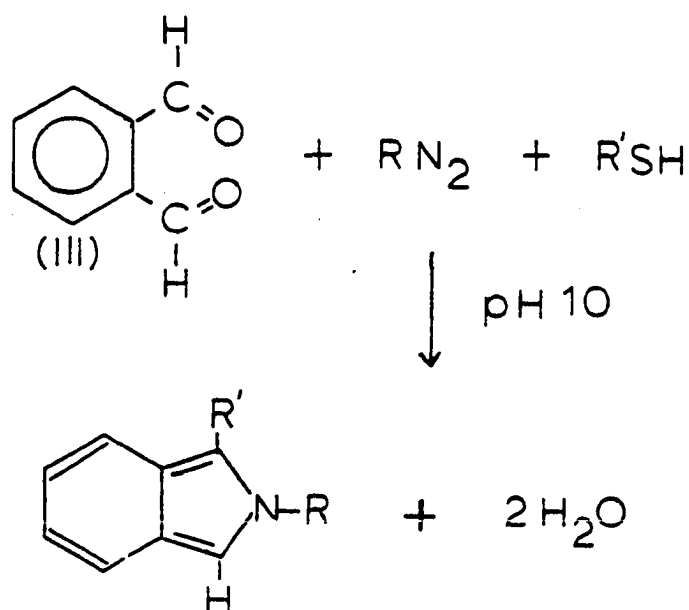
Early workers concluded that the observed need for a reducing agent to maintain good reproducibility was caused by the oxidative effects of dissolved oxygen (46). Later work suggests that the reducing agent reduces ninhydrin (I) to hydrindantin (I'),



and the hydrindantin plays an important role in the color forming mechanism (47). Upon standing, the stannous chloride containing ninhydrin reagent forms insoluble tin salts, complicating accurate reagent delivery. Titanous chloride was found to be as effective as  $\text{SnCl}_2$  without forming insoluble salts (48,49).

The ninhydrin reaction is a general reaction for all primary amines giving a near quantitative yield of blue reaction product ( $\lambda_{\text{max}} = 570 \text{ nm}$ ). Proline and hydroxyproline (secondary amines) give products that absorb at 440 nm; the sensitivity for the secondary amino acids is less than that for the primary amino acids, and the reaction times are longer (50).

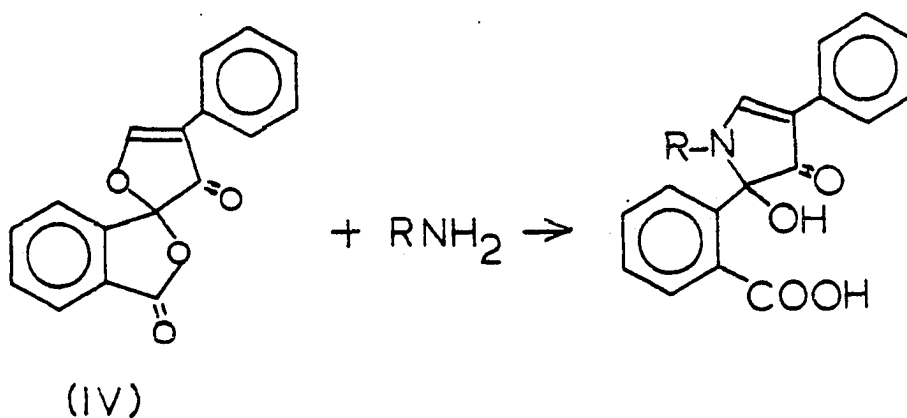
Fluorometric detection is accomplished by post-column addition of either o-phthalaldehyde (OPA) (51) or fluorescamine (52). The OPA method utilizes a pH 10 borate buffer containing OPA (III) and 2-mercaptoethanol (53).



The OPA reagent reacts with all primary amino acids to give an intense blue fluorescence. The OPA method is reported to be 50X more sensitive than the ninhydrin method (54). Proline and hydroxyproline do not react with the OPA reagent. However, Roth (55) reported that the addition of sodium hypochlorite oxidizes proline to a primary amine, and allows the formation of the corresponding fluorescent compound. The major

complication in this method is that primary amino acids are destroyed by excess hypochlorite. This has resulted in detection schemes utilizing complicated hypochlorite reagent stream switching mechanisms (56,57). Ishida et al. (58) claimed that through careful control of the hypochlorite concentration, switching need not be employed. They maintain that the detectability of amino acids remains stable, and is only slightly depressed if the hypochlorite concentration is kept low. Two separate chromatographic runs may also be done (59). Another oxidant, chloramine-T, is claimed to be useful with OPA to detect proline (60).

Fluorescamine (4-phenylspiro-[furan-2(3H), 1'-phthalan]-3,3'-dione) (IV) reacts rapidly with primary amines at alkaline pH to form fluorophores (excitation 390 nm, emission 475 nm) (61-63).



The reaction half-times for most amino acids are 200-500 ms (64). Secondary amines do not react with fluorescamine. However, Weigele et al. (65) showed that proline can be oxidatively decarboxylated by N-chlorosuccinimide to yield 4-amino-n-butylaldehyde, which reacts with fluorescamine in the manner of a primary amine. As in the case of hypochloride addition to OPA, complicated switching must be used to implement this scheme (66). Hydroxyproline can be determined with a slight adjustment of this method (67). Sharp baseline shifts occur during oxidant addition.

b. Pre-derivatized methods      The more polar amino acids are poorly retained by reverse-phase columns. However, pre-derivatized amino acids are well retained by reverse-phase columns, and efficient separations are possible. The most commonly used derivatizing agents are phenylthiohydantoin (PTH), dansyl chloride (Dansyl, Dns), and OPA.

PTH derivatives are a product of the Edman degradation procedure (68,69) for sequencing proteins. The reverse-phase chromatography (RP-HPLC) of these derivatives is an important simplification of the simultaneous determination of amino acids in protein hydrolysates, and has been applied frequently (70-74). PTH forms derivatives with all amino acids, allowing

colorimetric determinations with detection limits of 5-50 pmole.

5-dimethylaminophthalenesulfonyl (Dansyl, Dns) (75) reacts with free amines to yield compounds having intense yellow fluorescence (76,77). Tapuhi et al. (78) were the first to report the application of RP-HPLC to Dns derivatives. Detection limits of 0.05-1 pmole have been reported (79,80).

OPA derivatives, previously described, have also been separated by RP-HPLC (81,82).

When pre-column derivatizations are used, certain problems arise that do not arise when post-column derivatizations are used: 1) incomplete and/or secondary reactions; 2) sample contamination; and 3) derivative instability (83).

Ion-pairing has been used to accomplish RP-HPLC of amino acids. This method is not, strictly speaking, a pre-derivatization technique; and relies upon post-column addition to provide spectrophotometric detection (84,85).

### 3. Chromatographic separations of amino acids with electrochemical detection

#### a. Detection of derivatized amino acids

The general experience among electroanalytical chemists that the quantitative determination of aliphatic amines

and amino acids in aqueous solutions cannot readily be achieved by conventional voltammetry and amperometry is illustrated here by selected quotations. Adams (86) stated: "...aliphatic amines are difficult to anodically oxidize in any quantitative fashion." Malfoy and Reynaud (87) claimed: "Among the 20 amino acids present in the proteins only tryptophan and tyrosine are selectively oxidized at a gold, platinum or carbon electrode. Histidine is oxidizable only at a carbon electrode." Joseph and Davies (88) reported: "Most amino acids are not electroactive...." They proceeded to describe the a priori derivatization of amino acids with OPA to enable their electrochemical detection following RP-HPLC (89). The OPA derivative contains an electroactive isoindole grouping (82) that is electrochemically active at glassy carbon. Since OPA-derivatives suffer stability problems, Allison et al. (90) investigated using OPA derivatives formed with structurally different thiol compounds (91,92). The fluorescence of these more stable derivatives is markedly lower, but the electrochemical detection is not affected. Detection limits of 30-150 fmol were reported.

b. Direct detection of underivatized amino acids The direct detection of underivatized amino acids at a constant electrode potential was reported

recently by Hui and Huber (93); Krafil and Huber (94) at an oxide-covered Ni electrode in alkaline solutions. The detection reaction had been diagnosed by Fleischman et al. (95) to occur with direct chemical involvement of the oxide. The amino acids reduce  $\text{NiO}(\text{OH})_2$  to  $\text{Ni}(\text{OH})_2$  with subsequent anodic oxidation of  $\text{Ni}(\text{OH})_2$  back to  $\text{NiO}(\text{OH})_2$ . Disadvantages of using the Ni electrode result from 1) a long start-up time, during which the thickness of the oxide layer is stabilized and the background current decays to a steady value; and 2) the finite solubility of the oxides in the alkaline electrolyte solutions.

Amino acids can be potentiometrically detected using either Cu-selective membrane electrodes, or solid copper electrodes. Potentiometric techniques detect the presence of amino acids through the decrease in free  $\text{Cu}^{++}$  concentration caused by the complexation of the  $\text{Cu}^{++}$  by the amino acids (the  $\text{Cu}^{++}$  is either present in the eluent or added to the column effluent prior to the detector cell. The use of a Cu-selective membrane electrode (96) is complicated because the response time of the electrode is slow; hence, severe peak tailing occurs, and detection limits are poor. Alexander et al. (97); Alexander and Maitra (98) reported direct potentiometric response for amino acids at Cu, without addition of any

$\text{Cu}^{++}$  reagent. The detector response was decidedly nonlinear and the direction of curvature varied for differing amino acids. Detection limits were not given, but the data presented suggest them to be 50-100 ppm. The electrode response is quickly poisoned by sulfur-containing amino acids, presumably due to irreversible adsorption of these amino acids to the Cu electrode.

Kok et al. (99,100) reported an amperometric response for amino acids at Cu in alkaline solutions. No electrode poisoning was observed for sulfur-containing amino acids, and reproducibility was good. The gradual dissolution of the electrode due to the finite solubility of  $\text{Cu}^{++}$  causes a constant surface renewal, preventing electrode poisoning. Detection limits of 0.05-0.3 ppm were reported.

In an article reviewing wall jet electrochemical detectors, Fleet and Little (101) show the electrochemical detection of arginine in a methanol-borate eluent at carbon. He indicates that other amino acids give similar results. No other results were presented and no subsequent publications were found. Fleet was granted a patent (102) for an electrochemical detector system based on a wall-jet detector, in combination with a two step potential waveform generator. The first potential



functions as a detection potential and the second potential functions as a cleaning potential. Fleet claims that virtually any organic compound can be detected by this system, yet only hydroxy-aromatic and phenolic detection were demonstrated. Once again no subsequent publications were found in regards to this detector system.

### C. Aminoglycoside Determinations

#### 1. Nonchromatographic techniques

Aminoglycoside antibiotics are commonly prescribed to combat gram-negative bacillary infections. Serious side-effects of these drugs may occur during treatments involving extensive dosages. Two such side effects: Nephrotoxicity--reversible renal dysfunction; and Ototoxicity--irreversible inner ear damage; have been correlated with high serum levels of various aminoglycoside antibiotics (103-109). The ability to determine serum concentration allows the monitoring of patient compliance with the drug therapy, and determines if overdosage is occurring. Currently, the three most commonly used techniques to determine aminoglycoside antibiotics are: microbiological, radioenzymatic, and radioimmuno assays (110). Liquid chromatographic

determinations are becoming more common, but only at larger research facilities.

a. Microbiological assay      Agar diffusion methods (111) are the most common microbiological assay procedures. Antibiotic standards and unknown samples are placed in wells cut into agar plates that contain test organisms known to be sensitive to the antibiotic being tested. The diameter of the growth inhibition zones for the standards are measured and plotted versus log concentration. Unknown concentrations are determined from the standard plot. Incubation takes 3-6 hours, and the detection limit is about 0.5-1.0 ppm (112). Interference from other antimicrobial agent(s) is the most serious disadvantage. Separation by electrophoresis prior to microbiological assay has been used (113) to eliminate some interferences.

b. Radioenzymatic assay      Enzymes that attach modifying groups to certain aminoglycosides (114) can be used to incorporate radioactive tags ( $C^{14}$ ,  $H^3$ ) into the aminoglycosides. Numerous such methods have been reported for the radioactive measurement of aminoglycoside concentrations (115-117). Each assay requires 2-3 hours, the detection limits are similar to microbiological

assays, but microbiological assays are less expensive (118).

c. Radioimmuno assay Radioimmuno assays are sensitive techniques for determining aminoglycoside antibiotic concentrations (119-124). The theory of radioimmuno assays will not be discussed here, as an excellent review is presented by Chalt and Ebersole (125). The assays can be done in 2-3 hours, and the detection limits (1.0-10 ppb) are far better than required by routine clinical purposes. This procedure is more expensive than either microbiological or radioenzymatic assays (110).

## 2. Chromatographic techniques

Aminoglycoside antibiotics lack chromophores, thus eliminating standard spectrophotometric methods unless derivatization is used. As described for the detection of amino acids, OPA can be adapted for both pre-column (126-128) and post-column (129-131) derivatization of aminoglycosides. Detection limits of 0.1-1.0 ppm have been reported. Post-column derivatization by fluorescamine is also feasible with similar detection limits (132).

1-fluoro-2,4-dinitrobenzene (FDNB) (133) reacts with both primary and secondary amines in a pH 9.3 buffer at 80° C in 30 minutes (134). Obviously, the reaction times eliminate post column addition. Chromatography following derivatization with UV detection has detection limits of 0.5-1 ppm (135-137). Pre-injection clean-up of the derivatization mixture is necessary.

### III. EXPERIMENTAL

#### A. Electrodes and Rotators

Current-potential curves (I-E) were obtained by cyclic, linear-scan voltammetry at a Pt rotated disk electrode (RDE,  $0.460 \text{ cm}^2$ ; Pine Instrument Co., Grove City, PA) using a model PIR rotator (Pine Instrument Co.). Several flow-through detector designs were utilized. The initial detector was of a Pt wire-tip design (Figure III-1) described by Hughes (138). A second Pt flow-through detector, with much reduced dead volume (Dionex Corp., Sunnyvale, CA), consisted of a Pt disk working electrode ( $0.008 \text{ cm}^2$ ), a carbon counter electrode, and a silver-silver chloride reference electrode in a sandwich-type arrangement (Figure III-2). The third flow-through detector, a Pt wire-tip detector of simple design (Figure III-3), is identical in design to that described by Austin (139).

#### B. Potentiostats

A model RDE3 potentiostat (Pine Instrument Co.) was used for cyclic voltammetry. Potential-step waveforms were potentiostated by either a model UEM (Dionex Corp.) microprocessor-controlled potentiostat or a microcomputer controlled potentiostat.

Figure III-1. Pt wire-tip flow-through cell

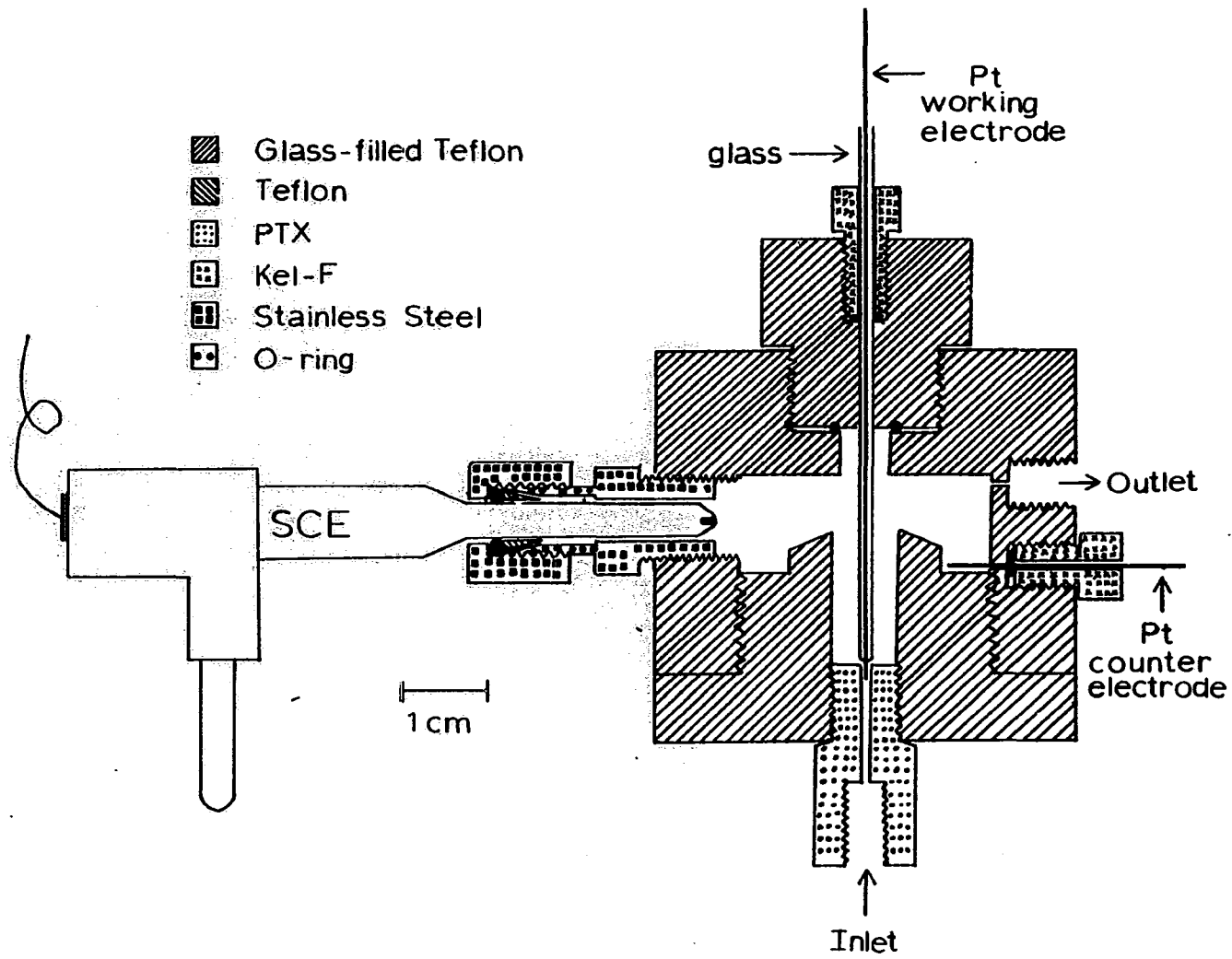
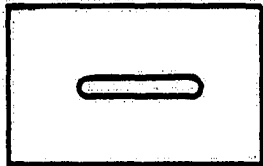
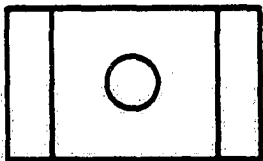


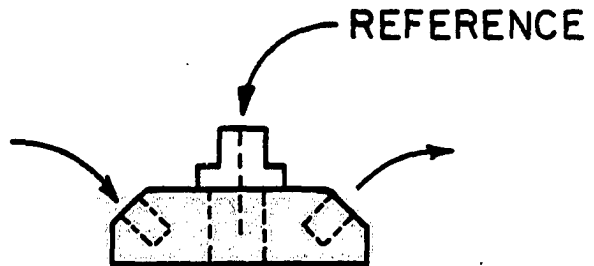
Figure III-2. Dionex flow-through cell



TOP  
VIEW



SIDE  
VIEW



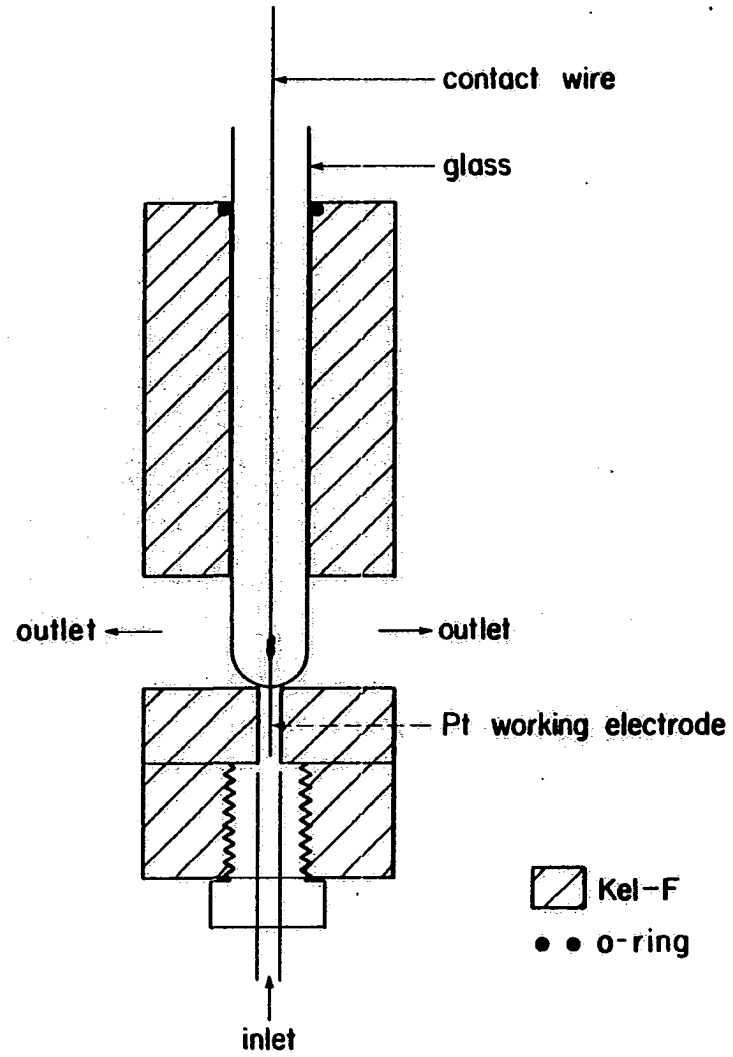
WORKING



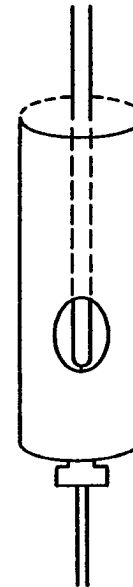
COUNTER



Figure III-3. Simple Pt wire-tip flow-through cell

Cross-Sectional View



Side View



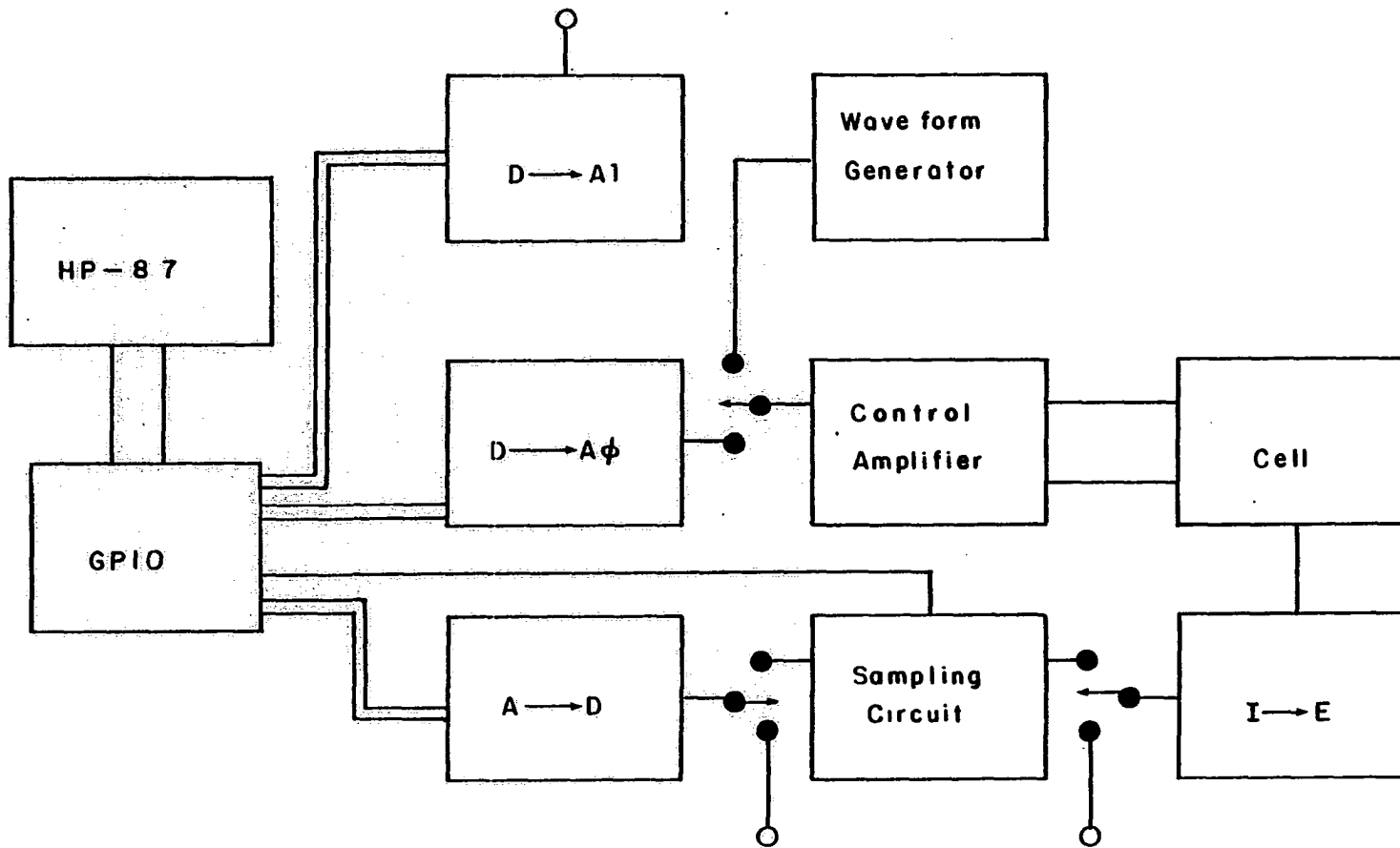
-  Kel-F
-  o-ring

## 1. Interface/Potentiostat

Data acquisition and potential control are accomplished through the use of the Interface/Potentiostat (I/P). The computer hardware consisted of an HP-87 computer (Hewlett-Packard, Corvallis, OR) with an HP 82980A Memory module, 87-15003 I/O ROM, HP82940A GPIO interface, HP82902M flexible disc drive, and an Epson MX-80F/T dot matrix printer (Epson America, Inc., Torrance, CA). The I/P was constructed by this author.

Figure III-4 shows a block diagram of the I/P. Data are transferred from the I/P to the HP-87 through the GPIO interface. The GPIO is a general purpose parallel interface that allows the selection of either 8-bit or 16-bit ports. For use with the I/P, the GPIO was configured to four, 16-bit ports (two input, two output). The interface section of the I/P consists of two 12-bit digital-to-analog converters (AD DAC80, Analog Devices, Norwood, MA), one 12-bit analog-to-digital converter (AD ADC80, Analog Devices), and appropriate support circuitry. The potentiostat section consists of a control amplifier which has as its input either a triangular waveform generator for use in cyclic voltammetry or a computer controlled digital-to-analog converter for use in pulsed amperometry.

Figure III-4. Block diagram of the interface/potentiostat



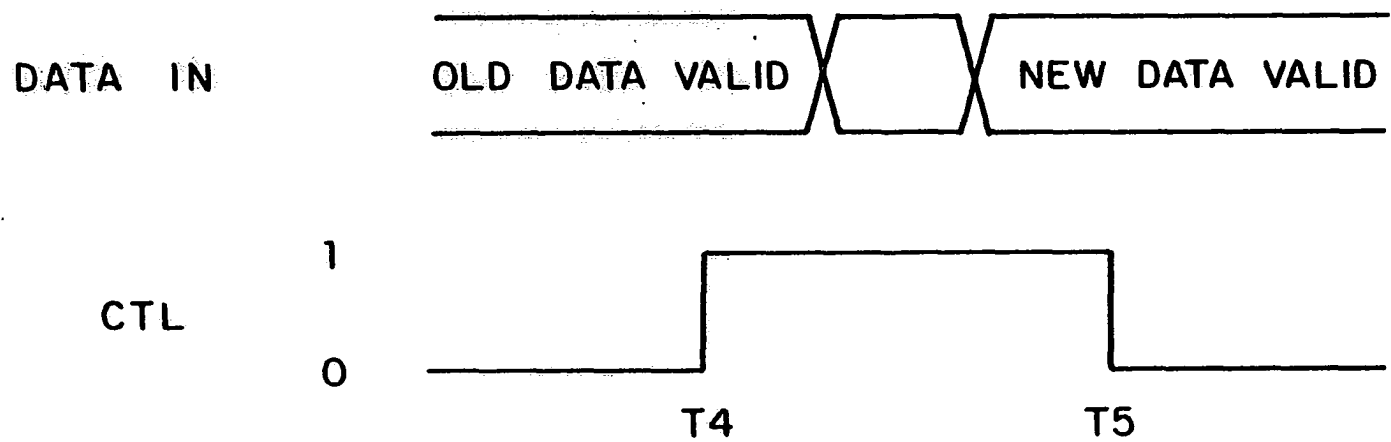
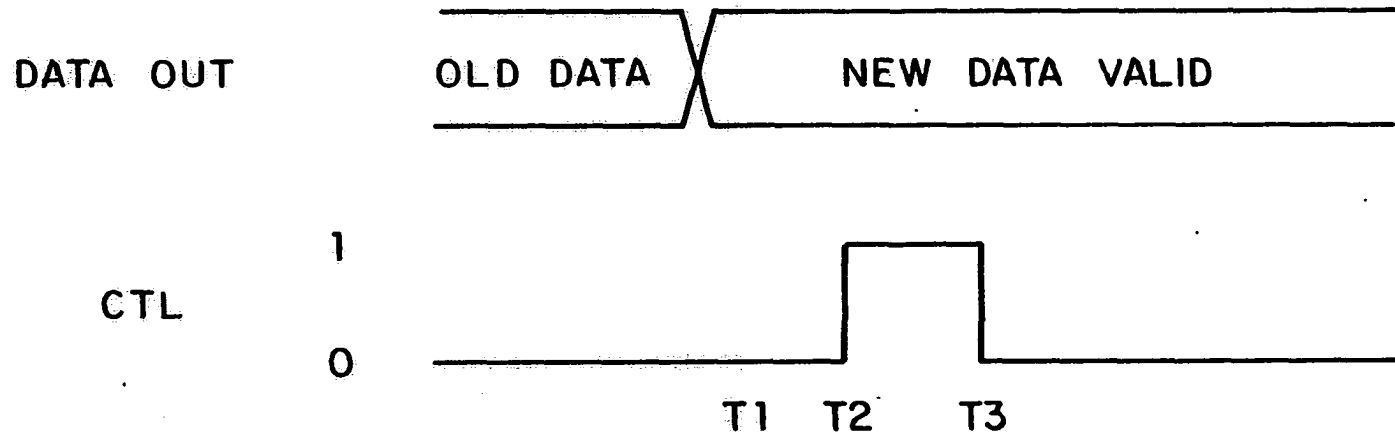
In the cyclic voltammetry mode the output of the current-to-voltage converter of the potentiostat was directly and continuously monitored. In the pulsed mode, sampling circuitry was added at the output of the current-to-voltage converter, and the signal was necessarily monitored by the computer controlled analog-to-digital converter.

a. GPIO      The use of 16-bit ports eliminated the need for two input/output (I/O) operations normally needed for accessing 12-bits with an 8-bit port (an 8-bit byte and a 4-bit nibble). This allowed for faster I/O operating times as all 12 bits were accessed on one pass. The output operations are conducted by one 16-bit port with two control lines (CTL0, CTL1). Through simple multiplexing with the appropriate data buffering, the two separate control lines provide for two separate channels. The same is true for the input operations. Two control lines (CTLA, CTLB) provide two separate input channels. However, for this work only one input channel was supported.

Since the converters are in a state of constant readiness, "strobe handshakes" were utilized to provide simple, fast control of data conversions. The input strobe handshake was operated in the BUSY-to-READY mode. Figure III-5 shows the essential actions of the data and

Figure III-5. GPIO handshake timing diagram





control lines. For outputting, the new data are placed on the data lines at T1 and the conversion start is signalled by the CTL stobe at T2. The conversion is accomplished in less than 5  $\mu$ s. T3 is the point at which the new data are latched. For inputting, the conversion is started by the CTL strobe at T4, the data are inputted some short time after T5.

Direct control of the control lines is possible, and two control lines (RESA, RESB) were made available for external use (i.e. recorder pen control).

b. Digital-to-analog conversion Two analog output channels are made possible by latching the digital input to one AD DAC80 with bistable latches (74LS75), while the data lines are changed to present new data to the remaining AD DAC80. CTLO latched or unlatched the data for channel 0 while CTL1 latched or unlatched channel 1 (Figure III-6). The AD DAC80s were operated in the bipolar mode ( $\pm 2.5$  V).

c. Analog-to-digital conversion The analog signal being sampled can be amplified and/or offset to maximize the accuracy of the analog conversion (Figure III-7). The signal is sampled by a voltage follower (A1) with adjustable gain and passed through a summing amplifier (A2) at which either positive or negative offset is applied. A sample-and-hold circuit (AD582,

Figure III-6. Digital-to-analog converter

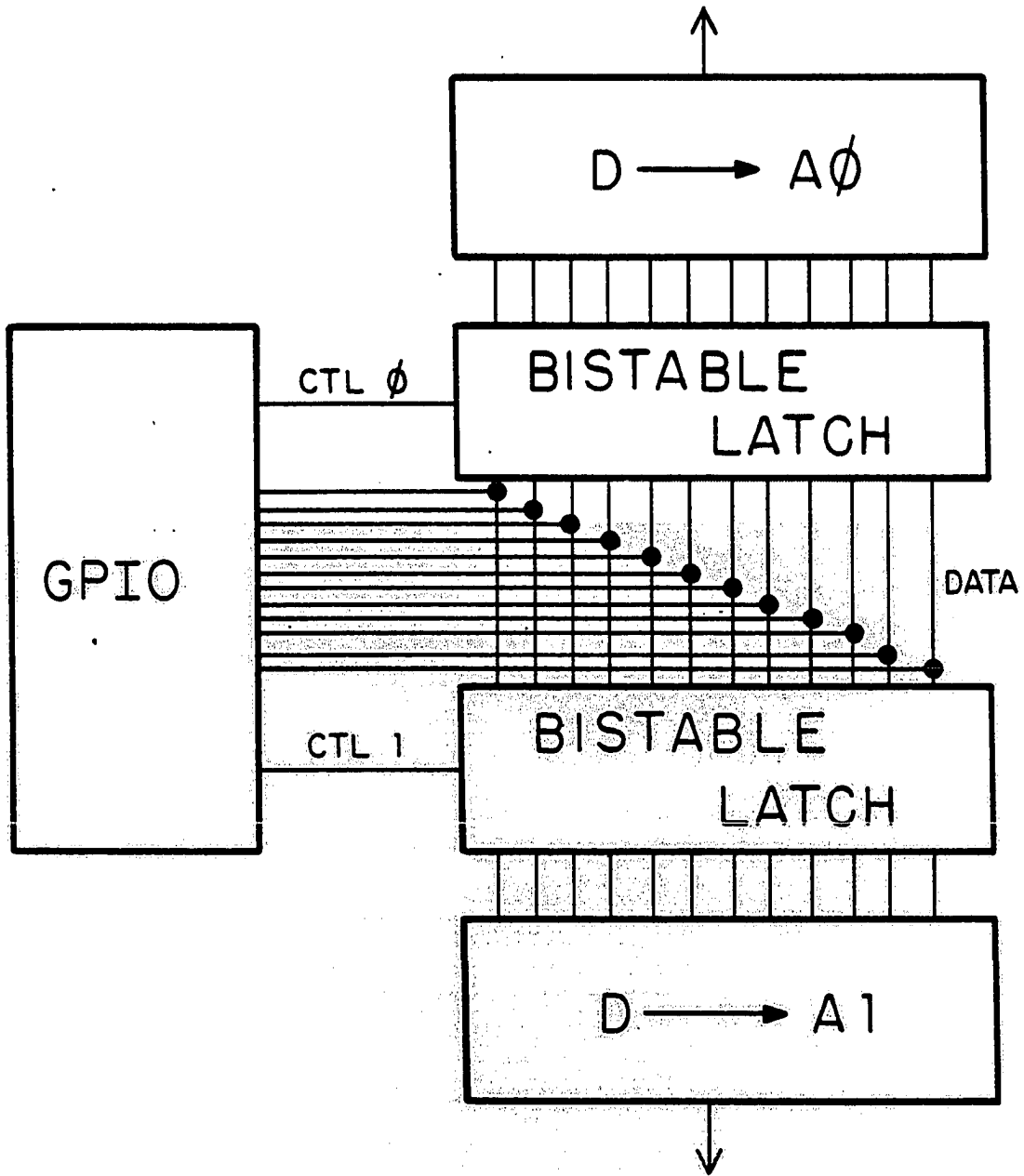
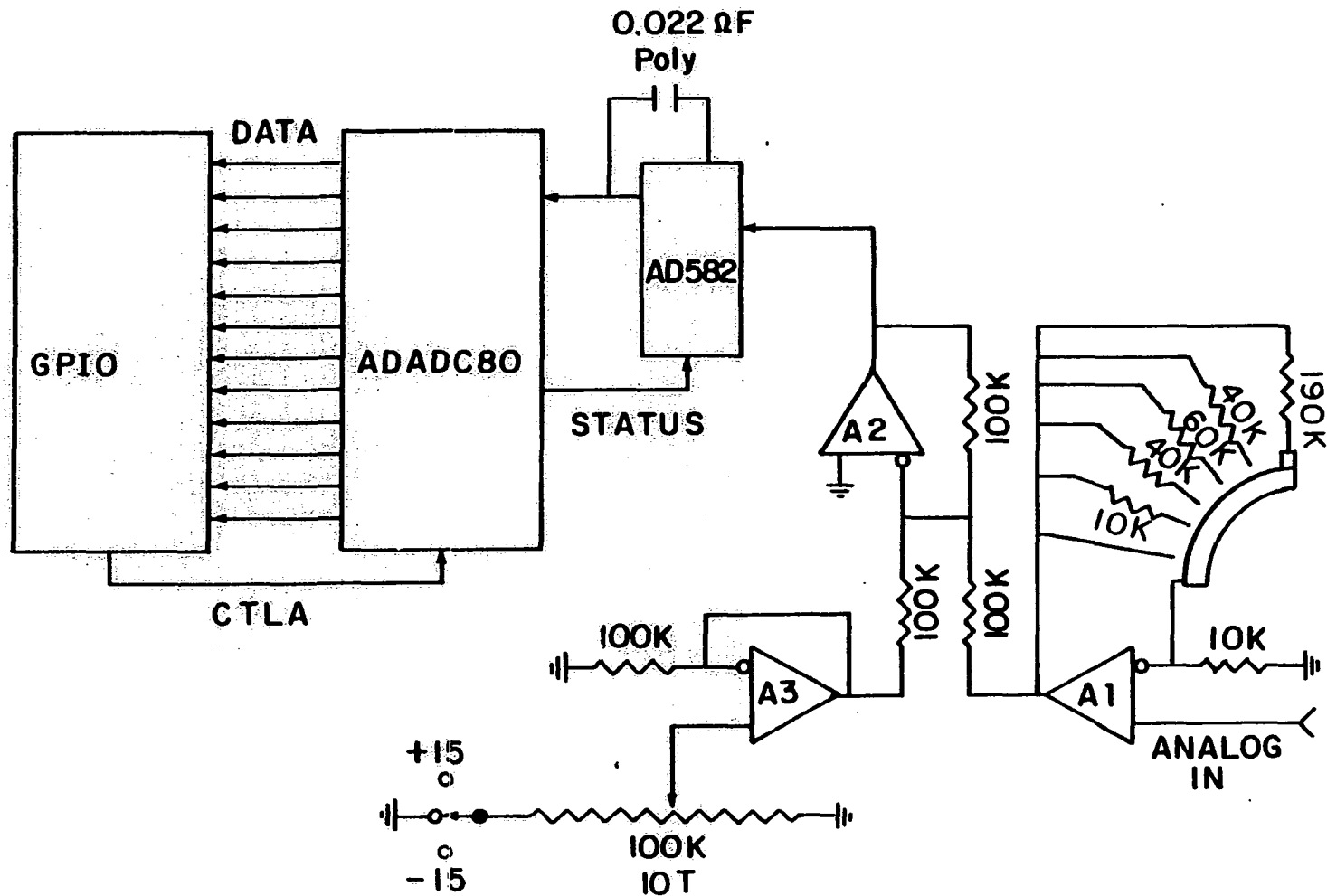


Figure III-7. Analog-to-digital converter



Analog Devices) holds the analog signal on the status command from the AD ADC80 for the duration of the analog conversion. The digital data is inputted to the HP-87 through the GPIO. The AD ADC80 was operated in the bipolar mode ( $\pm 10$  V).

d. Control amplifier and current-to-voltage converter Potentiostatic control of the electrode was maintained in the customary "three electrode" manner. The circuitry used is shown in Figure III-8. The working electrode is maintained at virtual ground by the current-to-voltage converter (A4), the counter electrode is driven relative to the reference electrode by the control amplifier (A5).

e. Triangular waveform generator Cyclic, linear-scan voltammetry was done by switching the input of the control amplifier to the output of the triangular waveform generator. The design of the waveform generator is that used by Pratt (140) and is represented here in Figure III-9.

f. Pulsed signal sampling circuit The potentiostat, when operated in the computer controlled pulsed mode, presented a special current sampling problem. In order to provide accurate current measurements, the sampling period and sampling delay, i.e. the time after application of the detection potential and prior

Figure III-8. Potentiostatic control diagram



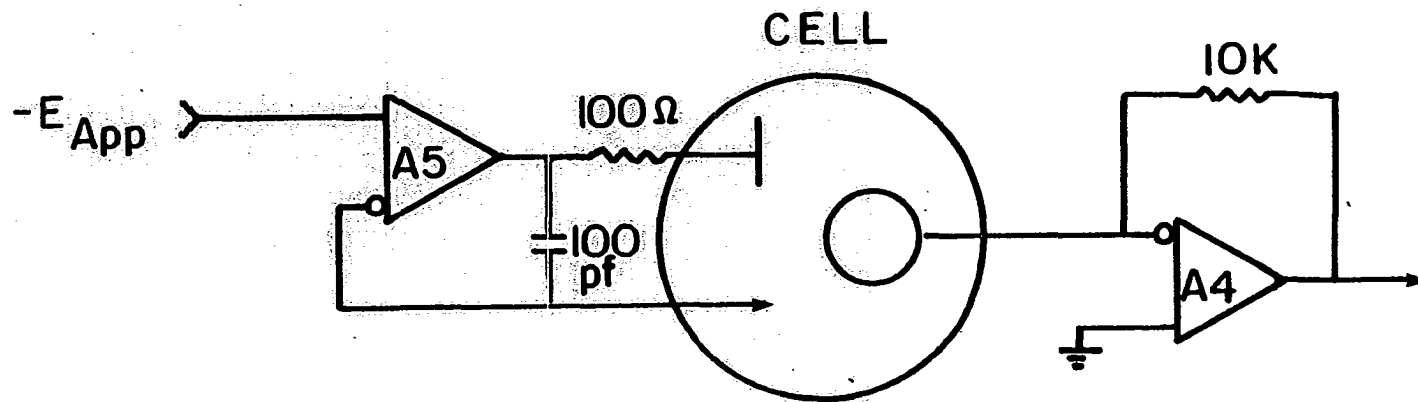
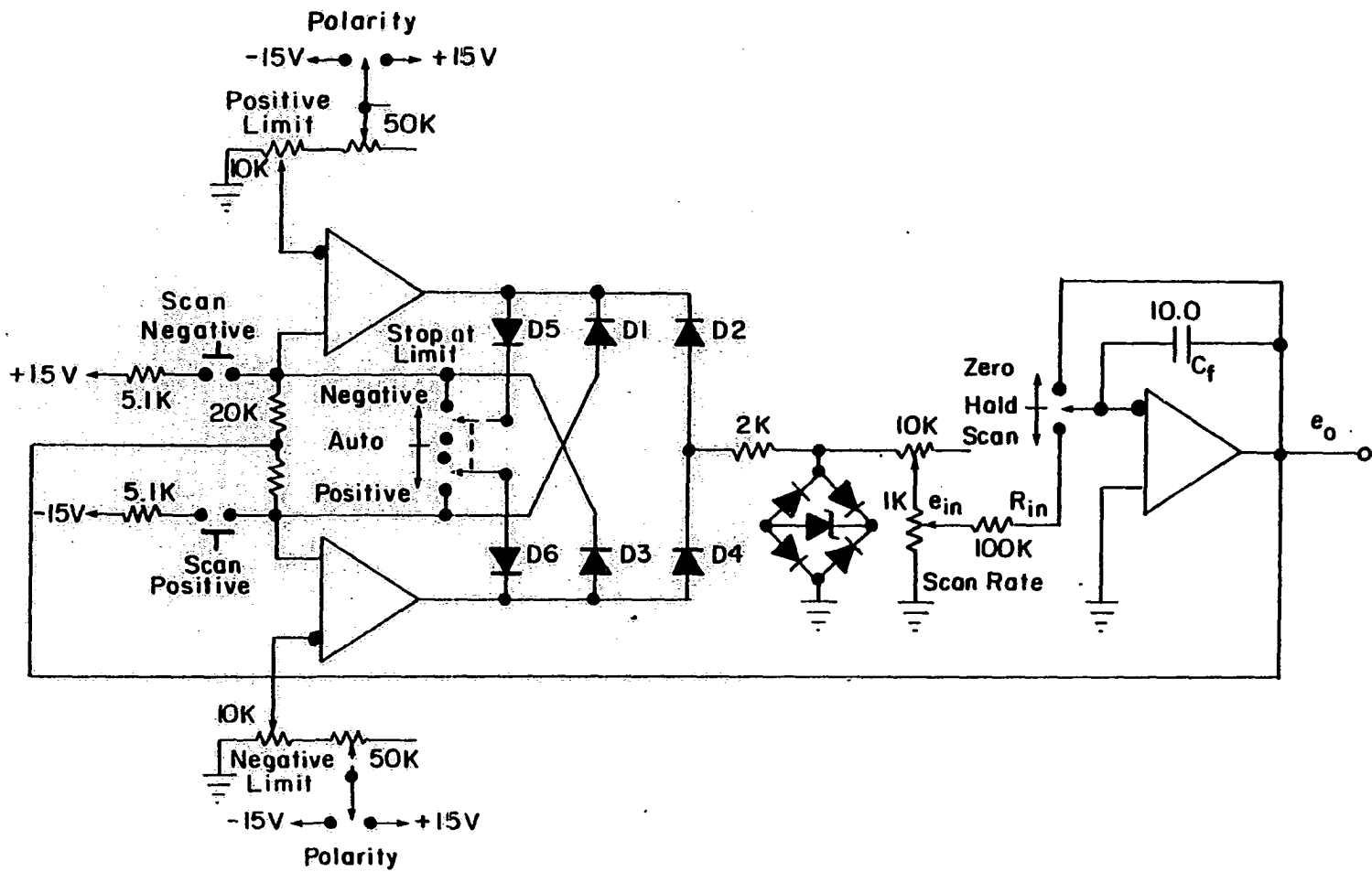


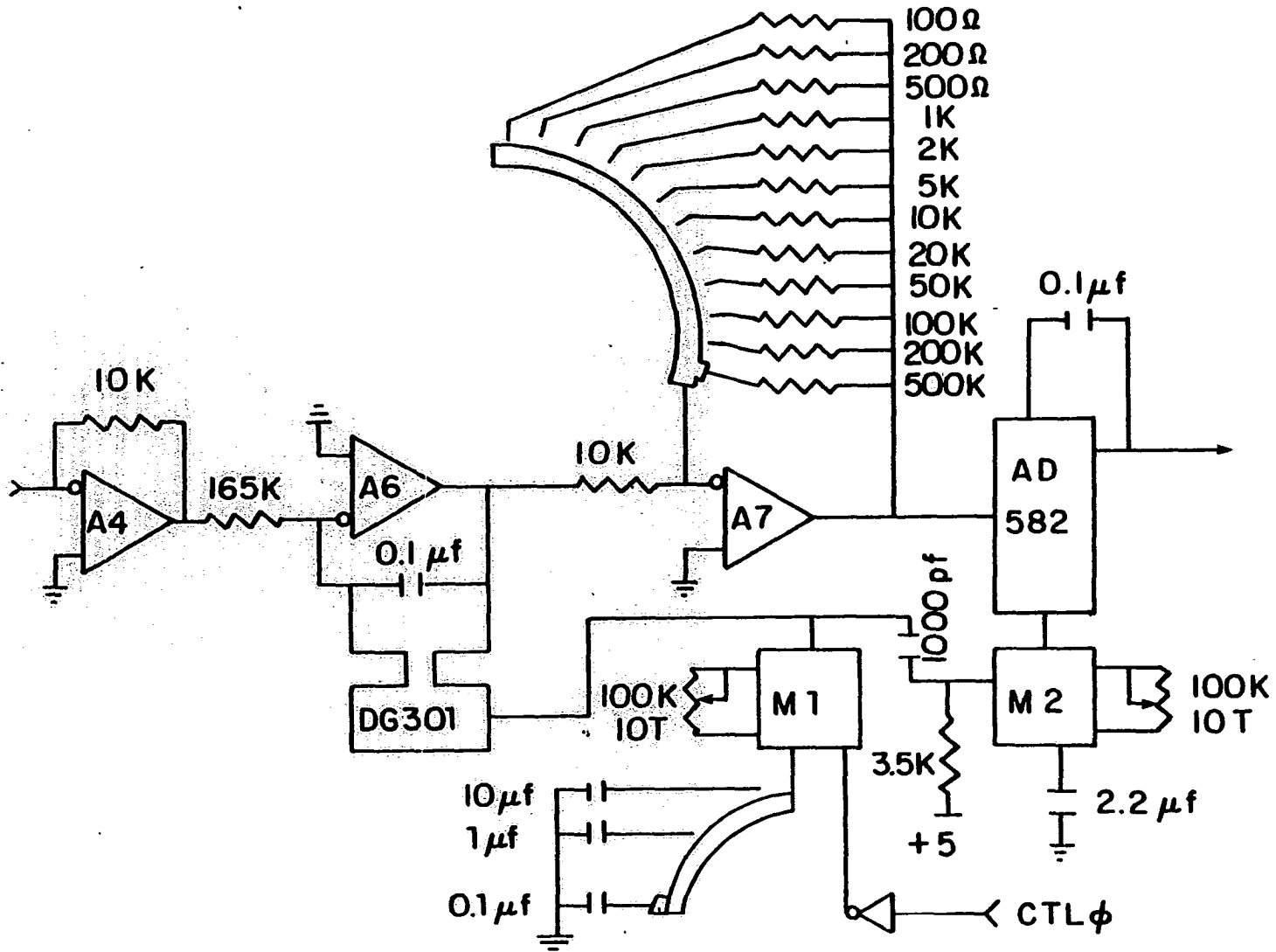
Figure III-9. Triangular waveform generator



to the sampling period; must be accurately reproduced. In addition, a minimum sampling delay time of 35 ms is desirable. Due to programming constraints, the minimum sampling delay possible with full computer control is about 130 ms, therefore the sampling delay and sampling period timing control was done by monostables on board the pulsed signal sampling circuit.

The circuit is shown in Figure III-10. The CTL0 strobe that signals the initiation of a potential pulse is used to trigger the sampling delay monostable (M1). This monostable (through the external adjustment of capacitance and resistance values) sets the sampling delay period by turning on the digital switch (DG 301CJ, Siliconix, Santa Clara, CA) and grounding the integrator (A6) capacitor for the duration of the sampling delay. At the end of the sampling delay the integrator is allowed to charge, and the sampling period monostable (M2) is triggered. M2 controls the sample-and-hold circuit (AD582). Once triggered, the output of M2 goes HI causing the sample and hold circuit to sample the integrator output for  $16 \frac{2}{3}$  ms, at which point the output of M2 returns LO, and the signal is held. In this manner, the integration is allowed to proceed for  $16 \frac{2}{3}$  ms, minimizing 60 Hz noise contributions to the signal. The output of the integrator is amplified (A7) prior to the sample-and-hold

Figure III-10. Pulsed signal sampling circuit



operation. The analog-to-digital conversion takes place any time prior to the application of the next potential pulse. Figure III-11 displays an example of the timing sequence.

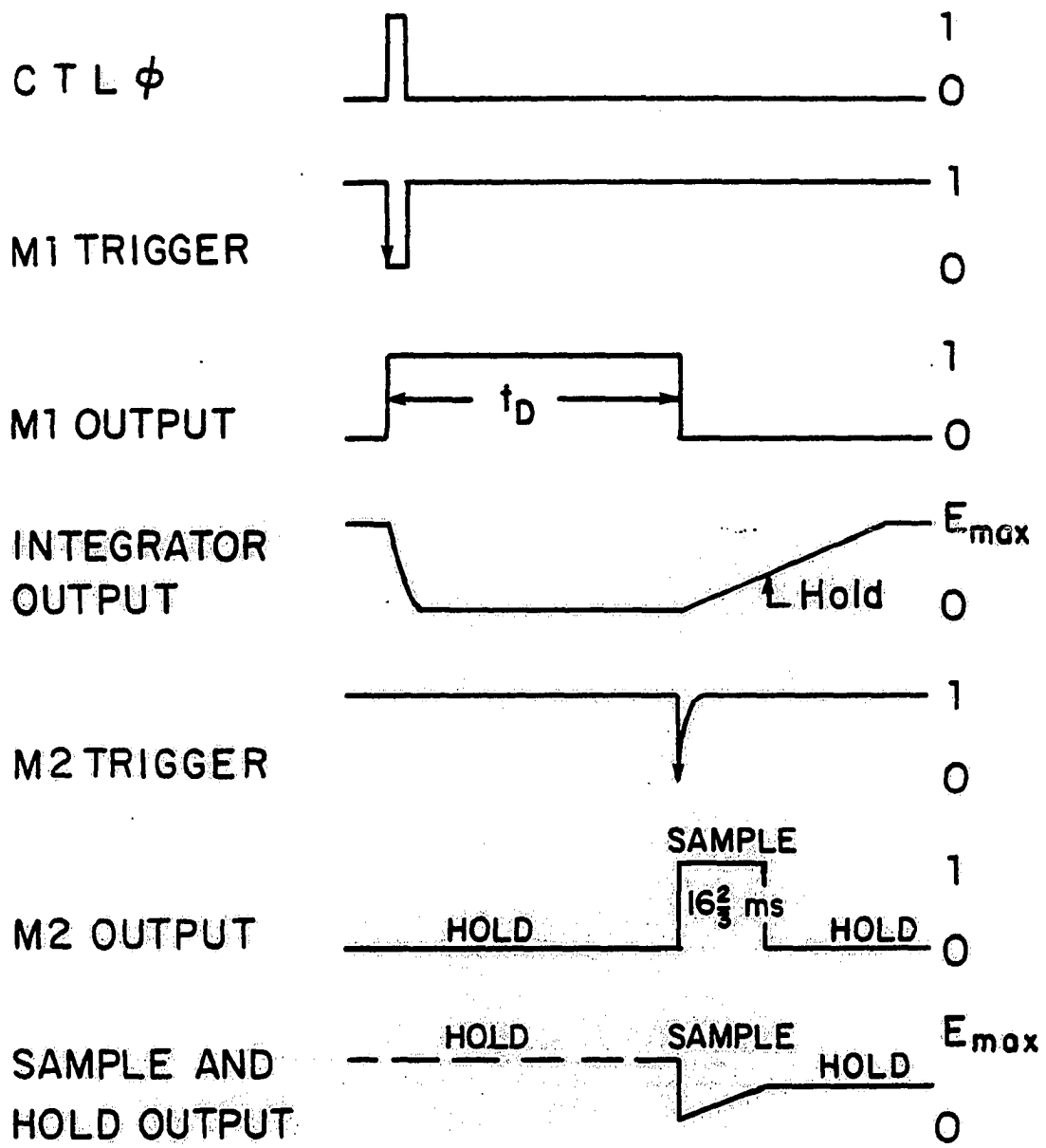
Current measurements done with the computer controlled pulsing potentiostat are noisier than similar measurement done with the Dionex UEM. Therefore, the I/P was used for the application of pulse waveforms comprised of more than three potential steps. The S/N ratio of the I/P was acceptable for these applications.

### C. Flow-Injection Apparatus

Flow injection detection was performed with a CMA-1 chromatographic module and a PMA-1 pumping module (Dionex Corp.) without the chromatographic column in the system. The PMA-1 module features a constant-flow/constant-pressure feedback system. This microprocessor controlled feedback system provides virtually pulse-free flow. A neutral guard column was placed in-line prior to the injection valve to provide sufficient backpressure (ca. 100 p.s.i.) to allow the pressure feedback system to function properly. The entire system exposes the eluent to only chemically inert nonmetallic materials. The injection sample loop volume was 50  $\mu$ l.

Figure III-11. Pulsed signal sampling circuit timing diagram





#### D. Liquid Chromatography

An AS6 anion exchange column (P/N 035391, Dionex Corp.) was used to separate both carbohydrates and amino acids. Temperature control was achieved by a circulated water jacket (Chemistry Shop). Aminoglycosides were separated on a MPIC-NS1 neutral polystyrene column (P/N 035321, Dionex Corp.). All chromatography employed the flow-injection apparatus with the column in-line.

Coupled-column chromatography was used for the separation and determination of aminoglycosides. A HPIC-CG1 cation exchange column (P/N 030831, Dionex Corp.) was used as the concentrator column. The CMA-1 module was configured to allow eluent changes and column switching (Figure VIII-4).

#### E. Chemicals

All chemicals were reagent grade. Water was distilled, demineralized, and passed through an activated carbon column prior to use. All eluents were passed through a 0.45  $\mu$ m filter prior to use. NaOH eluents used in the separations of carbohydrates and amino acids were prepared from a saturated stock solution (18M) using freshly boiled water to minimize carbonate contamination.

#### IV. ELECTROCHEMICAL SURVEY OF SELECTED COMPOUNDS

##### A. Introduction

As mentioned earlier, triple-step amperometry has been demonstrated to be a sensitive detection scheme for carbohydrates and simple alcohols (6-9). The preliminary goal of the research described in this dissertation was to expand the scope of triple step amperometric detection. This chapter describes the initial investigations done to realize this goal.

A cyclic, linear-scan voltammetry experiment at a Pt rotated disk electrode will quickly determine whether or not a compound is electroactive in a given electrolyte. Once electroactivity is ascertained, the ability to detect the compound through the use of constant (DC) amperometry is checked. If the compound is electroactive, yet DC amperometry fails (e.g. because the analytical current decays due to loss of surface activity) the compound becomes a prime candidate for pulse amperometric detection (PAD).

The following sections contain the results of preliminary investigations into the electroactivity of various groups of organic compounds and their detectability by PAD.

## B. Carboxylic Acids

Hydroxycarboxylic acids were chosen for examination to investigate the influence of the carboxylic acid group upon the easily detected alcohol moiety. No discernible difference was noted for the hydroxycarboxylic acid vs. similar aliphatic alcohols, as all the hydroxycarboxylic acids tested were electroactive.

Carboxylic acids display varied anodic activity at Pt. Formic acid is easily oxidized at any pH, while acetic acid appears to be nonelectroactive at all pH's. Anodic activity is seen for propionic acid at pH's < 7. Oxalic, malonic, and succinic acids; all dicarboxylic acids, have virtually no anodic activity at any pH. Table IV-1 contains the results of the investigation of carboxylic acid electroactivity.

## C. Amines

During the application of triple-pulse amperometry to the chromatographic analysis of urine, as described by Hughes (138), a large peak was identified as resulting from urea. No further work was done by Hughes to explore the electrochemical reactivity of the amine functionality. Hence, urea was seen as a starting point for research in this direction. Primary, secondary, and tertiary

Table IV-1. Electroactivity of selected carboxylic acids at Pt

	Compound	Structure	Result
carboxylic acids	formic acid	CHOOH	oxidized at any pH
	acetic acid	CH <sub>3</sub> COOH	not oxidized at any pH
	propionic acid	CH <sub>3</sub> CH <sub>2</sub> COOH	oxidized at < pH 7
hydroxycarboxylic acids	hydroxyacetic acid	HOCH <sub>2</sub> COOH	oxidized at any pH
	tartaric acid	(COH) <sub>2</sub> (COOH) <sub>2</sub>	oxidized at any pH
	citric acid	HOCCOOH (CH <sub>2</sub> COOH) <sub>2</sub>	oxidized at any pH
dicarboxylic acids	oxalic acid	(COOH) <sub>2</sub>	not oxidized at any pH
	malonic acid	CH <sub>2</sub> (COOH) <sub>2</sub>	not oxidized at any pH
	succinic acid	(CH <sub>2</sub> ) <sub>2</sub> (COOH) <sub>2</sub>	not oxidized at any pH

aliphatic amines were found by cyclic voltammetry to be irreversibly electroactive at Pt in basic electrolytes. The electroactivity lessened as the degree of alkyl substitution on the nitrogen increased. Table IV-2 summarizes the results.

Table IV-2. Electroactivity of selected aliphatic amines at Pt

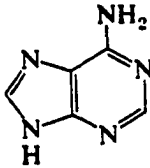
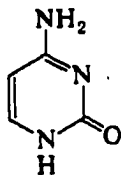
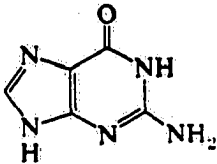
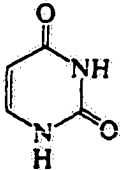
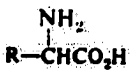
Compound	Structure	Results
urea	$\text{CO}(\text{NH}_2)_2$	oxidized at pH > 11
methyl amine	$\text{CH}_3\text{NH}_2$	oxidized at pH 13
diethyl amine	$(\text{CH}_3\text{CH}_2)_2\text{NH}$	oxidized at pH 13
tetra-ethyl amine	$(\text{CH}_3)_4\text{N}^+$	not oxidized at any pH

Combining the knowledge that both amines and some carboxylic acids were detectable made the detection of amino acids plausible. Indeed, all amino acids were found by cyclic voltammetry to be irreversibly electroactive at Pt in electrolytes of pH > 7. Proteins, heterocyclic

bases, and aminoglycosides were also found to be irreversibly electroactive at Pt in basic electrolytes. Table IV-3 lists the results of initial experimentation with various amine compounds.

With the exception of quaternary amines, PAD was successfully applied to the detection of all the amines examined, whereas DC amperometry failed due to rapid loss of sensitivity with time. PAD of amino acids, and aminoglycosides is described in Chapters VII and VIII, respectively.

Table IV-3. Electroactivity of selected amines at Pt

	Compound	Structure	Results
Hetero-cyclic bases	adenine		oxidized at pH 13
	cytosine		oxidized at pH 13
	guanine		oxidized at pH 13
	uracil		oxidized at pH 13
Amino acids			oxidized at pH > 7
Amino-glycosides		see page 125	oxidized at pH > 9
Proteins	-globulin	complex	oxidized at pH 13
	albumin	complex	oxidized at pH 13



V. THE EFFECT OF pH ON  
PULSED AMPEROMETRIC DETECTION  
AT PLATINUM ELECTRODES

For cases where a substantial background signal is present due to the formation of surface Pt oxide, the necessity of exactly matching the pH of the samples and the carrier stream to eliminate blank peaks has been noted. The exact match of pH is only critical for application of PAD to Flow-Injection Analysis (FIA) and not for liquid chromatography (LC) because for LC the solvent peak is separated from the analyte peak,

The decay of anodic current with time ( $i-t$ ) corresponding to oxide formation following a positive change in applied potential is adequately described for Pt electrodes by (141)

$$i = c\eta/t$$

where  $c$  is a constant and  $\eta$  is the applied overpotential for oxide formation. In the absence of surface active species,  $\eta$  at a constant applied potential ( $E$ ) is a function of the hydrogen ion activity ( $a_H$ ) as described by

$$\eta = E - E_0 + 0.0591p a_H$$

where  $E_0$  is a constant and  $p = -\log_{10}$ . Hence for

the evaluation of  $i$  at a fixed  $t$ , a plot of  $i$  vs.  $p a_H$  is predicted to have a slope of  $0.0591c/t$ .

Typical PAD peaks are shown in Fig. V-1 for eight successive injection of aqueous samples of NaOH into a carrier reference stream of 0.251 M NaOH. Injection of eight samples of the reference solution into the reference stream produced no peaks (central portion of Fig. V-1). A plot of anodic peak height ( $\Delta i$ ) vs.  $pC_{base}$  is shown in Fig. V-2. The value of  $\Delta i = 0$  corresponding to the injection of the reference solution,  $pC_b = pC_{b,ref}$  is indicated by the arrow. The observed linearity (slope = 133,  $s_{xy} = 1.0$  @ 90% confidence,  $r^2 = 0.9978$ ) did not extend to values of  $pC_{base}$  much beyond one-half decade, probably because of activity effects. The technique is equally applicable for pure concentrated solutions of strong acids, and data are shown for  $H_2SO_4$  in Fig. V-2 using 1.0 M as the concentration of the carrier reference stream. The linearity of the plot for  $H_2SO_4$  (slope = 72.9,  $s_{xy} = 4.7$  @ 90% confidence,  $r^2 = 0.9909$ ) is not nearly so great as for NaOH, probably because  $pC_{acid} = p a_H$  due to the second ionizable proton of  $H_2SO_4$ . The detection limit for both cases is approximately  $pH = 0.005$  (S/N = 2).

Figure V-1. Detection peaks for injection of alkaline solutions in 0.251 M NaOH

Conditions:  $V_i = 50 \mu\text{l}$   
 $V_f = 1.0 \text{ ml min}^{-1}$

Waveform:  $E_1 = 550 \text{ mV (225 ms)}$   
 $E_2 = -1300 \text{ mV (200 ms)}$   
 $E_3 = -200 \text{ mV (200 ms)}$

$pC_{\text{NaOH}}$ : (A) = 0.900  
(B) = 0.700  
(C) = 0.600  
(D) = 0.500  
(E) = 0.300

Carrier Stream:  $pC_{\text{NaOH}} = 0.600$

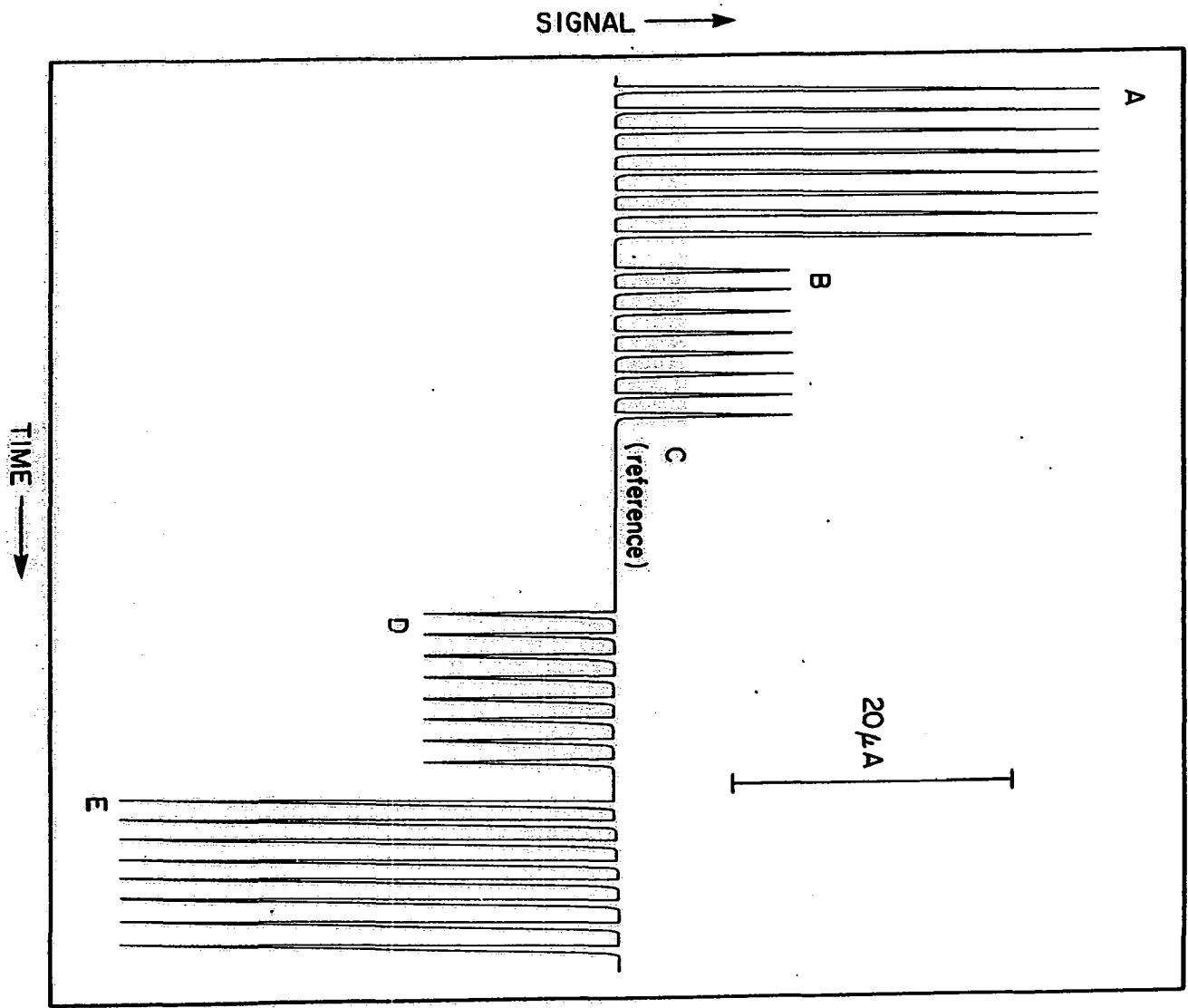
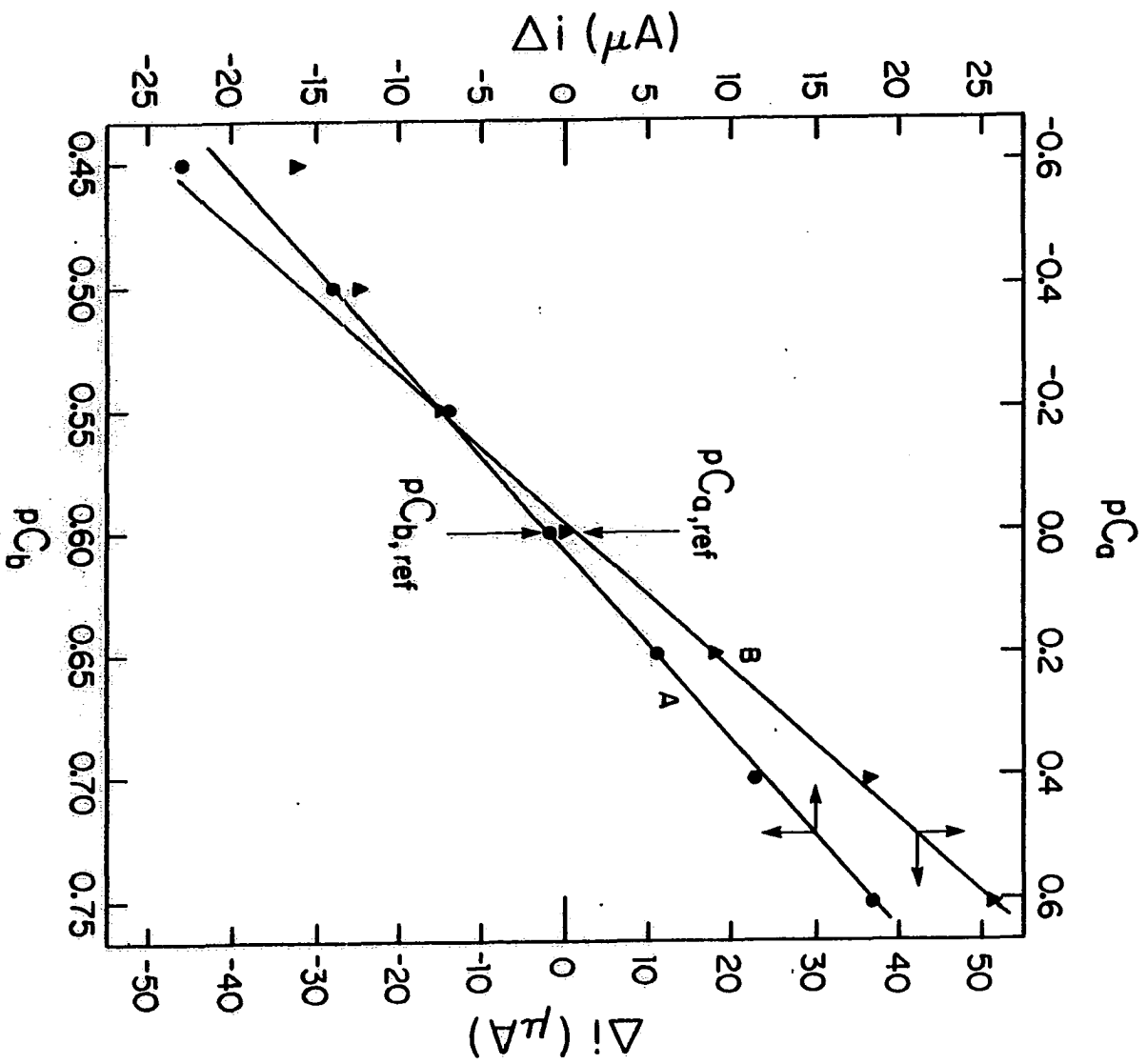


Figure V-2. Calibration curves for alkaline (A) and acidic (B) samples

Conditions:  $V_s = 50 \mu\text{l}$   
 $V_f = 1.0 \text{ ml min}^{-1}$

Waveform: (A) as in Figure V-1

(B)  $E_1 = 1400 \text{ mV (225 ms)}$   
 $E_2 = -250 \text{ mV (200 ms)}$   
 $E_3 = -150 \text{ mV (200 ms)}$



A useful application of this phenomenon is for frequent assay, by flow-injection technique, of production streams of acids and bases, especially for highly concentrated strong acids and bases for which the  $H^+$ -selective glass electrode is lacking in sensitivity. The application for quality control is most likely for the purpose of noting the occurrence of a small difference in concentration between the reference and injected solutions rather than for the quantitative determination of that difference over an extended range of concentration. Alternately, the sample solution can be pumped as the carrier stream with occasional injections of standard reference solutions. In this manner, extended range calibration curves would not be required and  $\Delta i$  vs. pC is linear.

VI. PULSED AMPEROMETRIC DETECTION  
OF ELECTROINACTIVE ADSORBATES  
AT PLATINUM ELECTRODES

A. Introduction

The oxidation of many species (i.e. amines occur at potential values positive of the value at which Pt oxide formation begins. Thus when PAD is applied to the detection of these species, the total current measured in the detection pulse results from the formation of surface oxide as well as the faradaic reaction of the adsorbed species. The large background is observed to be sufficiently stable to permit DC offset at the recorder input and sensitive determinations of very small analytical signals is still possible. The investigations of the application of PAD to such species as these led to the observation of "negative" peaks (i.e. the anodic peak current is less than the background current) if the current is sampled after a very short delay (e.g.  $\ll 100$  ms) following the detection potential pulse, whereas "positive" peaks are obtained for long delay times. This chapter will detail the present understanding of the  $i-t$  response of Pt, and show the applicability of PAD for the quantitative determination of  $\text{Cl}^-$  and  $\text{CN}^-$  in a flow-injection system. Explanation is given for the



non-linear response observed for electroactive species which has been attributed to control of the signal by the prevailing adsorption isotherm (6).

### B. Competitive Adsorption

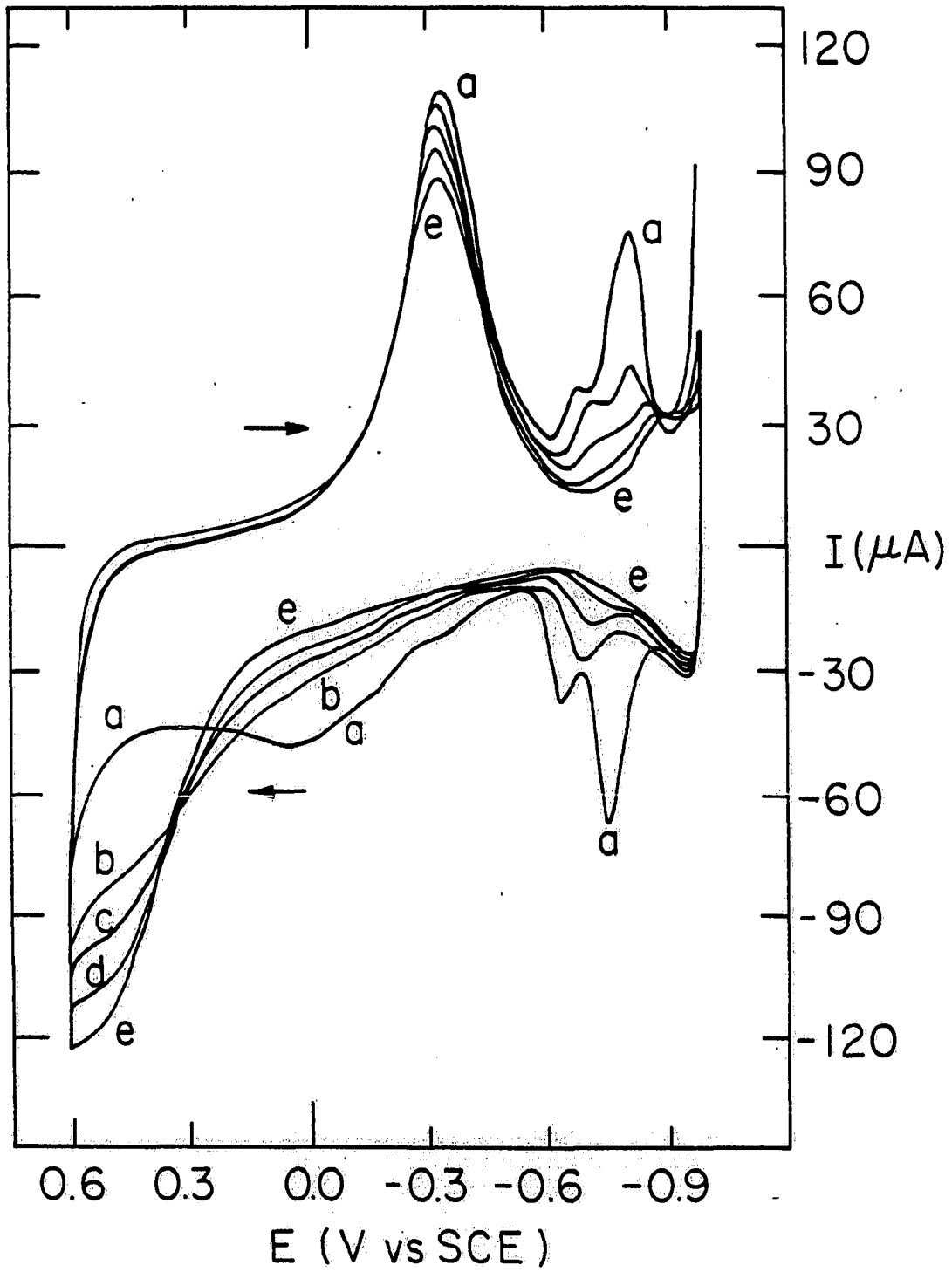
It was noted by cyclic voltammetry that adsorbed glycine in alkaline solutions suppressed the anodic current for oxide formation on a Pt electrode in the potential region just prior to that in which adsorbed glycine is oxidized. It is concluded that the adsorbed glycine inhibits the formation of oxide at the surface sites occupied by glycine molecules, and only at more energetic potential values can the glycine be oxidatively desorbed with concomitant oxide formation at the liberated Pt sites.

Since detection of glycine based on suppression of oxide formation produces rather minimal signals,  $\text{CN}^-$  was chosen as a model compound for the suppression studies due to its known ability to form stable coordination compounds with noble metal ions (142). The voltammetric response for KCN at Pt in 0.25 M NaOH is illustrated in Figure VI-1. As expected, the extent of oxide suppression is large, even for as little as 15  $\mu\text{M}$   $\text{CN}^-$ . These results are consistent with the conclusions of Angerstein-Kozłowska et al. (37), for acid solutions,

Figure VI-1. Current-potential curves for  $\text{CN}^-$  at a Pt RDE  
in 0.25 M NaOH

Conditions:  $\Phi = 6.0 \text{ V min}^{-1}$ ,  $W = 400 \text{ rev min}^{-1}$

Concentrations(M): a - 0.0, b -  $1.5 \times 10^{-5}$ ,  
c -  $1.0 \times 10^{-4}$ , d -  $4.0 \times 10^{-4}$   
e -  $8.0 \times 10^{-4}$



that it is the two reversible stages of PtOH formation which are suppressed by the adsorbate. If oxide suppression is to be observed in basic solution, the suppressing species must compete with the highly concentrated  $\text{OH}^-$  for surface sites. Thus  $\text{CN}^-$  with its strong Pt complexing strength is able to suppress oxide formation in alkaline solutions whereas  $\text{Cl}^-$  with its relatively weak complexing strength is only able to suppress the oxide growth in acidic solutions.

### C. Current Responses in the Presence of an Adsorbing Species

It becomes apparent when examining Figure VI-1 that if PAD is applied to the  $\text{CN}^-$  system, or any system that has the same tendencies for oxide suppression, there are two unique types of response depending on the detection potential (i.e. the first step of the triple-step waveform:  $E_1$ ). For  $-0.3 < E_1 < 0.15$  V, currents are larger in the absence of the adsorbate. Whereas for  $E_1 > 0.2$  V, currents are larger in the presence of the adsorbate. Cyanide displays an almost ideal suppression behavior for this work in that the charge suppressed is equal (~~±5%~~) to the additional charge passed once the delayed oxide formation is underway. It is concluded, therefore, that  $\text{CN}^-$  is not electroactive

under these conditions, and does not contribute a faradaic component to the signal obtained in the "positive" detection. An electroactive adsorbate will, of course, contribute a faradaic component to the total current observed in the region of PtO formation.

In order to exploit fully the usefulness of PAD, the  $i$ - $t$  response of the Pt electrode for a given potential step should be known. Figure VII-2 illustrates the  $i$ - $t$  responses for various systems in both acidic and basic solutions. The  $i$ - $t$  responses are dependent upon the applied potential-waveform, *i.e.* magnitude of the step from the preceding potential to the detection potential ( $E_3$  to  $E_1$  in the triple-step waveform). The  $i$ - $t$  curves for  $CN^-$  illustrate the basis for the two types of detection that are available in PAD depending upon the choice of  $E_1$  and delay time. Both "positive" and "negative" peak currents can be observed, relative to the baseline, for  $CN^-$  injected into a flowing stream of electrolyte, as demonstrated in Figure VI-3. The current varies  $< 2\%$  for 10 mV changes in potential at regions centered around both "positive" and "negative" detection potentials. The approximate baseline current resulting from the surface oxide formation in the absence of adsorbate is indicated for the two techniques.

Figure VI-2. Current-time curves for  $\text{Cl}^-$  and  $\text{CN}^-$  at Pt

Conditions: A1)  $E_1 = 720 \text{ mV}$ ,  $E_2 = 1600 \text{ mV}$ ,  $E_3 = -250 \text{ mV}$   
 $t_2 = 250 \text{ ms}$ ,  $t_3 = 250 \text{ ms}$

a -  $0.0 \text{ M Cl}^-$  in  $0.5 \text{ M H}_2\text{SO}_4$

b -  $5.0 \times 10^{-4} \text{ M Cl}^-$  in  $0.5 \text{ M H}_2\text{SO}_4$

A2)  $E_1 = 1300 \text{ mV}$ ,  $E_2 = 1600 \text{ mV}$ ,  $E_3 = -250 \text{ mV}$   
 $t_2 = 150 \text{ ms}$ ,  $t_3 = 250 \text{ ms}$

a -  $0.0 \text{ M Cl}^-$  in  $0.5 \text{ M H}_2\text{SO}_4$

b -  $5.0 \times 10^{-4} \text{ M Cl}^-$  in  $0.5 \text{ M H}_2\text{SO}_4$

B1)  $E_1 = 100 \text{ mV}$ ,  $E_2 = 700 \text{ mV}$ ,  $E_3 = -900 \text{ mV}$   
 $t_2 = 250 \text{ ms}$ ,  $t_3 = 425 \text{ ms}$

a -  $0.0 \text{ M CN}^-$  in  $0.25 \text{ M NaOH}$

b -  $5.0 \times 10^{-4} \text{ M CN}^-$  in  $0.25 \text{ M NaOH}$

B2)  $E_1 = 625 \text{ mV}$ ,  $E_2 = 700 \text{ mV}$ ,  $E_3 = -900 \text{ mV}$   
 $t_2 = 50 \text{ ms}$ ,  $t_3 = 425 \text{ ms}$

a -  $0.0 \text{ M CN}^-$  in  $0.25 \text{ M NaOH}$

b -  $5.0 \times 10^{-4} \text{ M CN}^-$  in  $0.25 \text{ M NaOH}$

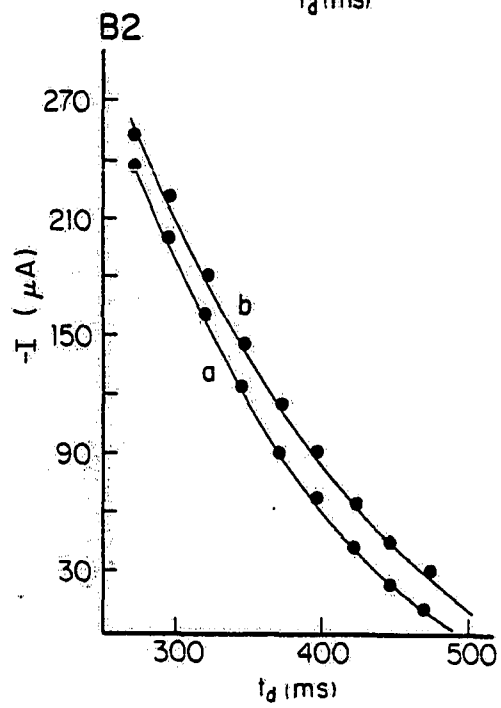
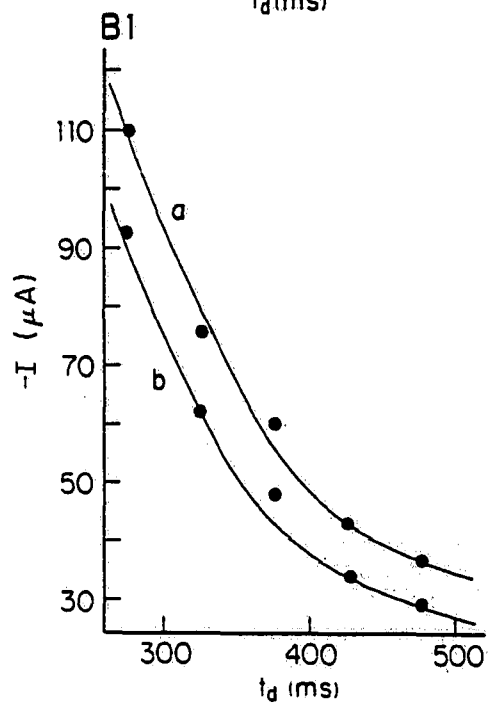
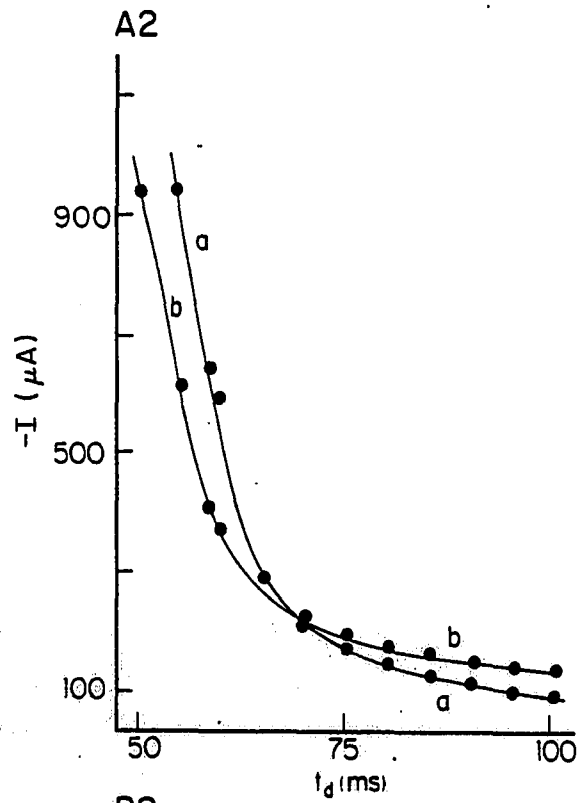
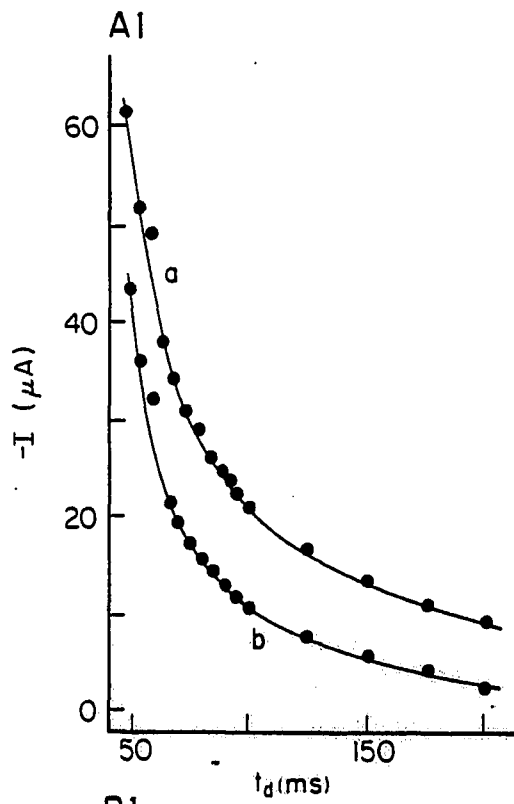


Figure VI-3. Pulsed amperometric detection of  $\text{CN}^-$  in 0.25 M NaOH

Conditions: A) Direct ("positive") detection

$$E_1 = 625 \text{ mV}, E_2 = 700 \text{ mV}, E_3 = -900 \text{ mV}$$

$$t_d = 400 \text{ ms}, t_2 = 50 \text{ ms}, t_3 = 425 \text{ ms}$$

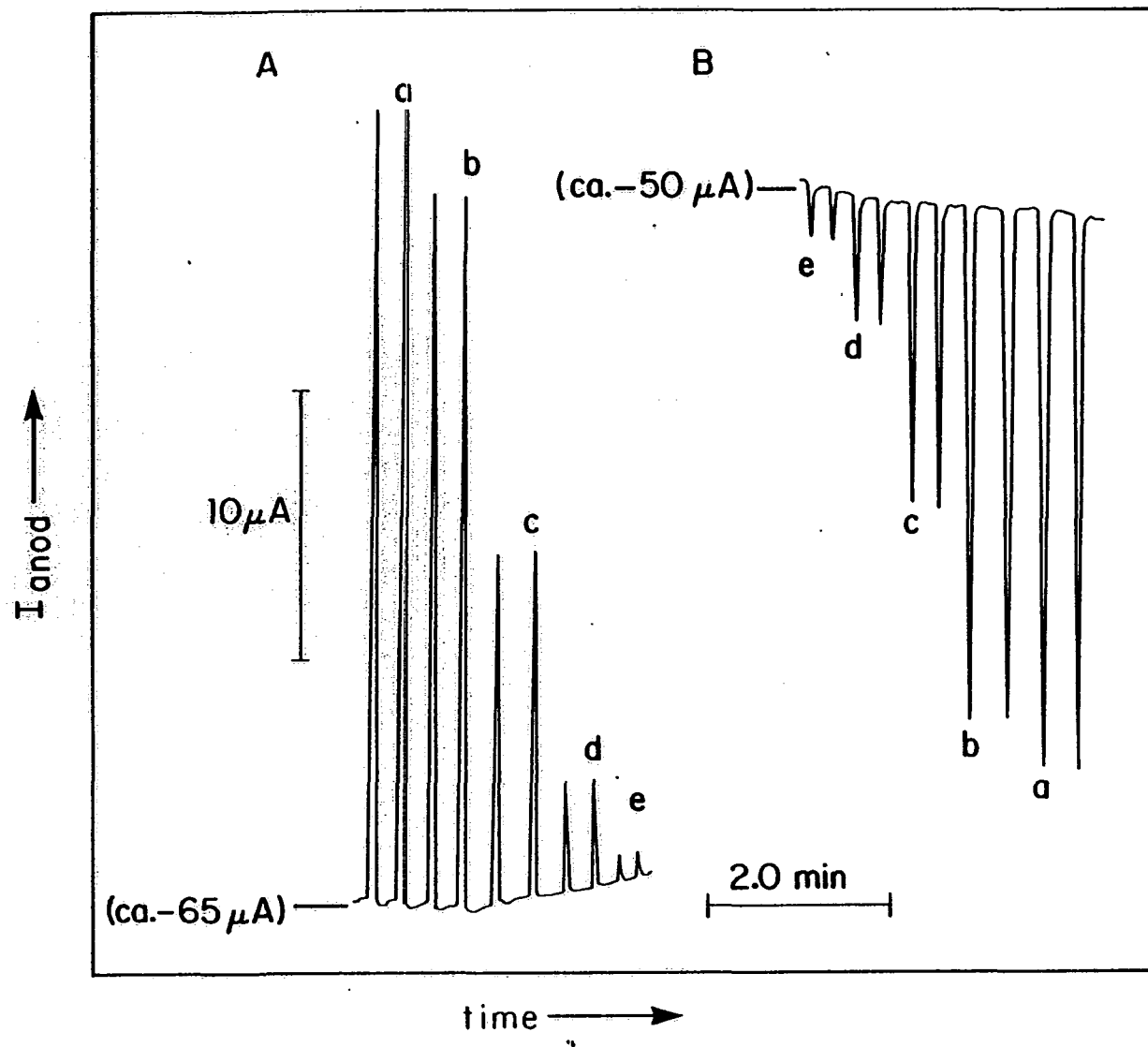
B) Indirect ("negative") detection

$$E_1 = 100 \text{ mV}, E_2 = 700 \text{ mV}, E_3 = -900 \text{ mV}$$

$$t_d = 400 \text{ ms}, t_2 = 250 \text{ ms}, t_3 = 425 \text{ ms}$$

Concentrations (M): a -  $1.0 \times 10^{-3}$ , b -  $7.5 \times 10^{-4}$   
c -  $1.0 \times 10^{-4}$ , d -  $7.5 \times 10^{-5}$   
e -  $2.5 \times 10^{-5}$





The application of PAD to the detection of  $\text{Cl}^-$  in acidic media also is feasible, concluded on the basis of the voltammetric response (Fig. VI-4). Both "positive" and "negative" peak-responses are possible, and both modes of detection were determined to be reproducible (rsd. <3%) and sensitive (lod. =  $1 \times 10^{-7} \text{M}$ , S/N = 2, in 50- $\mu\text{l}$  samples, i.e. 0.02 ng). Figure VI-5 displays an example of "negative" peaks for  $\text{Cl}^-$  detection. The "positive" detection of  $\text{Cl}^-$  for  $1.0 \text{ V} < E_1 < 1.2 \text{ V}$  is similar to the "positive" detection of  $\text{CN}^-$ . However, for  $E_1 > 1.2 \text{ V}$ ,  $\text{Cl}^-$  is oxidized to  $\text{Cl}_2$  and the peaks include a faradaic component, whereas the "positive" peaks for  $\text{CN}^-$  at  $E_1 > 1.2 \text{ V}$  do not. The potential for "negative" detection of  $\text{Cl}^-$  is significantly less than the value required for the oxidation of  $\text{Cl}^-$  to  $\text{Cl}_2$  on Pt. Hence, a faradaic current from the oxidation of  $\text{Cl}^-$  is precluded and the principle of the "negative" detection of  $\text{Cl}^-$  is identical to that of  $\text{CN}^-$ .

In the absence of an adsorbing analyte, the only contributions to the observed current resulting from an anodic potential step are the charging of the double layer and formation of  $\text{PtO}$ . Charging current is small, by comparison, and will be ignored here. The current response for oxide formation at a Pt surface free

Figure VI-4. Current-voltage curves for  $\text{Cl}^-$  at a Pt RDE in  
 $0.5 \text{ M H}_2\text{SO}_4$

Conditions:  $\phi = 6.0 \text{ V min}^{-1}$ ,  $W = 400 \text{ rev min}^{-1}$

Concentrations ( $\mu\text{M}$ ): a - 0.0, b - 1.0, c - 2.0, d - 5.0

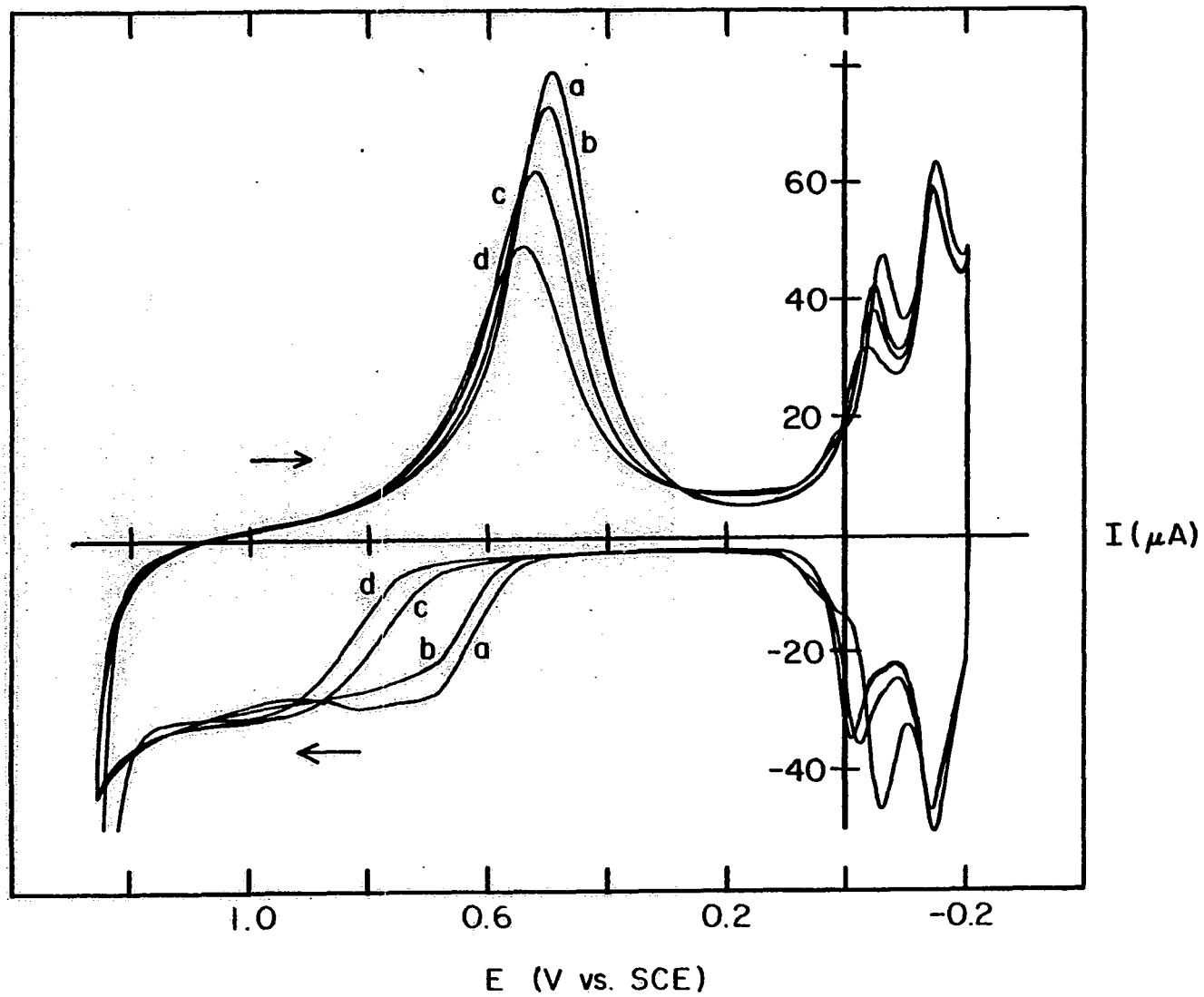


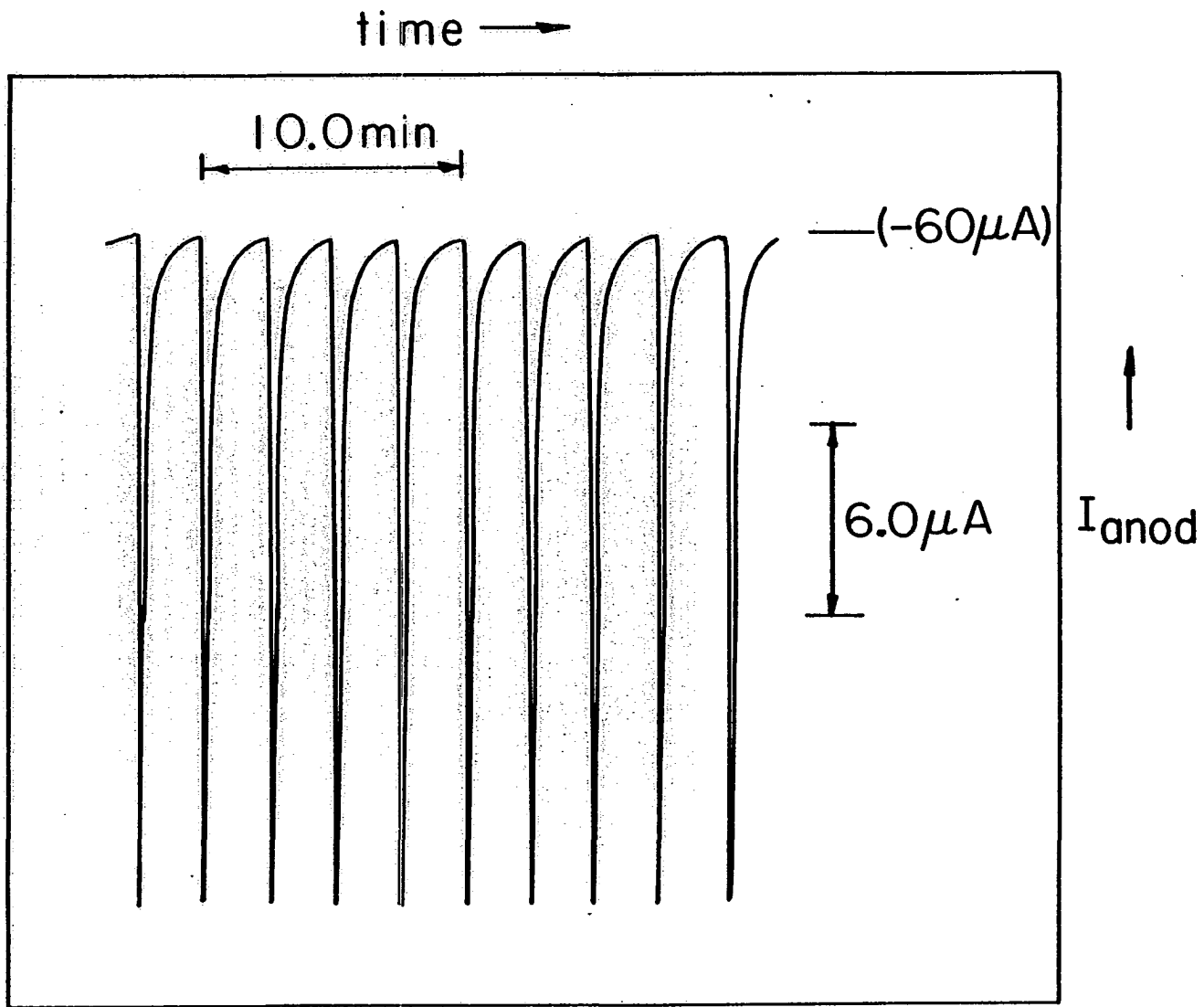
Figure VI-5. The indirect ("negative") detection of  $\text{Cl}^-$  in  $0.5 \text{ M H}_2\text{SO}_4$

Conditions:  $E_1 = 725 \text{ mV}$ ,  $E_2 = 1600 \text{ mV}$ ,  $E_3 = -200 \text{ mV}$

$t_d = 50 \text{ ms}$ ,  $t_2 = 250 \text{ ms}$ ,  $t_3 = 250 \text{ ms}$

$V_s = 50 \mu\text{l}$ ,  $V_f = 1.0 \text{ ml min}^{-1}$

Concentration:  $5.0 \times 10^{-4} \text{ M Cl}^-$  in  $0.5 \text{ M H}_2\text{SO}_4$



of adsorbate is described by Eq. (1)

$$i_{ox} = c(E-E_0)/t \quad (1)$$

where  $c$  is a constant,  $E-E_0$  is the applied overpotential for oxide formation, and  $t$  is the time after application of the potential step. Surface-oxide formation involves the conversion of adsorbed  $H_2O$  molecules at the Pt surface and Eq. (1) corresponds to the special case where  $\theta_{H_2O} = 1$  at  $t = 0$ . In the presence of an adsorbate,  $\theta_{H_2O} = 1 - \theta_{ad}$  and Eq. (1) is rewritten as

$$i_{ox} = c(E-E_0)/t \times (1-\theta_{ad}) \quad (2)$$

The formulation of Eq. (2) assumes, essentially, that the net result of an adsorbate is to decrease the effective surface area at which oxide formation occurs but does not alter the kinetics of the reaction (i.e.  $dc/d\theta_{H_2O} = 0$ ).

In the absence of adsorbates, plots of  $i_{ox}$  vs.  $1/t$  were linear, in accordance with Eq. (1). The  $i_{ox}-1/t$  plots obtained in the presence of an adsorbate are predicted to be linear only if the surface coverage by the adsorbate is constant (i.e.  $d\theta_{ad}/dt = 0$ ). Examination of the  $i$ - $E$  curve in Figure. VI-1 readily shows that adsorbed  $CN^-$  is desorbed simultaneously with oxide growth during the positive scan in the potential region  $E > 0.3$  V. Hence,  $i_{ox}-1/t$  plots, obtained by

the pulse technique in the presence of  $\text{CN}^-$ , are not expected to be linear. This was observed both for  $\text{CN}^-$  and  $\text{Cl}^-$ .

#### D. Determination of Surface Coverage

The magnitude of the "negative" detection peak, as defined by Eq. (3),

$$i_{\text{ox,sup,p}} = i_{\text{ox}} - i_{\text{ox,sup}} \quad (3)$$

results from oxide suppression and is proposed to be a measure of surface coverage by the adsorbate according to Eq. (4) where  $\theta_{\text{ad}}$  corresponds to the peak value.

$$i_{\text{ox,sup,p}} = c(E-E_0)/t - c(E-E_0)(1-\theta_{\text{ad}})/t$$

$$i_{\text{ox,sup,p}} = c(E-E_0)(\theta_{\text{ad}})/t \quad (4)$$

The relative peak surface coverage is defined as the ratio of  $i_{\text{ox,sup,p}}$  to  $i_{\text{ox}}$  for a fixed  $t$ , Eq. (5).

$$\frac{i_{\text{ox,sup,p}}}{i_{\text{ox}}} = \frac{c(E-E_0)(\theta_{\text{ad}})/t}{c(E-E_0)/t} = \theta_{\text{ad}} \quad (5)$$

under the assumption that the proportionality constant ( $c$ ) is independent of  $\theta_{\text{ad}}$ . The maximum suppression possible for oxide formation for a given adsorbate corresponds to the maximum surface coverage attainable for that adsorbate,  $\theta_{\text{ad,max}}$ . In effect, a limiting suppression current ( $i_{\text{ox,sup,max}}$ ) will be observed for a surface saturated with adsorbate ( $\theta_{\text{ad}} = 1.0$ ); this has been verified experimentally.



The decrease in  $\theta_{ad}$  for  $\text{Cl}^-$  was found to be approximately linear with time (Fig. VI-6) which is interpreted to represent zero-order kinetics with respect to  $\theta_{ad}$ , over the range of  $t$  represented in the figure, as given by Eq. (6) where  $\theta_{ad,0}$  is the value of  $\theta_{ad}$  for  $t = 0$ .

$$\theta_{ad} = \theta_{ad,0} - kt \quad (6)$$

The slope of the plot of  $\theta_{ad}$  vs.  $t$  (i.e.  $-k$ ) was determined also to increase with increasing positive values of  $E_1$ . This dependence on  $E_1$  is expected since desorption is influenced by  $\theta_{ox}$  which is, in turn, a potential-dependent quantity.

#### E. Adsorption Isotherm

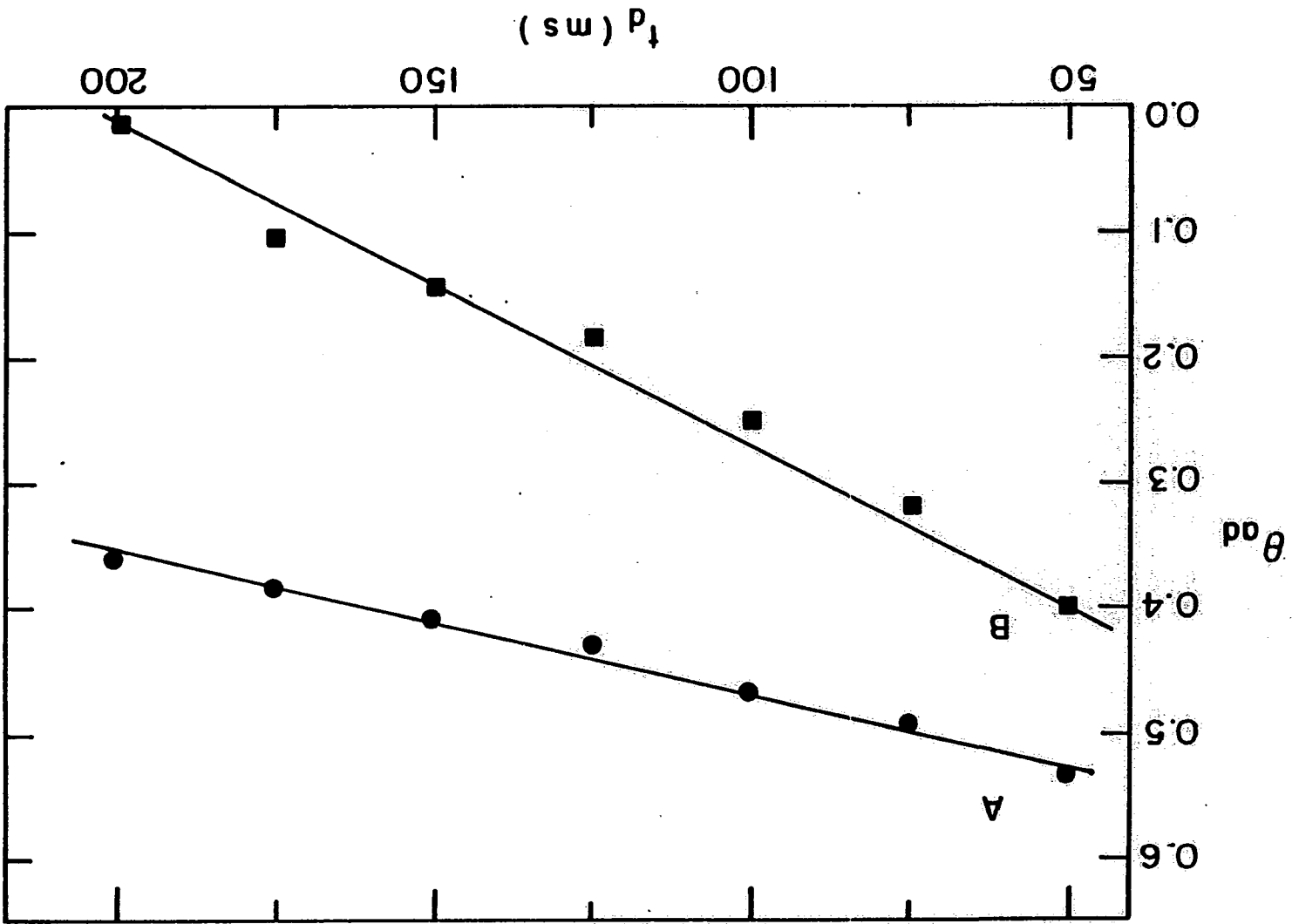
The Langmuir isotherm is considered to be the classic adsorption isotherm. Derived from first principles by Langmuir in 1918 (143), it assumes that there are no interactions between one adsorbed molecule and another, and that the surface is uniform. The rate of adsorption is assumed proportional to the fraction of unoccupied surface sites  $(1-\theta)$  and the bulk concentration of the adsorbate. The rate of desorption is assumed proportional to the fraction of occupied surface sites  $(\theta)$ . Thus

Figure VI-6. Plot of  $\theta_{ad}$  vs.  $t_d$  for  $\text{Cl}^-$  in

0.5 M  $\text{H}_2\text{SO}_4$

Conditions: A)  $E_1 = 700$  mV, remainder as in Fig. VI-5  
B)  $E_1 = 800$  mV, remainder as in Fig. VI-5

Concentration:  $5.0 \times 10^{-4}$  M  $\text{Cl}^-$  in 0.5 M  $\text{H}_2\text{SO}_4$



at equilibrium, the rates of adsorption and desorption are equated,

$$k_1(1-\theta)C = k_{-1}(\theta)$$

thus

$$\frac{\theta}{1-\theta} = KC$$

Temkin derived an isotherm based on the assumption of a non-uniform surface (144). Temkin assumed a surface on which a great many small areas have slightly varying standard free energies, at each of which the Langmuir isotherm is obeyed. The approximate form of the Temkin isotherm is

$$\theta = 1/f \ln(K_0 C)$$

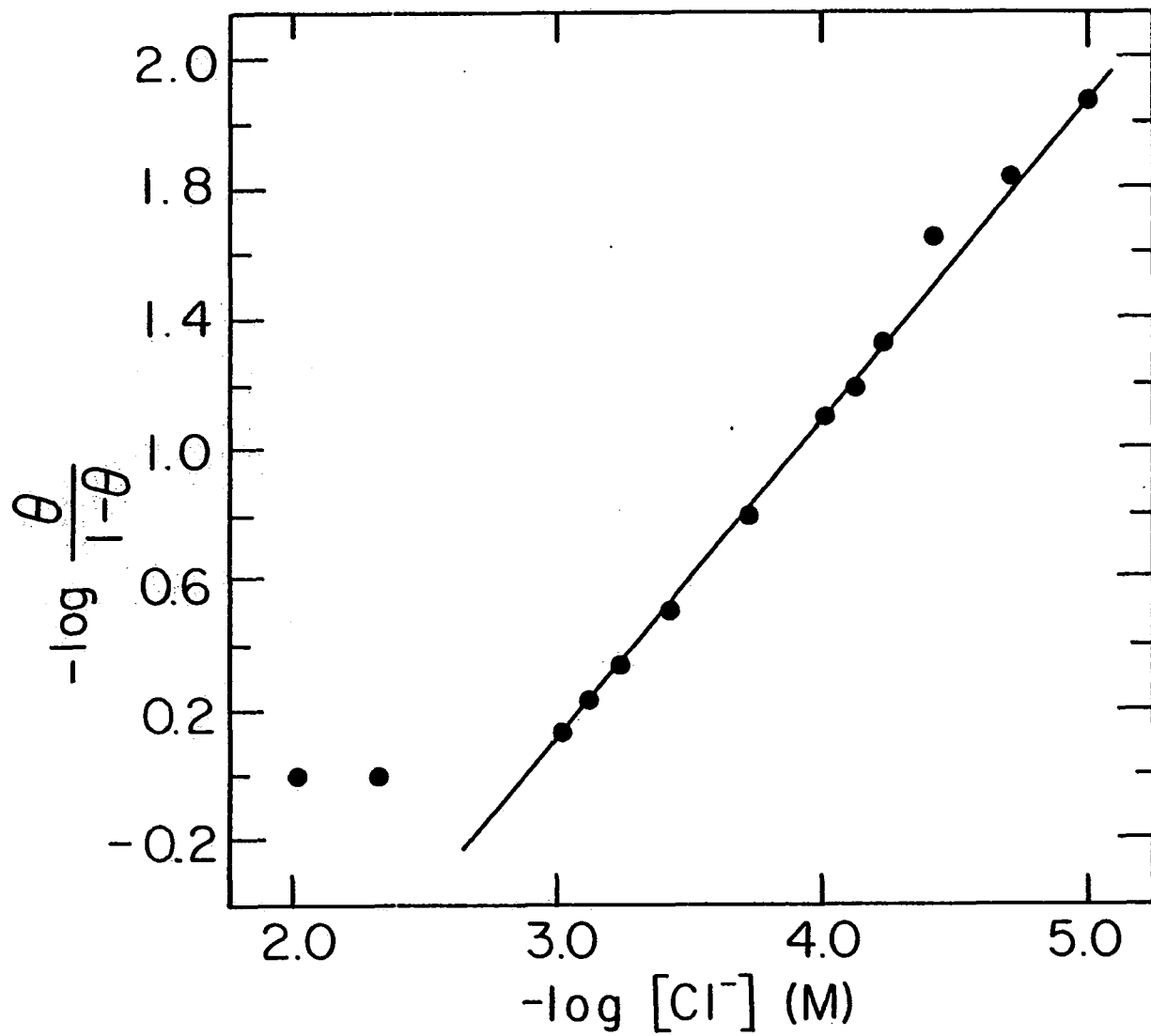
in which  $f = r/RT$ . The Temkin parameter,  $r$ , is assumed to be constant and independent of  $\theta$ .

Frumkin suggested a general isotherm which allowed long-range interactions between adsorbed species (145). The resulting isotherm is

$$\frac{\theta}{1-\theta} \exp(B\theta) = KC$$

Plots of  $i_{ox,sup,p}$  and  $\theta_{ad}$  vs.  $C$  have a distinct Langmuirian appearance. Figure VI-7 displays a plot of  $\log [\theta_{ad}/(1-\theta_{ad})]$  vs.  $\log [Cl^-]$ , which is linear with a slope of 1.0 as expected for control by the Langmuir isotherm. Only slight deviation from linearity occurs at large concentrations, which occurs

Figure VI-7. Plot of  $\log [\theta_{ad}/(1 - \theta_{ad})]$  vs.  $\log [Cl^-]$   
Conditions: as in Fig. VI-5



due to lateral interactions of the adsorbate for  $\theta_{ad} = 1$ .

The initial rate of adsorption for a species with fast adsorption kinetics at a uniformly accessible electrode (e.g. single crystal) is expected to be limited by mass transport. Likewise,  $\theta_{ad}$  (Eq. 5) measured for short adsorption times (i.e. the duration of  $E_3$ :  $t_3$ ), is expected to be proportional to the bulk concentration ( $C_b$ ) and  $t_3$ . This proportionality was not observed for the  $Cl^-$  system; the increase of  $t_3$  beyond 50 ms had no effect to increase the surface coverage. The integrated transport-limited flux to the electrode surface, calculated on the basis of measurements for an electroactive analyte ( $I^-$ ), requires  $t_3 \gg 1$  s to achieve the peak value of  $\theta_{ad}$  observed for  $Cl^-$  with  $t_3 = 50$  ms. However, the amount of analyte present in the diffusion layer at  $t_3 = 0$  must be considered. The integrated diffusion-limited flux to the surface during depletion of the diffusion layer (assuming a planer electrode) is calculated as follows:

$$\begin{aligned}
 N_{tot,dif} &= \int_0^{t_3} D \frac{dC}{dx} \Big|_{x=0} dt \\
 &= \int_0^{t_3} \frac{D^{1/2} C_b}{(\pi t)^{1/2}} dt
 \end{aligned}$$

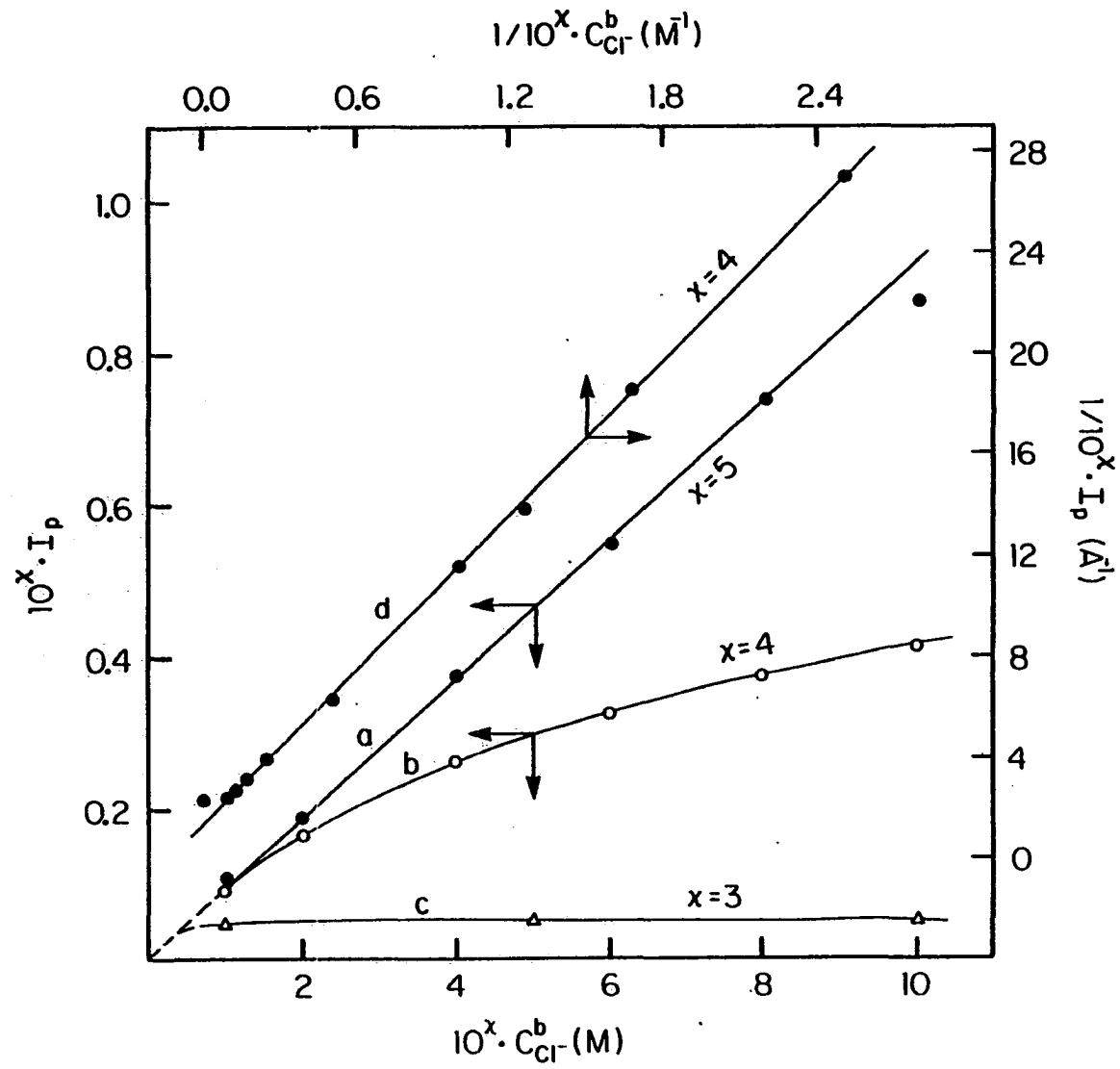
$$\begin{aligned}
&= \frac{D^{1/2} C^b}{\pi^{1/2}} t_3^{1/2} \\
&\approx \frac{2(10^{-5} \text{ cm}^2/\text{s})^{1/2} 10^{-7} \text{ mol/cm}^3}{(3.14)^{1/2}} t_3^{1/2} \\
&\approx 10^{-10} \text{ moles/cm}^2 \text{ (for } t_3 = 100 \text{ ms)}
\end{aligned}$$

Since a monolayer of  $\text{Cl}^-$  is about  $5 \times 10^{-9}$  moles/cm<sup>2</sup>, it is concluded that the majority of the  $\text{Cl}^-$  adsorbed at the reduced Pt surface originates from the diffusion layer. It is also concluded that a portion of the  $\text{Cl}^-$  adsorbed at the reduced Pt surface remains at the oxide-covered surface even for  $E_2$  in the region of  $\text{O}_2$  evolution for short  $t_2$ . This had not been anticipated. Evidence for the adsorption of  $\text{Cl}^-$  on PtO in anodic regions exists from radiochemical studies (146,147). If the oxidative cleaning process at  $E_2$  is not 100% effective, the adsorbed  $\text{Cl}^-$  will carry over into the next detection cycle. Also,  $\text{Cl}_2$  produced by the oxidative cleaning that does not diffuse from the electrode surface is reduced to  $\text{Cl}^-$  during the cathodic potential step ( $E_3$ ) and is available for adsorption. In FIA experiments, peak tailing is still present after many equivalent sample volumes of carrier stream have passed through the detector. Such tailing (Fig. VI-4) is not a result of the sample diffusion



Figure VI-8. Calibration curves for the direct ("positive") detection of  $\text{Cl}^-$  in 0.5 M  $\text{H}_2\text{SO}_4$

Conditions:  $E_1 = 1300 \text{ mV}$ ,  $E_2 = 1600 \text{ mV}$ ,  $E_3 = -250 \text{ mV}$   
 $t_d = 50 \text{ ms}$ ,  $t_2 = 150 \text{ ms}$ ,  $t_3 = 250 \text{ ms}$



profile and is attributed to the carry-over of  $\text{Cl}^-$ . Positive absolute errors occur if repetitive sample injections are closely spaced in time. It is concluded that it is by the depletion of the diffusion layer and through carry-over that Langmuir adsorption control of the current response for detection of  $\text{Cl}^-$  is observed for small  $t_3$  for both the "negative" and "positive" detection techniques.

For the case in which  $\text{Cl}^-$  is detected at potentials at which oxide formation and  $\text{Cl}^-$  oxidation occur simultaneously, plots of  $i_{\text{ox,p}}$  vs.  $C$ , are not linear. However, plots of  $\log[\theta_{\text{ad}}/(1-\theta_{\text{ad}})]$  vs.  $\log C$  are linear and it is concluded again that detection control is by Langmuir-type adsorption. As expected, a plot of  $1/i_p$  vs.  $1/C$  is linear (Fig. VI-8). This is significant in light of the fact that calibration plots for the PAD detection of carbohydrates, amino acids, and sulfur compounds are nonlinear, whereas plots of  $1/i$  vs.  $1/C$  are linear (148). It is concluded that the current response of these compounds is governed in the same manner as the responses for  $\text{Cl}^-$ .

VII. THE DIRECT ELECTROCHEMICAL DETECTION OF  
AMINO ACIDS AT A PLATINUM ELECTRODE IN  
AN ALKALINE EFFLUENT

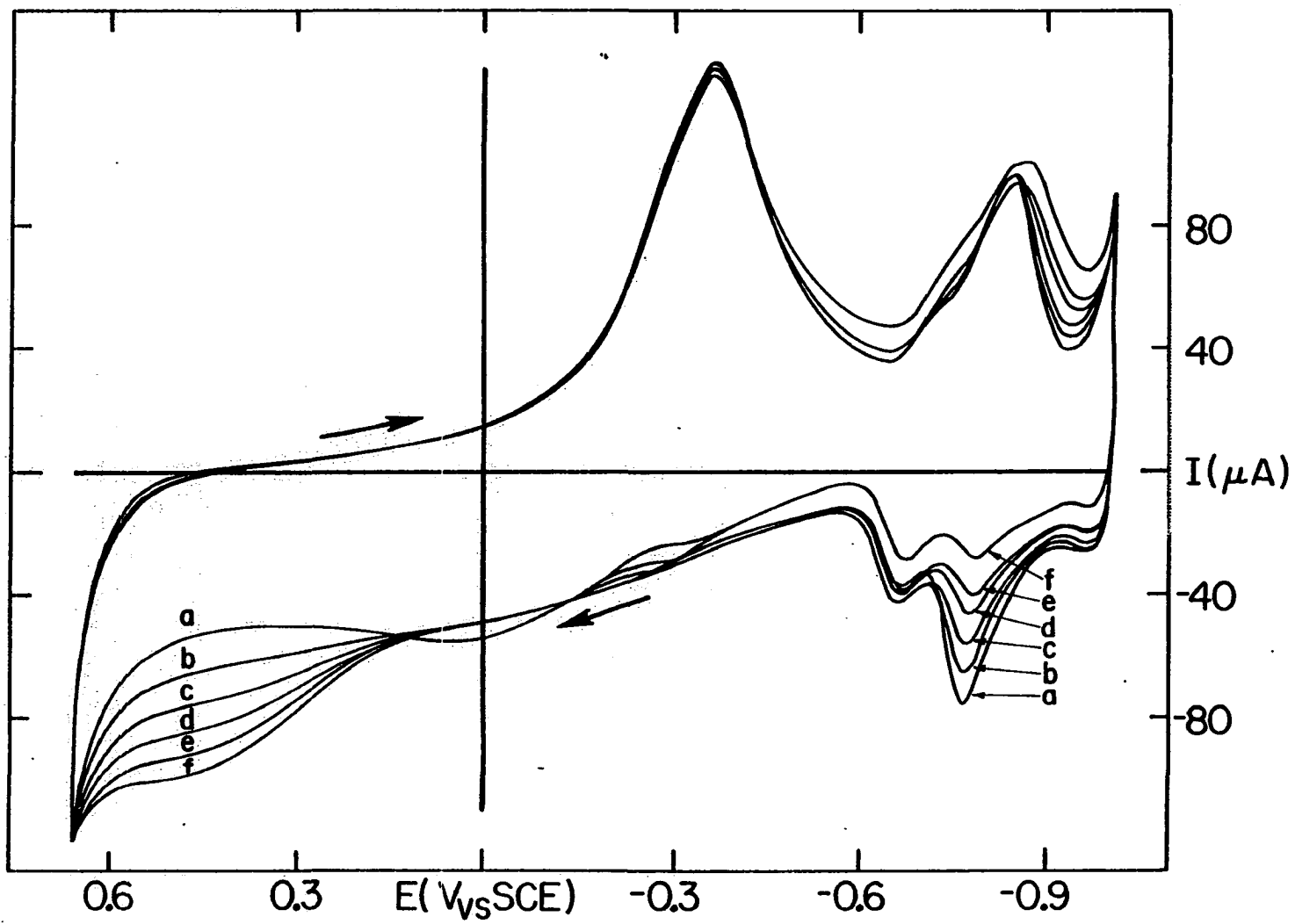
A. Cyclic Voltammetry

The voltammetric responses of amino acids at Pt electrodes in 0.25 M NaOH are illustrated adequately by the I-E curves for glycine obtained for a cyclic, linear-scan of potential as shown in Figure VII-1 for the Pt RDE. The residual response of the electrode (curve a) obtained in the absence of the amino acid is characterized by an anodic wave during the positive scan for  $E > -0.3$  V which corresponds to the formation of the oxide layer (PtOH and PtO). Rapid evolution of  $O_2$  (g) occurs for  $E > 0.6$  V. The oxide layer is cathodically reduced on the negative potential scan to produce the peak at  $-0.3$  V. The cathodic and anodic peaks in the region  $-0.6$  to  $-0.9$  V correspond to the electrochemical production and dissolution, respectively, of adsorbed atomic hydrogen. Rapid evolution of  $H_2$  occurs for  $E < -0.9$  V. Additions of the amino acid result in a decrease in the quantity of adsorbed atomic hydrogen which can be produced during the negative potential scan. This is explained if the amino acid is adsorbed at the electrode surface thereby depleting the number of available Pt sites.

Figure VII-1. Current-potential curves for glycine by cyclic, linear-scan voltammetry at a Pt RDE

Conditions: 0.25 M NaOH,  $\phi = 7.2 \text{ V min}^{-1}$ ,  
 $W = 400 \text{ rev min}^{-1}$

Concentrations (mM): a - 0.00, b - 0.050, c - 0.15,  
d - 0.35, e - 0.70, f - 1.20



Oxidation of the adsorbed amino acid produces an anodic wave on the positive potential scan in the region  $E = 0.3$  to  $0.6$  V, with the current increasing as a nonlinear function of the bulk concentration of the amino acid ( $C_b$ ). There is virtually no evidence for oxidation of the amino acid on the subsequent negative potential scan in the region  $E = 0.6$  to  $0.3$  V.

The anodic wave for the amino acid obtained on the positive potential scan was determined to vary in height as a linear function of the rate of potential scan and to be virtually independent of the rotational velocity of the RDE. Such behavior is consistent with the conclusion that the oxidation is a surface-controlled reaction.

Furthermore, the oxide film produced on the positive potential scan to  $0.65$  V prevents further detection of the amino acid on the negative potential scan.

Optimum detection of the amino acids occurs in electrolytes of  $\text{pH} > 13$ . However, detection is quite feasible in electrolytes of  $\text{pH} > 7$ .

#### B. Triple-step Waveform

Various triple-step potential waveforms were developed on the basis of the I-E curves in Figure VII-1. Two such waveforms are described in Table VII-1.

Table VII-1. Description of two triple-step potential waveforms for detection of amino acids at Pt electrodes in 0.25 M NaOH

Wave-form	Step	Potential (V)	Period (ms)	Function
A.	1	$E_1 = 0.50$	$t_1 = 250$ $t_d = 200$	anodic detection delay before sampling
	2	$E_2 = -.89$	$t_2 = 425$	reduction/adsorption
	3	$E_3 = 0.78$	$t_3 = 050$	anodic activation
B.	1	$E_1 = 0.55$	$t_1 = 200$ $t_d = 150$	anodic detection delay before sampling
	2	$E_2 = 0.75$	$t_2 = 150$	oxidative cleaning
	3	$E_3 = -.90$	$t_3 = 425$	reduction/adsorption

The potential required to oxidize the amino acids is significantly more positive than required for alcohols and carbohydrates in the same alkaline medium. Hence, the coverage of the electrode surface by oxide at the respective detection potentials is substantially greater for amino acids than for carbohydrates, and the corresponding residual current is slow to decay to a negligible value. The residual current is large for short delay periods ( $t_d$ ) prior to the analytical signal sampling. It was initially expected that long delay periods would be required to allow the residual current to decay to a negligible value so that sensitive current



measurement is feasible. This expected need for a long delay period can be obviated by the use of a large value for  $E_3$  with the step back to the detection potential  $E_1$  (i.e., waveform A). For  $E_3 > E_1$ , the oxide coverage produced during the short period  $t_3$  is greater than the equilibrium coverage for potential  $E_1$ . Hence, the step from  $E_3$  to  $E_1$  results in the immediate relaxation of oxide growth. Electrochemical reduction of PtOH and PtO does not occur at  $E_1$  and, therefore, the residual current is negligible after several milliseconds. The potential step from  $E_1$  to  $E_2$  does result in the rapid reduction of the oxide layer followed by the adsorption of unreacted amino acids from the bulk solution. Clearly, the surface-controlled oxidation of amino acids commences immediately upon the potential step from  $E_2$  to  $E_3$ . The analytical success obtained for these waveforms results because the period for decay of the faradaic current for the amino acids is slow relative to the combined time periods  $t_3 + t_d$ .

The initial assumption that the residual current must decay to a negligible value proved incorrect. It was found that the large background from the residual current is sufficiently stable to permit sensitive determinations of very small analytical signals. Thus, it was possible

to use waveforms similar to waveform B, with a DC offset at the recorder.

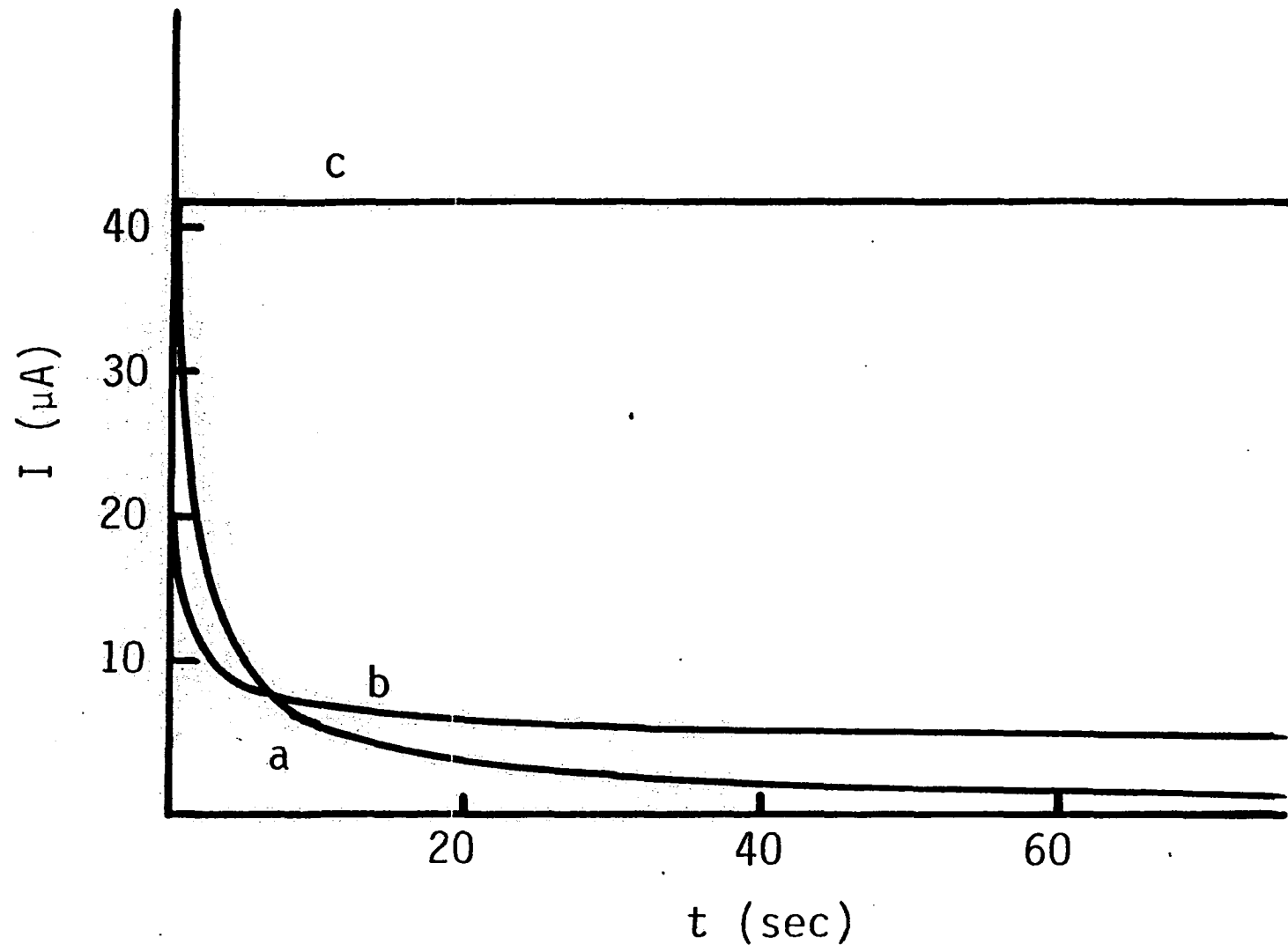
The difficulty associated with application of surface-controlled reactions for amperometric detection at a constant applied potential is illustrated for glycine in Figure VII-2. Prior to recording the current-time (*i-t*) data, the potential of the Pt RDE was cycled repeatedly in the manner used for obtaining Figure VII-1. The final scan was terminated at the negative limit, the potential was stepped to 0.5 V and the *i-t* curve recorded. The anodic signal in the presence of the amino acid (curve b) decreased rapidly. The residual response in the absence of the amino acid (curve a) is shown for comparison. The *i-t* curve for glycine is also shown in Figure VII-2 which was obtained using the triple-step waveform A (curve c); no pretreatment of the electrode was needed in conjunction with curve c. No decrease of the signal was observed over a 10 minute period. It should be noted that curve c actually contains a significant background current which was offset relative to curves a and b by a DC offset applied at the recorder.

There exists no one universal set of optimum potential and time parameters for the triple-step waveform. The waveform parameters can be optimized for a given experimental condition (e.g. known electrolyte

Figure VII-2. Current-time curves for glycine at a Pt RDE

Conditions: 0.25 M NaOH,  $W = 400 \text{ rev min}^{-1}$ ,

Curves: a - 0.00 mM glycine,  $E = 0.50 \text{ V}$ ; b - 0.50 mM glycine,  $E = 0.50 \text{ V}$ ; c - 0.50 mM glycine, waveform A



composition, detector configuration and electrode area), but upon changing a condition (e.g. changing detector cell design) the parameters will need further minor optimization. General effects of changing specific waveform parameters have been empirically determined and lead to the the following guidelines for the optimization of a potential waveform.

1. The potential sequence of waveform B (Table VII-1) is recommended, as this sequence was found to be universally applicable.
2.  $E_3$  must be sufficiently negative to cause rapid reduction of the oxide formed during  $t_2$ . Increasing  $t_3$  allows longer adsorption times, therefore larger responses. A plateau is usually reached at  $t_3 > 400$  ms.
3.  $E_2$  must be sufficiently positive to cause oxidative cleaning, yet not cause excessive  $O_2$  evolution leading to bubbles at the electrode surface. Bubbling is generally observed to occur for  $t_2 > 250$  ms.
4.  $E_1$  and  $t_d$  have a reciprocal relationship. Plots of  $i_p$  vs.  $t_d$  display maxima that shift to shorter  $t_d$  for more positive  $E_1$  values.

The response PAD has for one amino acid relative to another will usually not change as the parameters change, only absolute sensitivity will change. Therefore, when PAD is applied to chromatography, multiple chromatograms of the sample, recorded using slightly different waveforms will all have the same relative shape; only the current sensitivity will change.

### C. Flow-Injection Analysis

The waveforms are applied at a frequency of ca. 1 Hz which is sufficient for the "continuous" monitoring of a flowing stream. Waveforms were applied for the detection of various amino acids in the flow-through detector under conditions of flow-injection detection with repeated injections of 50 ul samples of the amino acids. The concentration of NaOH in the samples and the carrier stream was 0.25 M. Representative results are shown in Figure VII-3 for glycine. Over short time periods (3 hrs) precision is satisfactory for all amino acids by the flow-injection technique with a relative standard deviation < 3%. Figure VII-4 shows PAD's response for glycine recorded over a seven hour period. The illustrated response is for a detector that had been unused for one month prior to the experiment. The recording of the detector response was started

Figure VII-3. Peaks obtained for glycine over a short time span by flow-injection with PAD

Conditions: 0.25 M NaOH, 1.0 ml min<sup>-1</sup>  
0.50 mM glycine, 50 μl injections  
waveform B

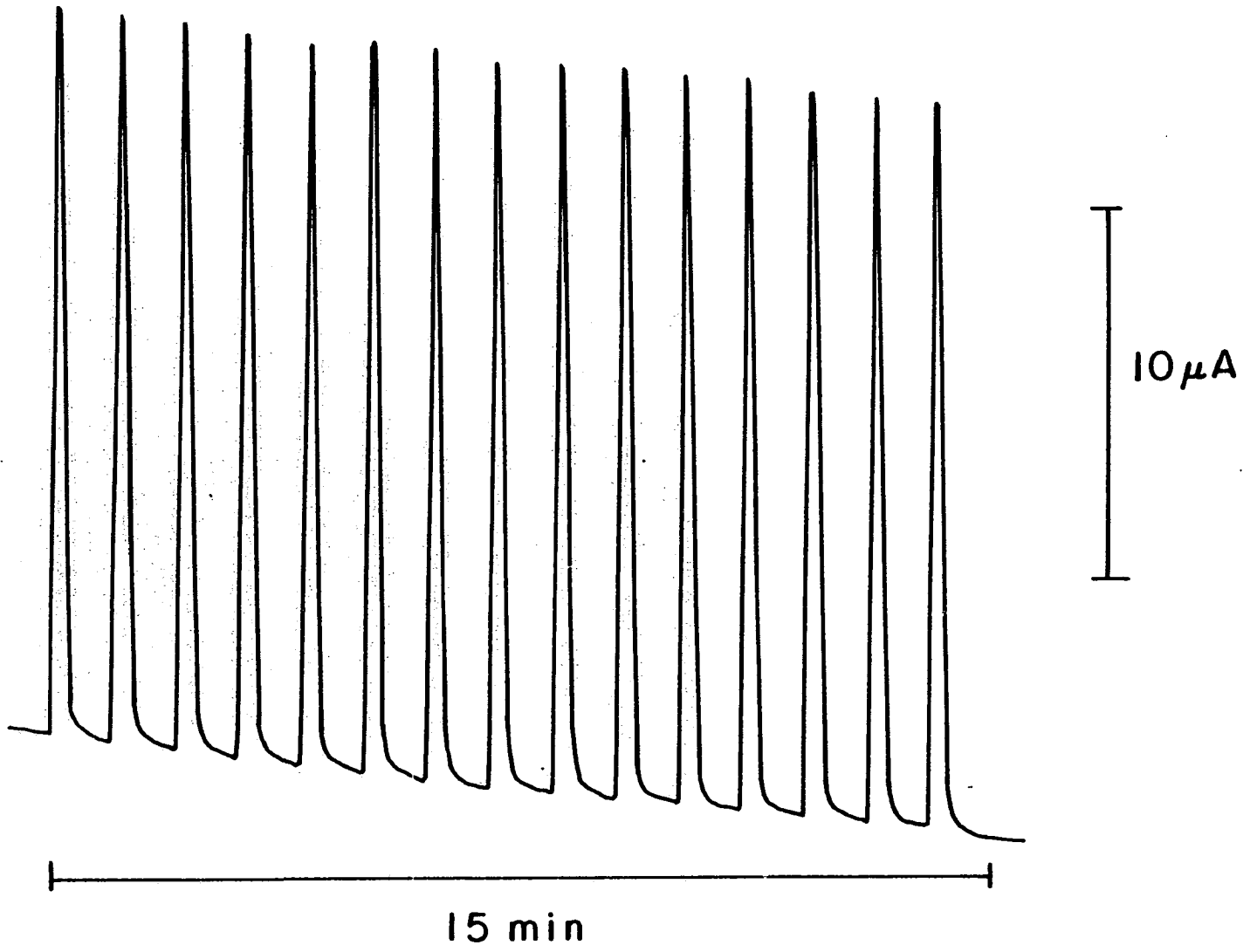
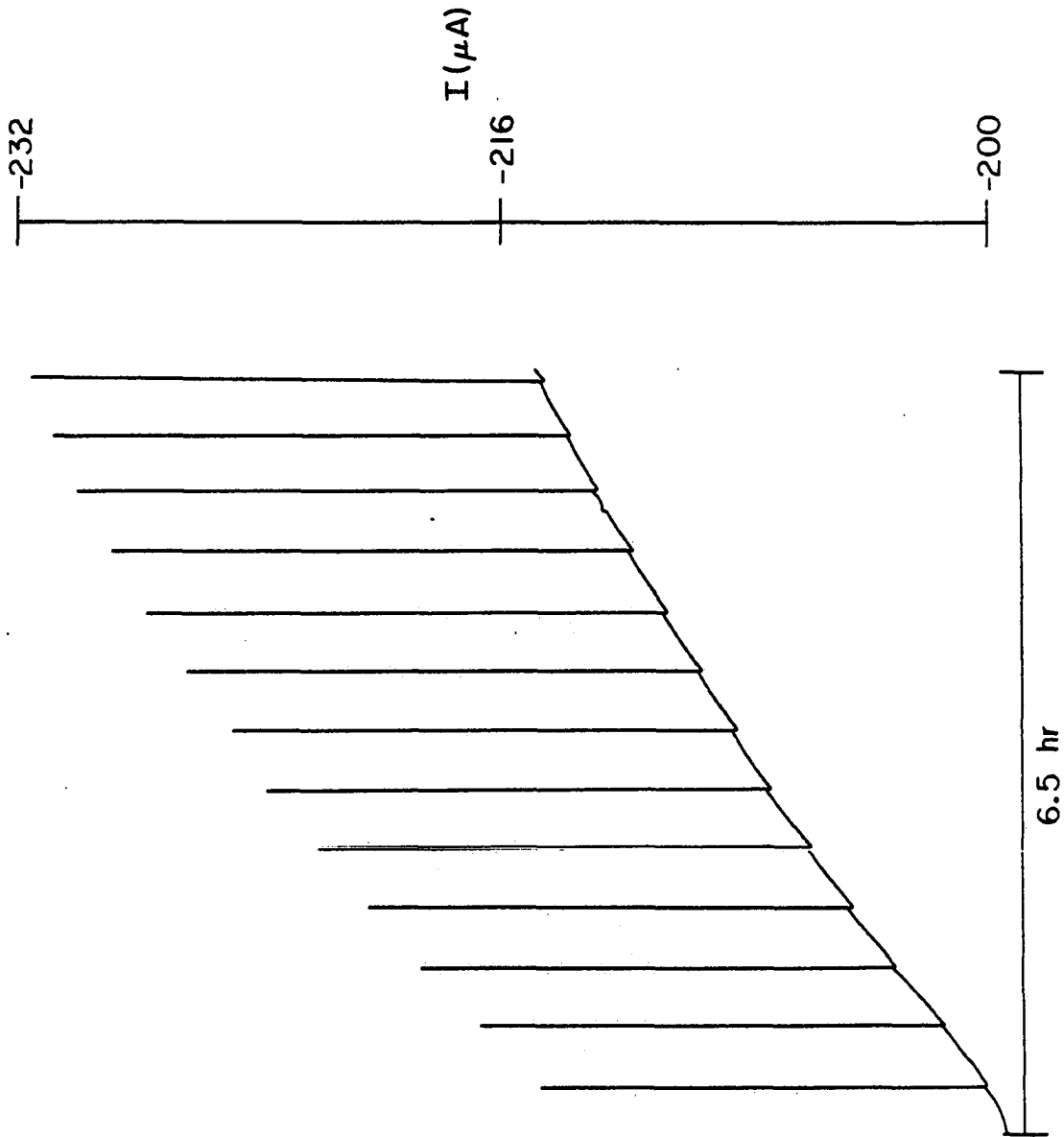




Figure VII-4. Peaks obtained for glycine over a long time span by flow-injection with PAD

Conditions: 0.25 M NaOH, 1.0 ml min<sup>-1</sup>  
0.50 mM glycine, 50 ul injections  
waveform B



immediately after the initial power-up. The rsd. of the peak heights is 5% overall. The rsd. decreases to < 3% after several hours of operation. Subsequent use of this detector showed that the baseline drift lessened as the detector use continued.

For the purpose of comparing the relative sensitivity for various amino acids, the responses for 20 amino acids normalized with respect to glycine are contained in Table VII-2.

Table VII-2. Relative sensitivities of 20 amino acids normalized to glycine

---

Electrolyte: 0.25M NaOH at 0.5 ml min<sup>-1</sup>  
Amino acids: 50  $\mu$ l, 5.0 x 10<sup>-4</sup> M

Amino Acid	Rel. Sens.	Amino Acid	Rel. Sens.
alanine	0.85	leucine	0.50
B-alanine	1.1	lycine	1.4
arginine	2.0	methionine	1.6
asparagine	1.3	phenylalanine	1.8
cysteine	1.3	proline	0.32
cystine	1.0	serine	1.1
glutamic acid	0.44	threonine	1.1
glycine	1.00	tryptophan	1.9
histadine	1.8	tyrosine	1.5
hydroxyproline	0.58	valine	0.40
isoleucine	0.47		

---

## D. Calibration

Calibrated plots for glycine ( $i_{\text{peak}}$  vs.  $C_b$ ), prepared from data obtained by the flow-injection technique, approached linearity at low concentrations ( $C_b < 0.6$  mM) but deviated significantly at higher concentrations (Fig. VII-5). This behavior is the same as that observed for the detection of alcohols and carbohydrates (6-8) by the triple-step technique, and is concluded to be the consequence of a reaction mechanism in which only adsorbed species are detected (see Chapter VI). Hence, the anodic signal is proportional to the surface coverage ( $\theta$ ) of the adsorbed analyte. Based on the Langmuir isotherm, which is expected to be valid for  $\theta \ll 1$  (small  $C_b$ ), plots of  $1/i_{\text{peak}}$  vs.  $1/C_b$  are predicted to be linear. This prediction is verified by the data in Figure VII-6 for glycine.

An attempt was made to ascertain "n"; the number of electrons participating in the electrochemical oxidation of glycine. Depending upon the assumption of a saturated surface coverage, n was found to range between 1 and 10. Adsorptional displacement experiments (see Chapter II) indicate that the saturated surface coverage ( $\theta_{\text{max}}$ ) is approximately 0.1. Based upon this  $\theta_{\text{max}}$ , n is approximately 10. If it is assumed that there exists

Figure VII-5. Calibration curves ( $i_{\text{peak}}$  vs.  $C_b$ ) for glycine by flow-injection with PAD

Conditions: 0.25 M NaOH,  $1.0 \text{ ml min}^{-1}$   
50  $\mu\text{l}$  injections, waveform B

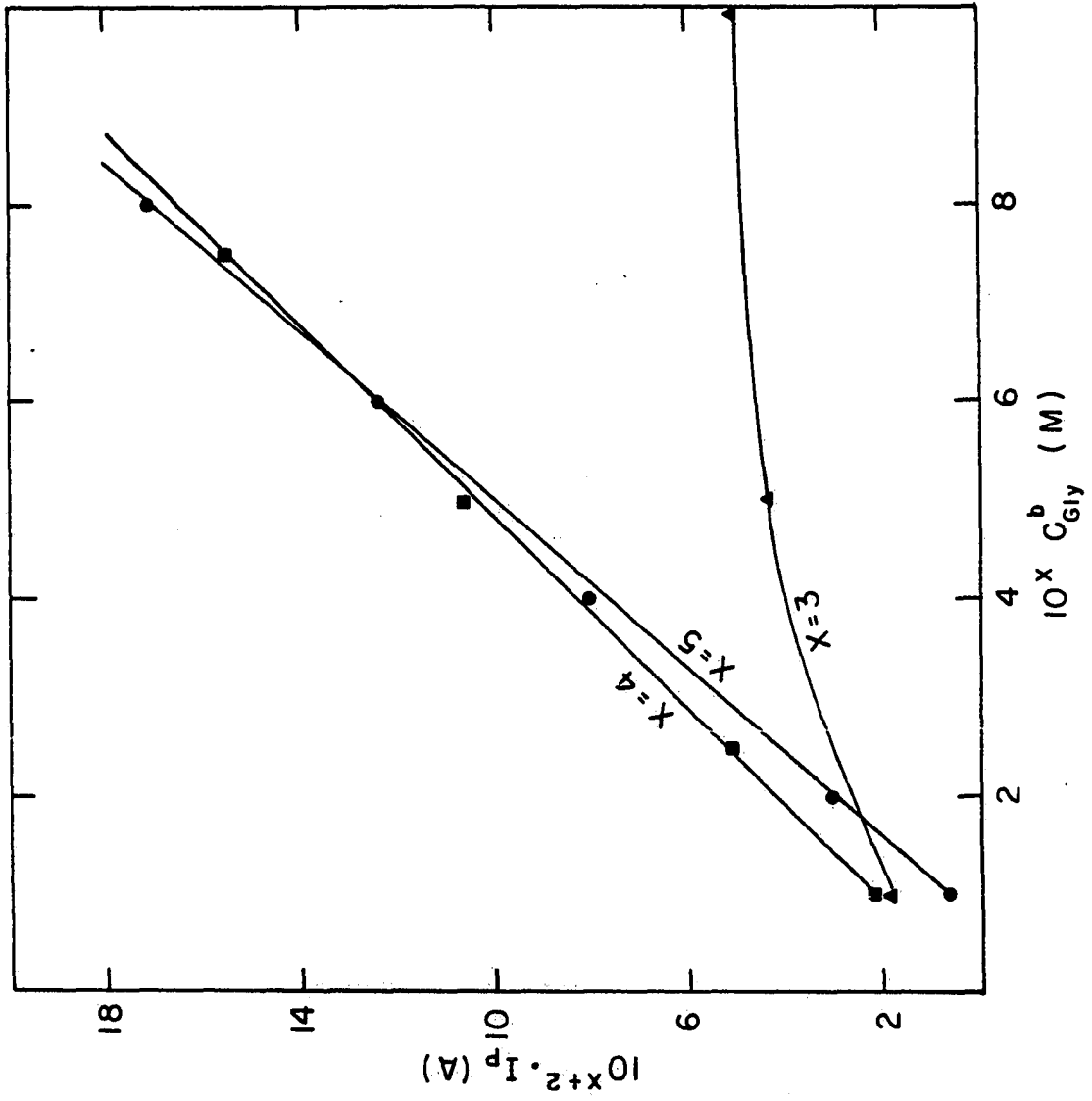
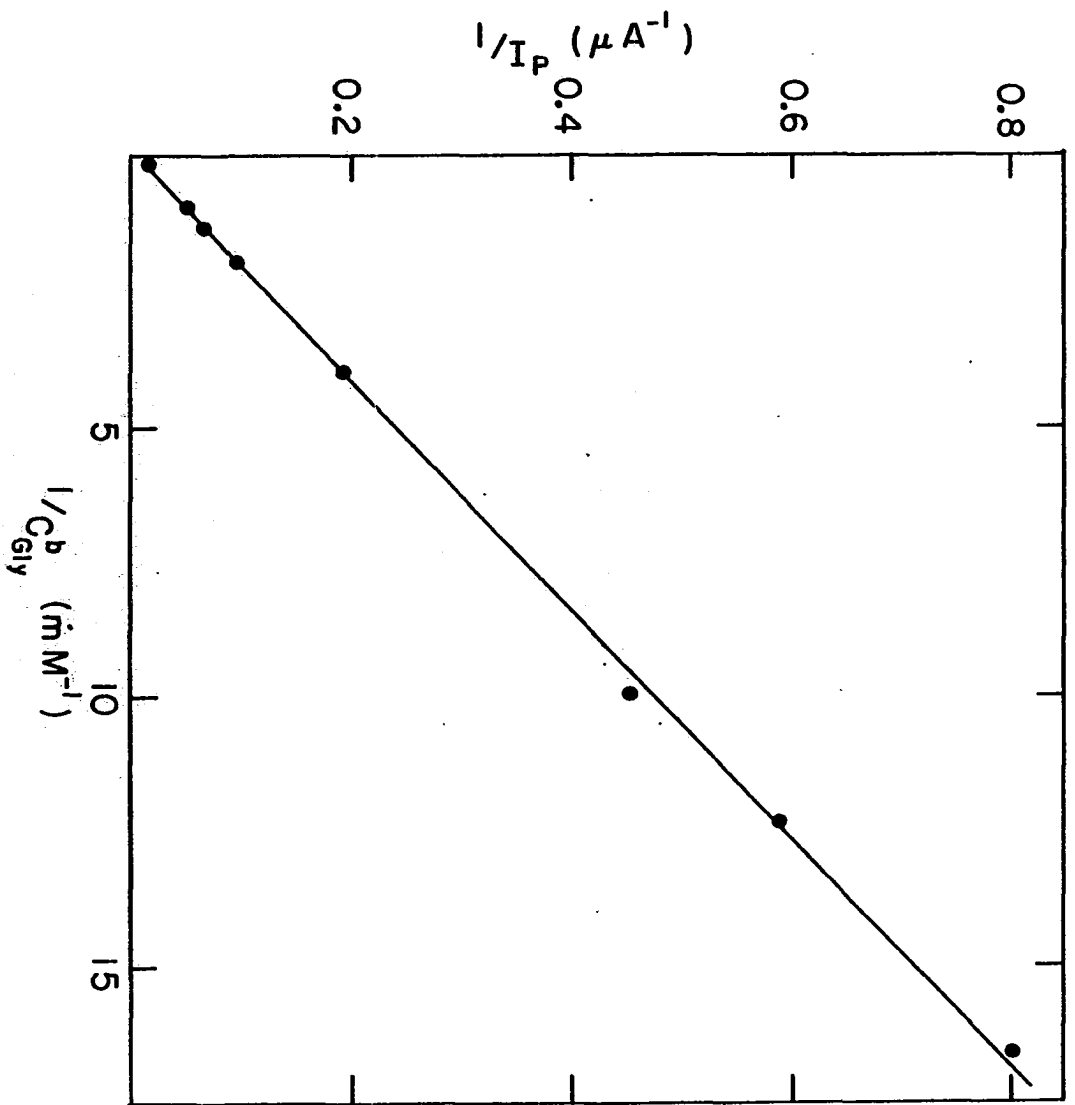


Figure VII-6. Calibration curve ( $1/i_{\text{peak}}$  vs.  $1/C_b$ ) for glycine by flow-injection with PAD

Conditions: 0.25 M NaOH,  $1.0 \text{ ml min}^{-1}$   
50  $\mu\text{l}$  injections, waveform B





a one to one Pt:glycine ratio ( $\theta_{\max} = 1$ ), then  $n = 1$ . Both of these assumptions have weaknesses. A  $\theta_{\max}$  of 1 is unlikely due to the size of glycine. A  $\theta_{\max}$  of 0.1 is also unlikely, as it would be expected that the saturated surface coverage would be higher than 0.1. The adsorptional displacement measurement of  $\theta_{\max}$  may be unreliable. The cathodic peaks for  $H^+$  are observed to shift negative rather than only decrease in magnitude. This indicates that the reduction of adsorbed  $H^+$  is being made more unfavorable by the presence of glycine. Rather than actually reducing the surface coverage of the adsorbed  $H^+$ , glycine may coordinate the  $H^+$  in close proximity to the surface. This coordinated  $H^+$  would still be reduced, and would cause  $\theta_{\max}$  to appear low. Therefore,  $\theta_{\max}$  is probably greater than the indicated value of 0.1. The determination of  $n$  will only be possible with the ability to accurately determine  $\theta_{\max}$ .

#### E. Liquid Chromatography

The applicability of PAD for amino acids in the flow-through detector is further demonstrated in Figures VII-7 and VII-8 for the chromatographic separation of a synthetic mixture of selected amino acids. It should be

Figure VII-7. Chromatogram of selected amino acids using PAD

Conditions: Column: Dionex AS6, 40° C  
Eluent: 0.25 M NaOH, 0.6 ml min<sup>-1</sup>  
Sample: 50 µl, 1.0 mM for each amino acid  
Waveform: A

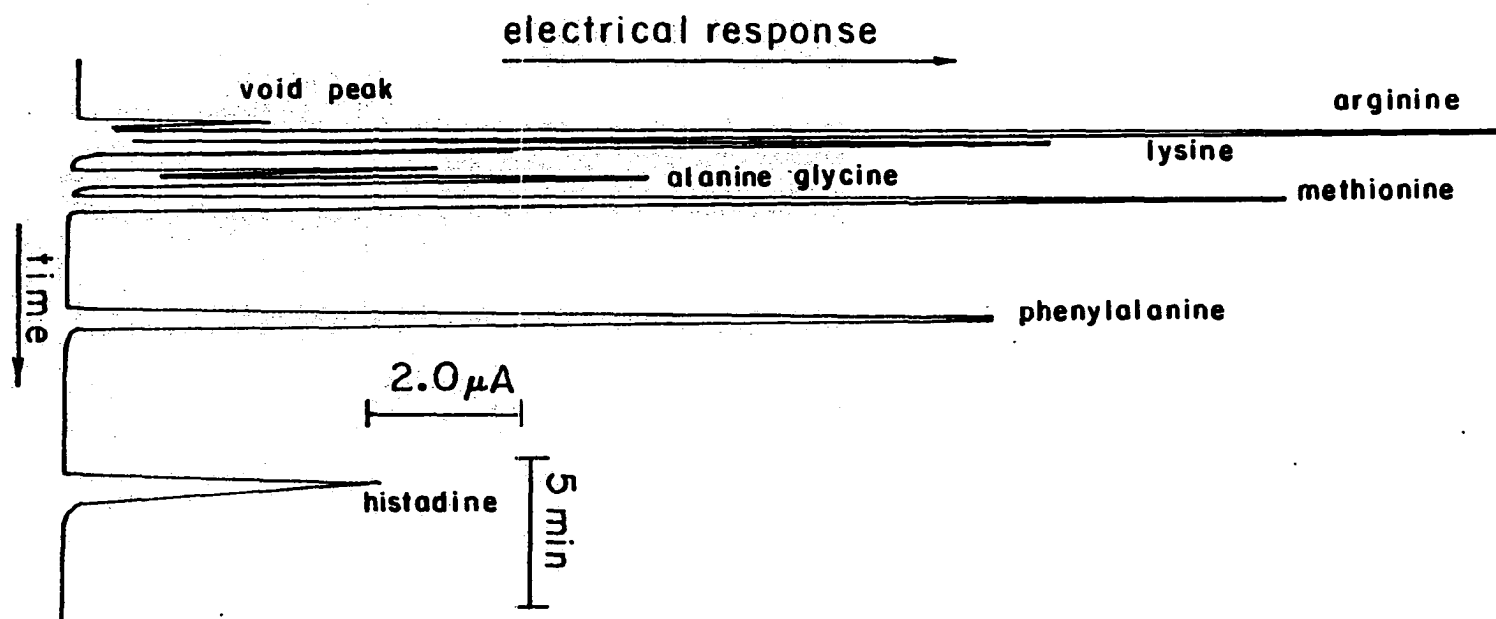
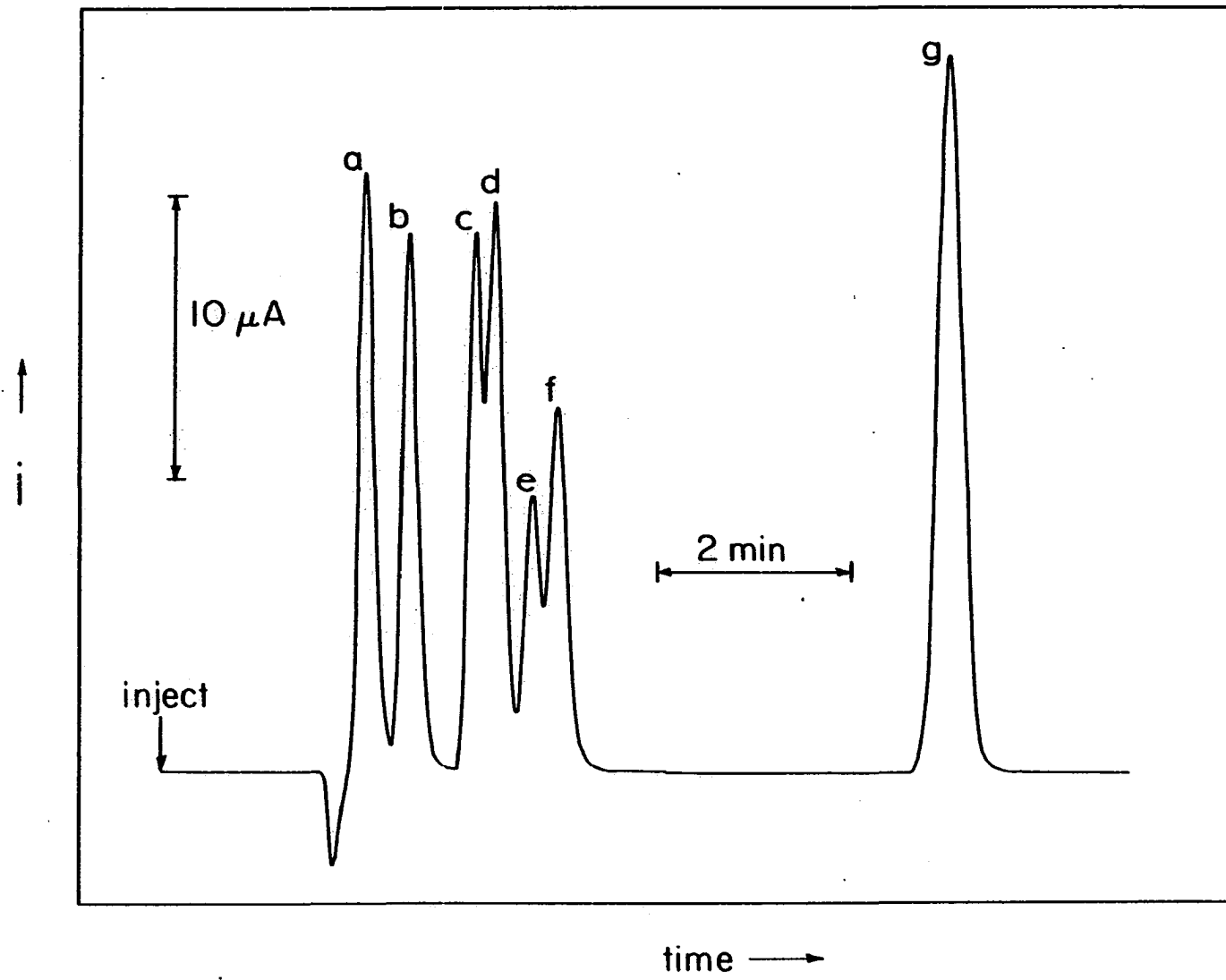


Figure VII-8. Chromatogram of amino acids

Conditions: Column: Dionex AS6, 40°C  
Eluent: 0.15 M NaOH, 0.7 ml min<sup>-1</sup>  
Sample: 50 µl  
Waveform: B  
Peaks: a - 20 ppm arg, b - 25 ppm lys  
c - 20 ppm asn, d - 50 ppm thr  
e - 100 ppm pro, f - 70 ppm hpr  
g - 60 ppm phe



noted that proline and hydroxyproline, both secondary amines, give good responses using PAD.

Table VII-3 lists capacity factor ( $k'$ ) values of 14 amino acids for four eluent compositions. Baseline resolution can be achieved for a mixture of approximately eight amino acids (arg, lys, ala, pro, gly, hpr, ser, phe) in 35 minutes using 0.05 M NaOH as the eluent. It should be emphasized with regard to Table VII-3 and Figures VII-7 that the feasibility of direct electrochemical detection of amino acids is being stressed and not the quality of the separation. Improved exchangers are presently being developed by the Dionex Corporation.

Table VII-3. Values of  $k'$  for 14 amino acids

---

Column: Dionex AS6

$$k' = \frac{t_R - t_o}{t_o}$$

AA	0.25M NaOH	0.1M NaOH	0.05M NaOH	0.01M NaOH 0.001M Borate
ala	0.38	0.89	1.48	1.73
arg	0.09	0.16	0.15	0.07
asn	0.34	0.87	1.60	1.57
gly	0.45	1.09	2.03	1.78
hpr	0.32	1.30	2.30	2.33
ile	0.38	0.89	1.50	1.10
leu	0.38	0.89	1.48	1.10
lys	0.17	0.39	0.65	0.67
met	0.59	1.07	1.86	1.44
phe	1.51	3.3	6.11	5.36
pro	0.47	1.08	1.83	1.99
ser	0.55	1.39	2.66	2.13
thr	0.38	0.89	1.33	0.97
val	0.37	0.88	1.20	0.90

---

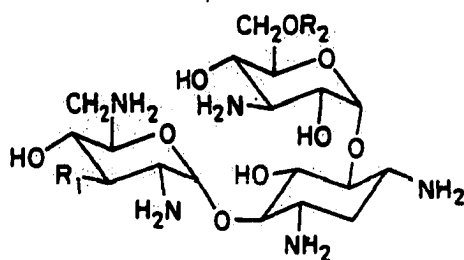
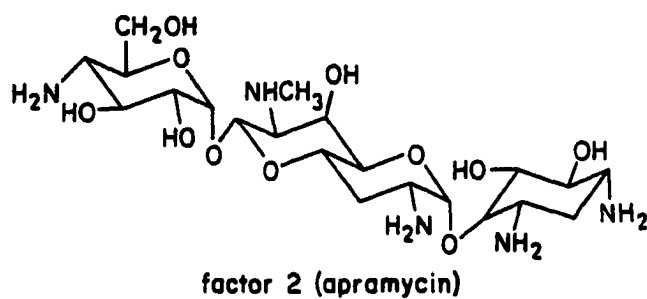
VIII. LIQUID CHROMATOGRAPHIC SEPARATION  
OF AMINOGLYCOSIDES WITH PULSED  
AMPEROMETRIC DETECTION

A. Introduction

Nebramycin factors are a group of closely related aminoglycosides which are produced by fermentation of Streptomyces tenebrarius (149). The structures of the nebramycin factors used in this work are illustrated in Figure VIII-1. The nebramycin factors 6 and 2, also known as tobramycin and apramycin, respectively, are important antibiotics. Their production by fermentation usually results in a complex mixture of the various nebramycin factors plus a variety of products commonly associated with growth of the producing microorganism. The ability to monitor the nebramycin factors in the fermentation broth as well as their determinations in biological fluids is desirable. Single-column and coupled-column chromatography combined with PAD are demonstrated here for the separation of these compounds, as well as the determination of tobramycin and apramycin in blood serum. Novel chromatographic conditions employ the alkaline electrolyte (0.25 M NaOH) necessary for the sensitive detection as the chromatographic effluent. This allows for direct monitoring of the chromatographic effluent by



Figure VIII-1. Structure of nebramycin factors

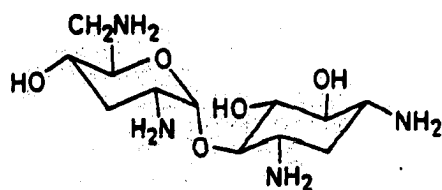


factor 4, R<sub>1</sub>=OH, R<sub>2</sub>=CONH<sub>2</sub>

factor 5 (kanamycin B), R<sub>1</sub>=OH, R<sub>2</sub>=H

factor 5', R<sub>1</sub>=H, R<sub>2</sub>=CONH<sub>2</sub>

factor 6 (tobramycin), R<sub>1</sub>=H, R<sub>2</sub>=H



PAD, eliminating the need for cumbersome post-column addition of reagents. The coupled-column technique allows for on-line sample preconcentration and pretreatment, if necessary. In this manner, the blood serum was analyzed with deproteination and filtration as the only pre-injection step.

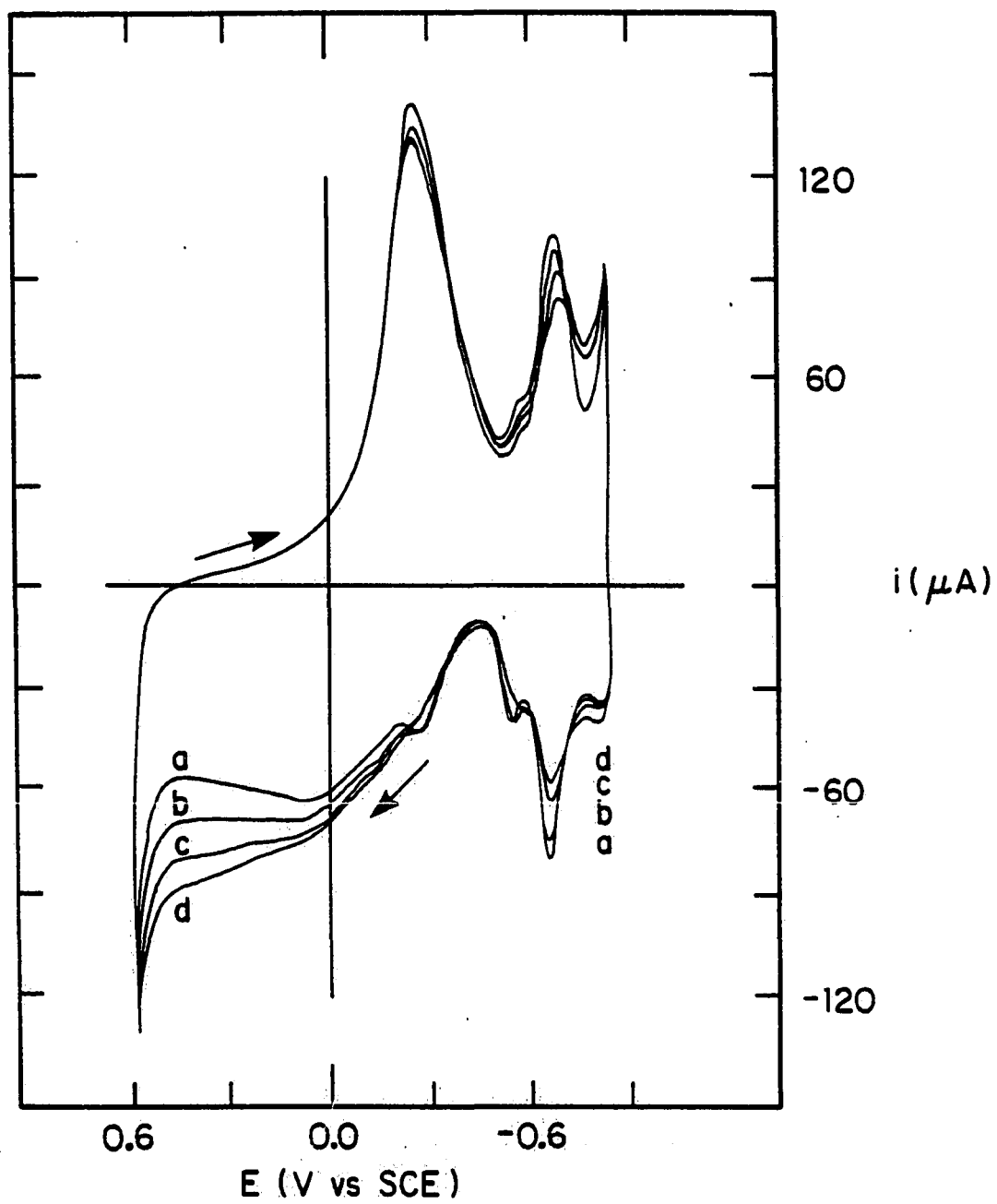
#### B. Cyclic Voltammetry

Current-potential (I-E) curves for tobramycin at the Pt RDE in 0.25 M NaOH are shown in Figure VIII-2. These curves adequately represent the voltammetric response of all the nebramycin factors tested and it is concluded that all the aminoglycosides react by a common mechanism. The presence of the aminoglycoside results in an increased anodic signal during the positive scan in the region of PtO production ( $E > 0.0$  V). This signal exhibits no dependence on the electrode rotation speed, but varies linearly with potential scan rate. This behavior is characteristic of surface-controlled processes and it is concluded that the anodic reaction is the surface-catalyzed oxidation of aminoglycoside which has been adsorbed in the potential region where surface oxide does not exist ( $E < -0.2$  V). Direct evidence for the presence of adsorbed aminoglycoside is the suppression of the peaks for adsorbed hydrogen.

Figure VIII-2. Current-potential curves for tobramycin at  
a Pt RDE in 0.25 M NaOH

Conditions:  $\phi = 6.0 \text{ V min}^{-1}$ ,  $W = 900 \text{ rev min}^{-1}$

Concentrations (ppm): a - 0.0, b - 1.0,  
c - 5.0, d - 20.0



## C. Triple-step Waveforms

Two triple-step potential waveforms (Table VIII-1) for pulsed amperometric detection of aminoglycosides were designed on the basis of the I-E curves in Figure VIII-2.

Table VIII-1. Description of two triple-step potential waveforms for detection of aminoglycosides at Pt electrodes in 0.25 M NaOH

Wave-form	Step	Potential (V)	Period (ms)	Function
C.	1	$E_1 = 0.55$	$t_1 = 250$ $t_d = 200$	anodic detection delay before sampling
	2	$E_2 = 0.70$	$t_2 = 125$	oxidative cleaning
	3	$E_3 = -.90$	$t_3 = 425$	reduction/adsorption
D.	1	$E_1 = 0.70$	$t_1 = 125$ $t_d = 75$	detection and cleaning delay before sampling
	2	$E_2 = -1.3$	$t_2 = 225$	rapid reduction
	3	$E_3 = -.20$	$t_3 = 400$	adsorption

Waveform C was established in the customary manner with the step for oxidative cleaning to a potential greater than for detection ( $E_2 > E_1$ ), followed by the negative step for reduction with adsorption. As mentioned in Chapter VII, there is significant flexibility in the

design of potential waveforms which are suitable for PAD, as illustrated by waveform D. In this case, the detection potential ( $E_1$ ) was chosen to be sufficiently large so that significant oxidative cleaning occurred during the detection period; hence, a more energetic oxidative cleaning pulse was not needed subsequent to  $E_1$ . The value of  $E_2$  caused very rapid reduction of the surface oxide and  $E_3$  allowed adsorption of analyte for the next detection cycle. The main benefit derived from this waveform structure is the freedom to adjust  $E_3$  to a potential of maximum analyte adsorption. The structure of waveform C requires that  $E_3$  be a large negative value to provide for rapid oxide reduction. In the case of aminoglycosides, the maximum adsorption potential is about -0.2 V, which does not cause rapid PtO reduction. Hence, when waveform C is used, the adsorption potential is significantly different than the observed maximum adsorption potential. This results in decreased sensitivity as compared to waveform D.

#### D. Chromatography

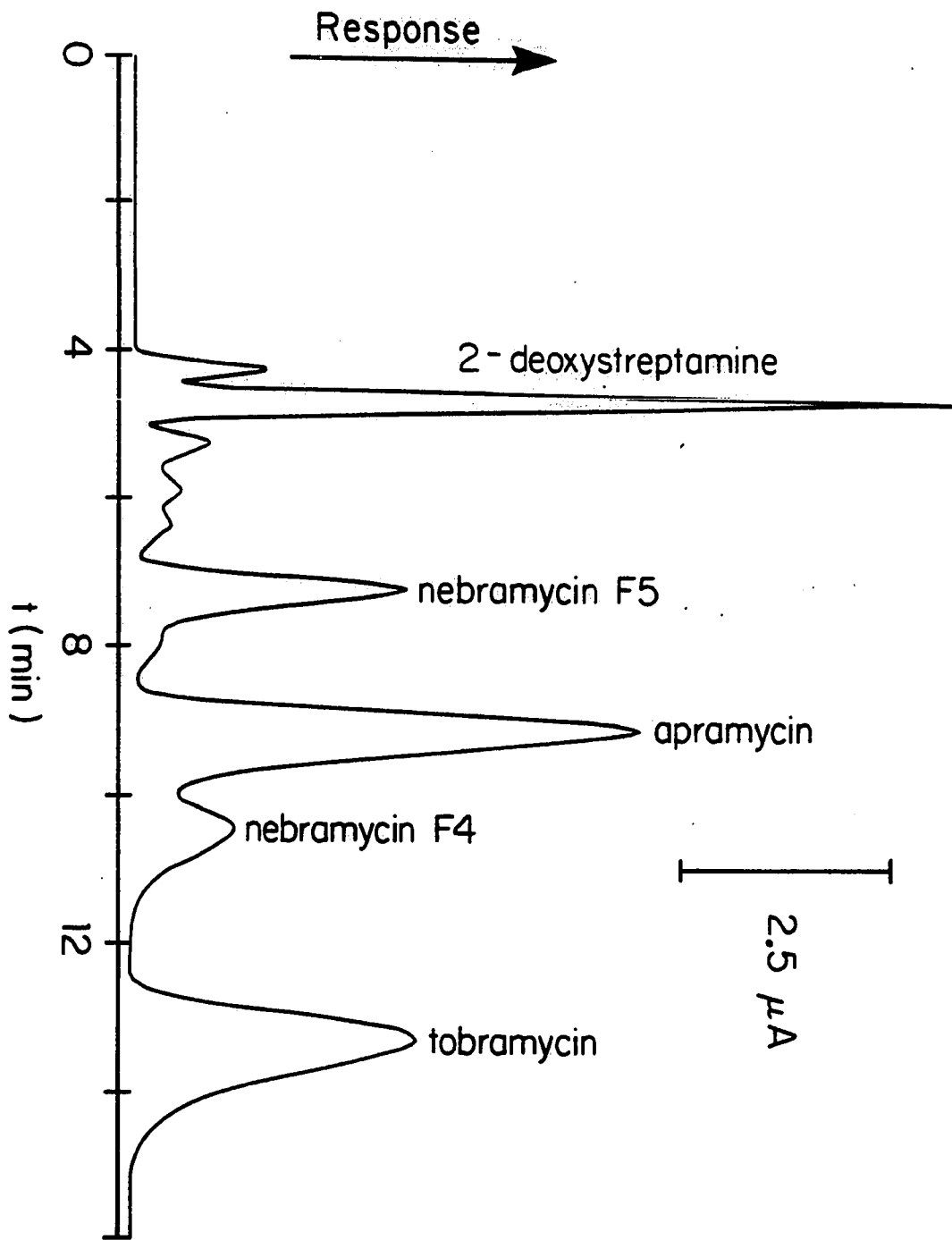
The chromatogram (single-column) for a 50  $\mu$ l injection of the indicated nebramycin factors at the 100 ppm level is shown in Figure VIII-3. Resolution is satisfactory. The limit of detection for a 50  $\mu$ l

Figure VIII-3. Chromatogram of a mixture of several nebramycin factors

Conditions: waveform C, single column,  $0.6 \text{ ml min}^{-1}$

Sample: 50  $\mu\text{l}$  injection, 100 ppm each compound





injection was 0.8 ppm for tobramycin (S/N = 2). The detectability was improved significantly by use of the dual-column technique to allow for on line preconcentration of the aminoglycosides from larger samples. Aminoglycosides are polyvalent in acidic solutions and, as such, are strongly retained on a high capacity cation-exchange column in the manner of Schmidt and Slavin (150) using a pH 5.2 phosphate buffer. Figure VIII-4 shows the switching configuration of the CMA-1 in the dual-column mode. The valving is configured such that the sample could be injected onto the preconcentrator column by the phosphate buffer (1 mM) adjusted to pH 5.2 and subsequently backflushed to the separator column by the eluent (0.25 M NaOH). This procedure allows also the clean-up of samples by an extended wash period in which weakly adsorbed components of the sample are eluted from the cation column by the buffer. A 20 minute wash period was found to be suitable for the deproteinated serum samples.

The effect of sample size on peak shape for the dual-column technique is illustrated in Figure VIII-5. As evidence, relatively large samples can be preconcentrated without significant peak broadening, in spite of the long wash period.

Figure VIII-4. Valving diagram

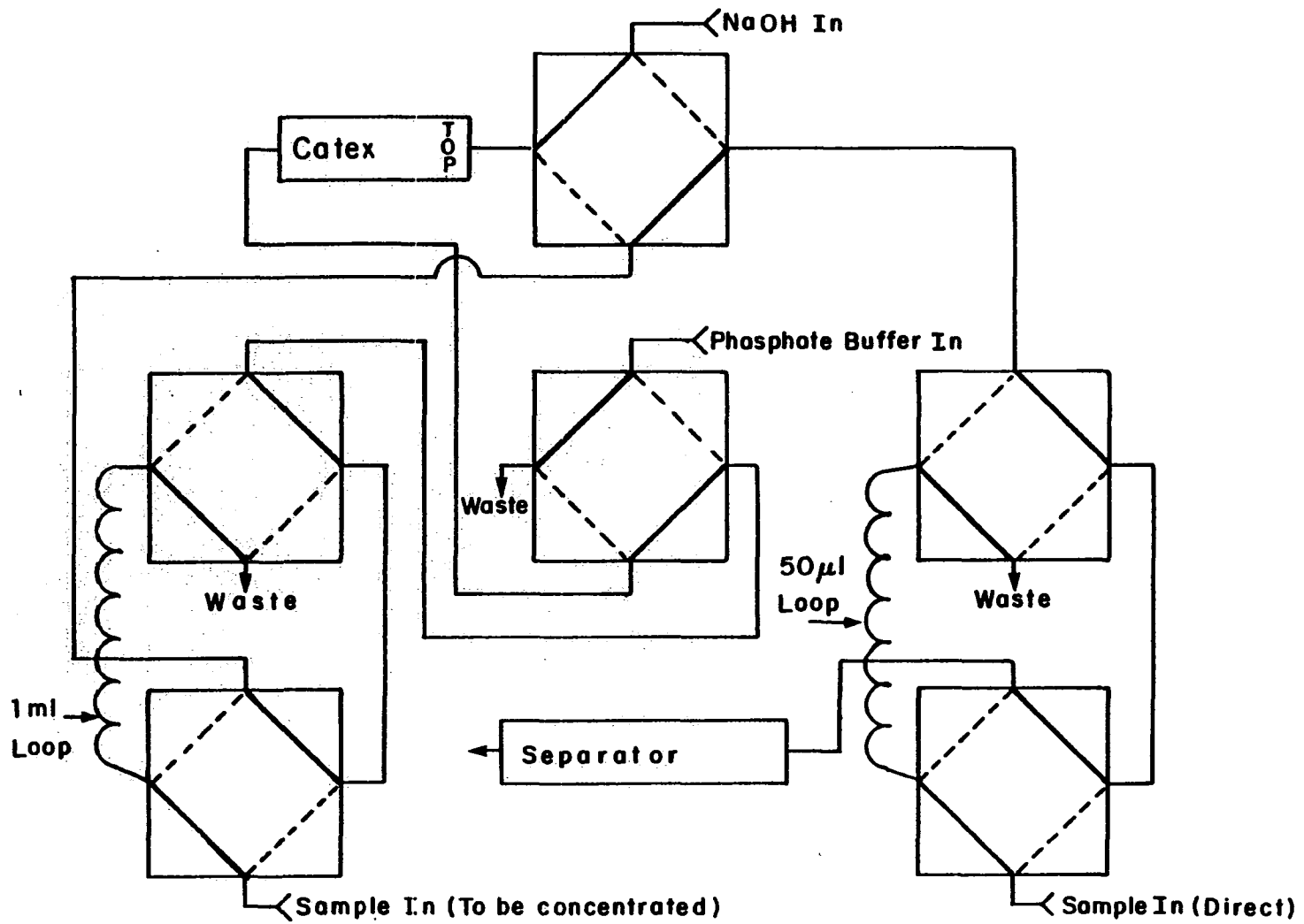
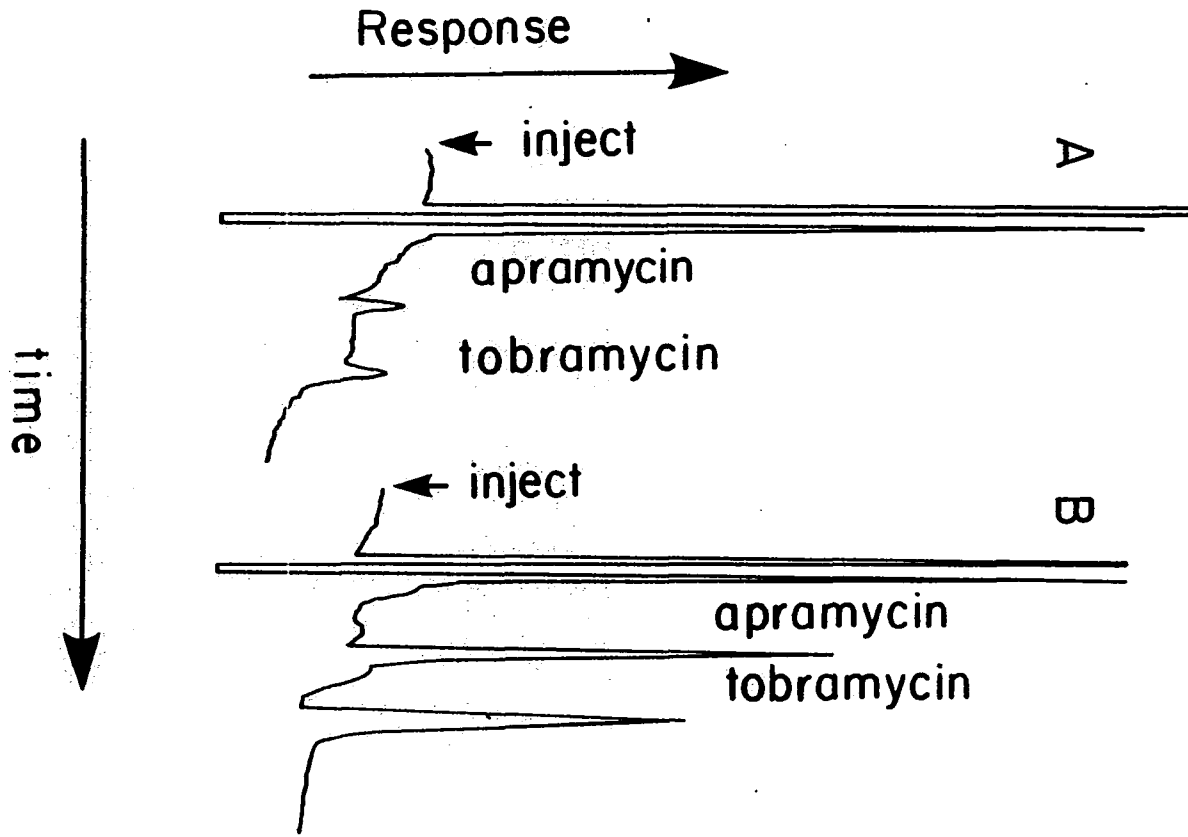


Figure VIII-5. Effect of sample size in dual-column separations

Conditions: waveform D, 6 min wash,  $0.6 \text{ ml min}^{-1}$

Samples: A - 1.0 ml (0.8 ppm), B - 5.0 ml (0.8 ppm)



The chromatogram for a 1.0 ml sample of blood serum spiked with 0.6 ppm each of tobramycin and apramycin is shown in Figure VIII-6 for the dual column technique. The first peak is concluded to result from amino acids retained by the cation column but only weakly retained by the separator column. For antibiotic levels exceeding 1 ppm in 50  $\mu$ l samples (50 ng), preconcentration was not needed but was still found desirable for the benefit of sample washing.

The chromatogram for a sample of fermentation broth is shown in Figure VIII-7 using the single-column technique. The peak with the longest retention (nebramycin F5') is well resolved from its hydrolysis product, tobramycin. This is of particular interest since nebramycin F5' is a main component of tobramycin fermentation. Additional development of the chromatography is needed to obtain satisfactory resolution of all components of this complex sample.

#### E. Calibration

Calibration curves for tobramycin and apramycin are shown in Figure VIII-8. For the short range of dilute concentrations examined, the plot of peak current ( $I_p$ ) vs. concentration (C) is approximately linear for both the single-column technique (SC; tobramycin: slope = 0.0465,

Figure VIII-6. Chromatogram of spiked blood serum  
Conditions: waveform D, 20 min wash, 0.6 ml min<sup>-1</sup>  
Samples: 1.0 ml injection, 0.6 ppm each component



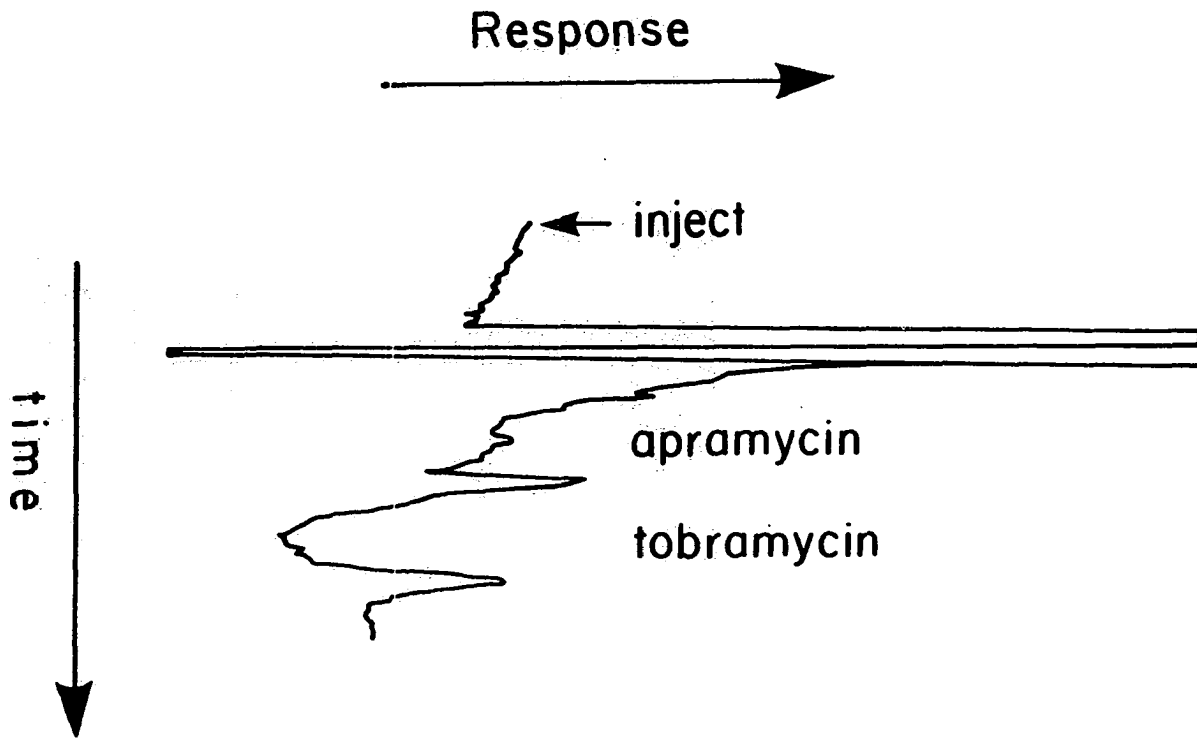


Figure VIII-7. Chromatogram of fermentation broth

Conditions: waveform D, dual-column,  $0.6 \text{ ml min}^{-1}$

Sample: 21:1 dilution,  $50 \mu\text{l}$  injection

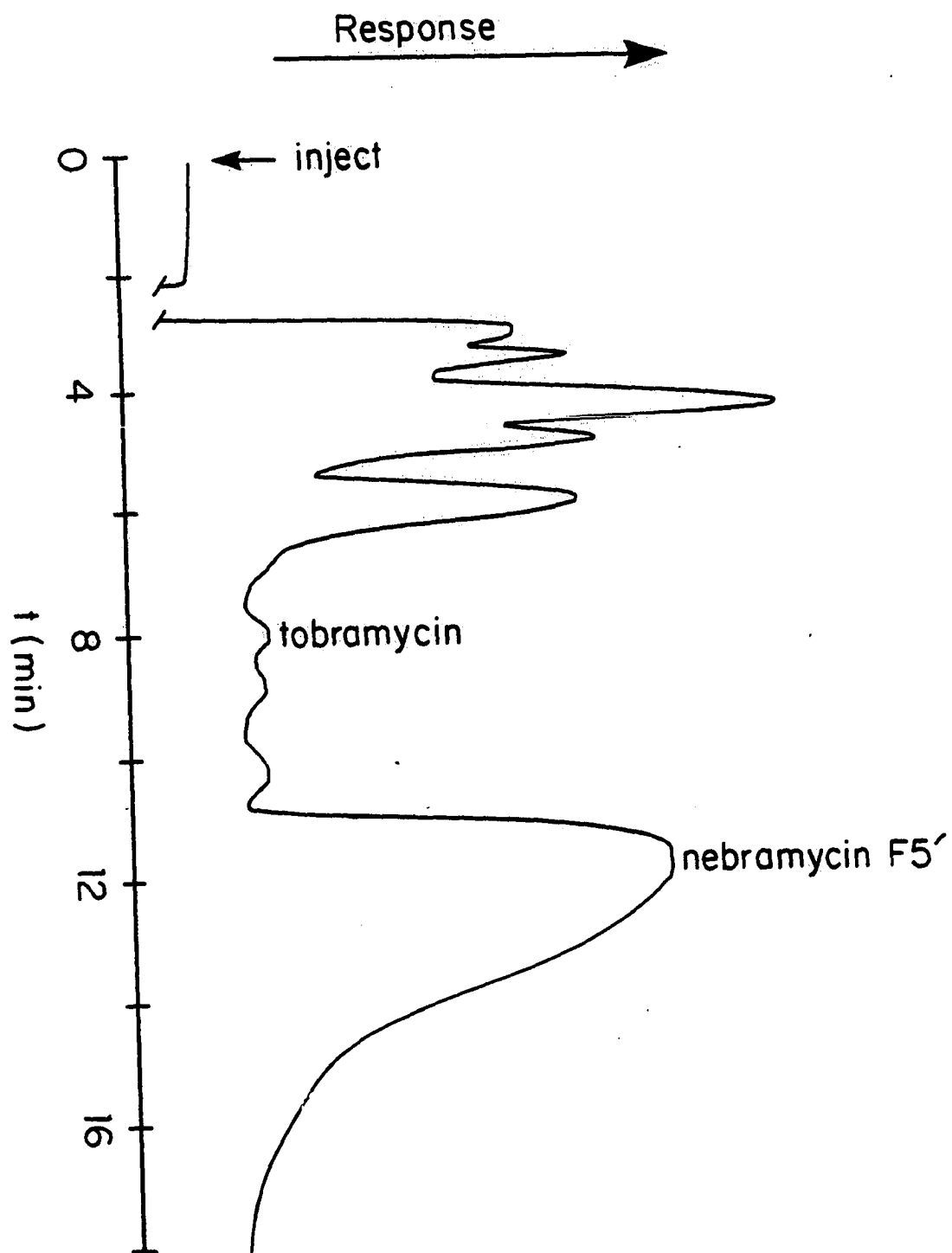
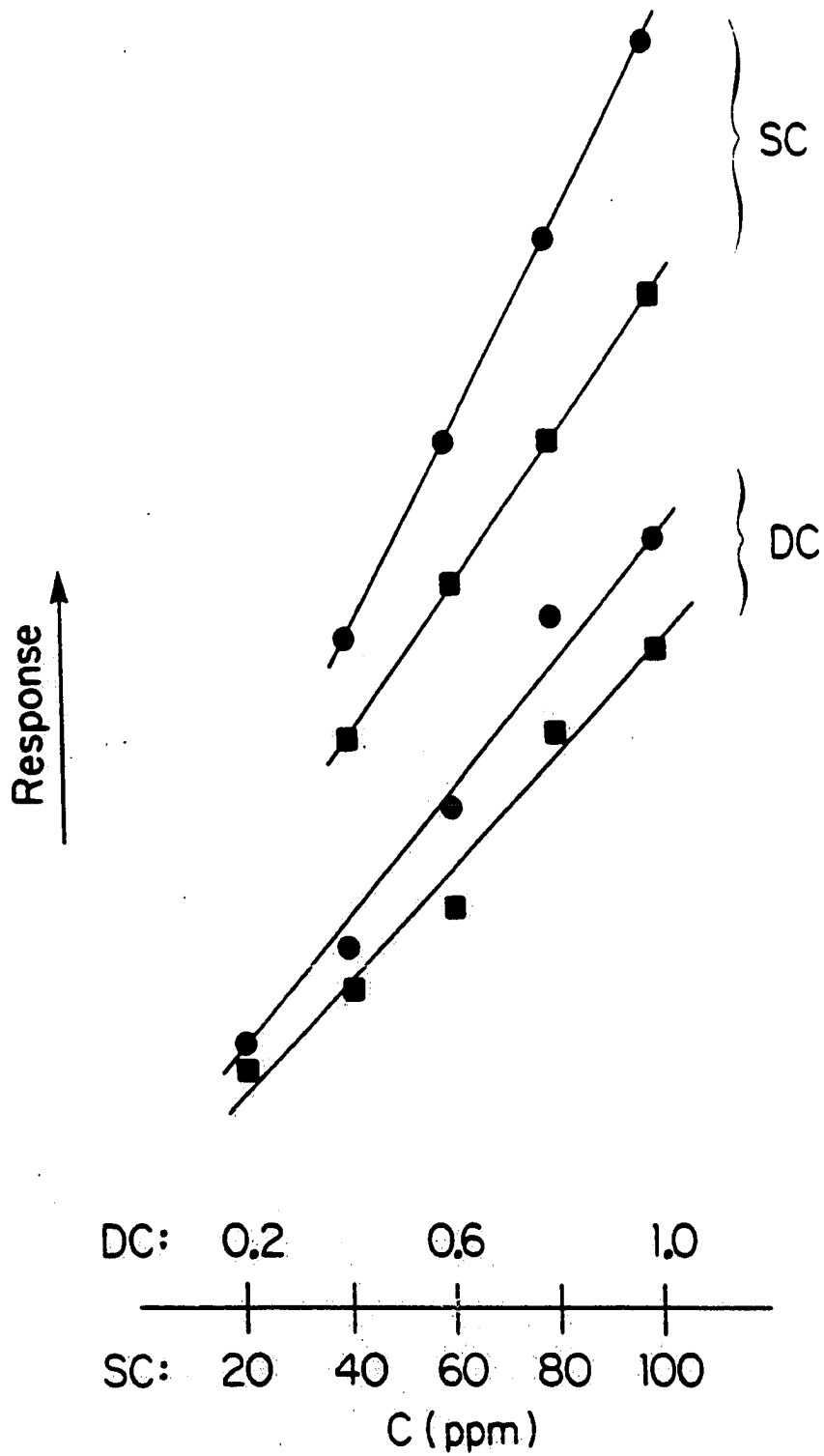


Figure VIII-8. Chromatographic calibration curves

Conditions: waveform D,  $0.6 \text{ ml min}^{-1}$

Curves: ● - apramycin, ■ - tobramycin  
SC - single column,  $50 \mu\text{l}$  injection  
DC - dual column,  $1.0 \text{ ml}$  injection



$s_{xy} = 0.0158$ ,  $r^2 = 0.9999$ ; apramycin: slope = 0.0623,  $s_{xy} = 0.0039$ ,  $r^2 = 0.9999$ ) and the dual-column technique (DC; tobramycin: slope = 0.6630,  $s_{xy} = 0.0358$ ,  $r^2 = 0.9892$ ; apramycin: slope = 0.8125,  $s_{xy} = 0.0388$ ,  $r^2 = 0.9916$ ). For an extended concentration range to higher values, as it has been shown for other surface-controlled reactions (amino acids and carbohydrates) that the linearity of calibration is improved by plotting  $1/I_p$  vs.  $1/C$ . Similar behavior is expected for aminoglycosides. The explanation is as in Chapter VI; sensitivity is controlled by adsorption and the adsorption isotherm is a non-linear function of the concentration at high concentration, where there is a significant fraction of the electrode surface covered by the adsorbed analyte.

## IX. SUMMARY

Pulsed amperometric detection (PAD) is concluded to be a useful and reliable method of detecting compounds that have surface-controlled anodic reactions at noble-metal electrodes. Compounds, whose electroactivity is so irreversible that their reactions were once thought useless, have been shown to be easily detected and quantified. The successful detection of these electrochemically difficult compounds relies upon the ability of PAD to continually restore the surface activity of noble-metal electrodes through the use of triple-step potential waveforms. The analytical signal is measured during the application of a detection potential ( $E_1$ ). Two subsequent potential steps are applied to alternately oxidatively clean ( $E_2$ ) and reduce ( $E_3$ ) the electrode surface. Analyte adsorption is allowed to occur during the time spent at  $E_3$ . The adsorbed analyte is then detected when  $E_1$  is once again applied. There exists a large background component in the analytical signal due to the formation of surface oxide at the detection potential. However, it has been shown that this background is sufficiently stable to allow sensitive determination of very small analytical signals.

The substantial background current due to the formation of Pt oxide makes PAD sensitive to conditions that affect the oxide growth. It has been shown that slight changes in pH have large effects upon the rate of oxide growth. It has also been shown that both electroactive and electroinactive adsorbates strongly affect Pt oxide growth. It is by this means that PAD is useful, not only for the sensitive detection of electroactive species, but the detection of nonelectroactive species as well.

Calibration plots for compounds detected by PAD have nonlinear  $i_p$ - $C_b$  relationships. Through the study of the effects of nonelectroactive adsorbates ( $Cl^-$  and  $CN^-$ ) on Pt oxide growth, it was determined that Langmuir-type adsorption isotherms were being obeyed. Langmuirian behavior accounts for the nonlinearity of  $i_p$ - $C_b$  calibration curves. It also has been shown that a Langmuir isotherm predicts a linear  $1/i_p$ - $1/C_b$  relationship. Analytes detected by PAD have been demonstrated to have linear  $1/i_p$ - $1/C_b$  relationships, further supporting the conclusion that analyte adsorption is based on Langmuir isotherms.

PAD has been shown to be a general detection technique well suited for detection of analytes in a chromatographic effluent stream. With the appropriate



electrolyte used as a chromatographic eluent; sensitive, direct detection of amino acids and aminoglycosides have been demonstrated. Novel chromatographic conditions were implemented to provide good resolution of aminoglycoside antibiotic factors. A dual column technique was used to allow on-line clean up of biological samples. PAD coupled to this chromatography system has been shown to be able to make sensitive determinations (0.8 ppm for a 50  $\mu$ l injection) of aminoglycosides in human blood serum as well as antibiotic fermentation broths.

## X. FUTURE RESEARCH

The lack of specificity in PAD is apparent. Further work to develop chromatographic conditions suitable for the direct application of PAD is needed. Since most of the successful applications of PAD use strongly basic electrolytes, silica-based reverse-phase columns are unable to be used due to the rapid decomposition of the bonded phase. The application of nonsilica-based columns (e.g., polystyrene-based) should be explored. These columns would be able to withstand the pH extreme usually necessary for PAD.

Another alternative would be to study the usefulness of PAD in electrolytes of more mid-range pHs. And, since most existing chromatographic separations employ organic modifiers in the eluent; PAD using electrolytes of moderate pH, containing organic modifiers should be examined. In this manner, PAD might be made applicable to currently existing chromatographic procedures.

PAD's ability to respond to compounds that adsorb to Pt might be enhanced by using an electrolyte containing an electroactive adsorbate, which could be easily displaced by analyte adsorbates. The resulting large background current would greatly amplify the effect of adsorption of nonelectroactive species. In this manner, even adsorbates

that have low maximum surface coverages would be detected. If careful selection of the detection potential is exercised, electroactive adsorbates may even show "negative" peaks in the presence of a large excess of electroactive species in the electrolyte. This would allow further adaptation of existing chromatographic conditions, (e.g., some protein separations employ 10% methanol eluent concentrations) extending PAD's applicability.

## XI. BIBLIOGRAPHY

1. Breiter, N. W. Electrochim. Acta, 1963, 8, 973.
2. Giner, J. Electrochim. Acta, 1964, 9, 63.
3. Cabelka, T. D.; Austin, D. S.; Johnson, D. C. J. Electrochem. Soc., 1984, 131, 1597.
4. Brown, O. R. "Physical Chemistry of Organic Solvent Systems"; Plenum: New York, 1973.
5. Clark, D.; Fleischman, M.; Pletcher, D. J. Electroanal. Chem., 1972, 36, 137.
6. Hughes, S.; Meschi, P. L.; Johnson, D. C. Anal. Chim. Acta, 1981, 132, 1.
7. Hughes, S.; Meschi, P. L.; Johnson, D. C. Anal. Chim. Acta, 1981, 132, 11.
8. Hughes, S.; Johnson, D. C. J. Agric. Food Chem., 1982, 30, 712.
9. Edwards, P.; Haak, K. K. American Lab., 1983, 15(April), 78.
10. Damaskin, B. B.; Petrii, O. A.; Batrakov, V. V. "Adsorption of Organic Compounds on Electrodes"; Plenum: New York, 1971.
11. Shlygin, A. I.; Manzhelei, M. E. Uch. Zap. Kishinevsk. Univ., 1953, 8, 13.
12. Pavela, T. O. Ann. Acad. Sci. Fennicæ, Ser. A, 1954, 59.
13. Will, F.; Knorr, C. Z. Elektrochem. 1960, 258, 270.
14. Kolotyrkin, Y. M.; Chemodanov, A. N. Dokl. Akad. Nauk SSSR, 1960, 134, 128.
15. Breiter M. W.; Gilman, S. J. Electrochem. Soc., 1962, 109, 622.
16. Khazova, O.; Vasilev, Yu. B.; Bagotski, V. S. Elektrokhimiya, 1965, 1, 82.

17. Brummer, S. B. J. Phys. Chem., 1965, 69, 562.
18. Brummer, S. B.; Ford, J. I. J. Phys. Chem., 1965, 69, 1355.
19. Oikawa, M.; Mukaibo, T. J. Electrochem. Soc. Japan, 1962, 20, 568.
20. Bagotski, V. S.; Vailev, Yu. B. Electrochim. Acta., 1966, 11, 1439.
21. Gilman, S. Trans. Faraday Soc., 1966, 62, 466.
22. Franklin, T. C.; Sothorn, R. D., J. Phys. Chem., 1954, 58, 951.
23. Gilman, S. J. Phys. Chem., 1963, 67, 78.
24. Joliot, F. J. Chem. Phys., 1930, 27, 119.
25. Blomgren, E. A.; Bockris, J. O'M. Nature, 1960, 186, 305.
26. Wroblowa, H.; Green, M. Electrochim. Acta, 1963, 8, 679.
27. Green, M.; Dahms, H. J. Electrochem. Soc., 1963, 110, 466.
28. Green, M.; Dahms, H. J. Electrochem. Soc., 1963, 110, 1075.
29. Dahms, H.; Green, M.; Weber, I. Nature, 1962, 196, 1310.
30. Smith, R. E.; Urbach, H. B.; Harrison, J. H.; Hatfield, N. L. J. Phys. Chem., 1967, 71, 1250.
31. Heiland, W; Gileadi, E.; Bockris, J. O'M. J. Phys. Chem., 1966, 70, 1207.
32. Gileadi, E.; Rubin, B. T.; Bockris, J. O'M. J. Phys. Chem., 1965, 69, 3335.
33. Cabelka, T. D. Ph.D. Dissertation, Iowa State University, Ames, IA, 1981.

34. Angerstein-Kozłowska, H.; Conway, B. E.; Sharp, W. B. A. J. Electroanal. Chem., 1973, 43, 9.
35. Gilroy, D.; Conway, B. E. Can. J. Chem., 1968, 46, 875.
36. Reddy, A. K. N.; Genshaw, M. A.; Bockris, J. O'M. J. Chem. Phys., 1969, 48, 671.
37. Angerstein-Kozłowska, H.; Conway, B. E.; Barnett, B.; Mozota, J. J. Electroanal. Chem., 1979, 100, 417.
38. Sakaguchi S. J. J. Biochem., 1925, 5, 25.
39. Gale, E. F. Adv. Enzymol., 1945, 5, 67.
40. Itoh, H.; Kawashima, K.; Chibata, I. Agric. Biol. Chem., 1973, 38, 869.
41. Itoh, H.; Morimoto, T.; Chibata, I. Anal. Biochem., 1974, 60, 573.
42. Spackman, D. H.; Stein, W. H.; Moore, S. Anal. Chem., 1958, 30, 1190.
43. Pfeifer, R.; Karol, R.; Korpi, J.; Burgoyne, R.; McCourt, D. Am. Lab., 1983, 15(3), 78.
44. Ruhemann, S. J. Chem. Soc., 1910, 97, 2025.
45. Ruhemann, S. J. Chem. Soc., 1911, 99, 792.
46. Moore, S.; Stein, W. H. J. Biol. Chem., 1948, 176, 367.
47. Lamothe, P. J.; McCormick, P. G. Anal. Chem., 1973, 45, 1906.
48. James, L. B. J. Chromatogr., 1971, 59, 178.
49. James, L. B. J. Chromatogr., 1978, 152, 298.
50. Moore, S.; Stein, W. H. J. Biol. Chem., 1954, 211, 907.
51. Lee, H.; Forde, M. D.; Lee, M. C.; Bucher, D. J. Anal. Biochem., 1979, 96, 298.

52. Udenfriend, S.; Stein, S.; Bohlen, P.; Dairman, W.; Leimgruber, W.; Weigle, M. Science, 1972, 178, 871.
53. Benson, J. R.; Hare, P. E. Proc. Nat. Acad. Sci. USA, 1975, 72, 619.
54. Roth, M.; Hampai, A. J. Chromatogr., 1973, 83, 353.
55. Roth, M.; Anal. Chem., 1971, 43, 880.
56. St. John, P. A. Aminco Laboratory News, 1975, 31, 1.
57. Bohlen, P.; Mellet, M. Anal. Biochem., 1979, 96, 298.
58. Ishida, Y.; Fujita, T.; Asai, K. J. Chromatogr., 1981, 204, 143.
59. Bohlen, P.; Schroeder, R. Anal. Biochem., 1982, 126, 144.
60. Drescher, P.; Lee, K. S. Anal. Biochem., 1978, 84, 559.
61. Weigle, M.; De Bernardo, S. C.; Teng, J. P.; Leimgruber, W. J. Am. Chem. Soc., 1972, 94, 5927.
62. Conn, R. B.; Davis, R. B. Nature (London), 1959, 183, 202.
63. Udenfriend, S.; Stein, S.; Bohlen, P.; Dairman, W. Science, 1972, 178, 871.
64. Stein, S.; Bohlen, P.; Stone, J.; Dairman, W.; Udenfriend, S. Arch. Biochem. Biophys., 1973, 155, 202.
65. Weigle, M.; De Bernardo, S.; Leimgruber, W. Biochem. Biophys. Res. Commun., 1973, 50, 352.
66. Felix, A. M.; Terkelsen, G. Arch. Biochem. Biophys., 1973, 157, 177.

67. Felix, A. M.; Terkelsen, G. Anal. Biochem., 1973, 56, 610.
68. Edman, P. Acta Chem. Scand., 1950, 4, 283.
69. Edman, P.; Begg, G. Eur. J. Biochem., 1967, 1, 80.
70. Downing, M. R.; Mann, K. G. Anal. Biochem., 1976, 74, 298.
71. Zimmerman, C. L.; Apella, E.; Pisano, J. J. Anal. Biochem., 1976, 75, 298.
72. Zimmerman, C. L.; Apella, E.; Pisano, J. J. Anal. Biochem., 1977, 77, 569.
73. Henderson, L. E.; Copeland, T. D.; Oroszlan, S. Anal. Biochem., 1980, 102, 1.
74. Margolies, M. N.; Braner, A. J. Chromatogr., 1978, 148, 429.
75. Gray, W. R.; Hartley, B. S. Biochem. J., 1963, 89, 59p.
76. Gray, W. R.; Hartley, B. S. Biochem. J., 1963, 89, 379.
77. Gray, W. R. Biochem. J., 1970, 119, 805.
78. Tapuhi, Y.; Miller, N.; Kruger, B. L. J. Chromatogr., 1981, 205, 325.
79. Tapuhi, Y.; Schmidt, D. E.; Lindner, W.; Karger, B. L. Anal. Biochem., 1981, 115, 123.
80. Weiner, S.; Tichbee, A. J. Chromatogr., 1981, 213, 501.
81. Hill, D. W.; Walters, F. H.; Wilson, T. D.; Stuart, J. D. Anal. Chem., 1979, 51, 1338.
82. Lindroth, P.; Mopper, K. Anal. Chem., 1979, 51, 1667
83. De Jong, C.; Hughes, G. J.; Van Wieringen, E.; Wilson, K. J. J. Chromatogr., 1982, 241, 345.
84. Kraak, J. C.; Jonker, K. M.; Huber, J. F. K. J. Chromatogr., 1977, 142, 671.



85. Knox, J. H.; Hartwick, R. A. J. Chromatogr., 1981, 204, 3.
86. Adams, R. N. "Electrochemistry at Solid Electrodes"; Marcel Dekker: New York, 1969.
87. Malfroy, M.; Reynaud, J. A. J. Electroanal. Chem., 1980, 114, 213.
88. Joseph, M. H.; Davies, P. Current Separations, 1982, 4, 62.
89. Joseph, M. H.; Davies, P. J. Chromatogr., 1983, 277, 125.
90. Allison, L. A.; Mayer, G. S.; Shoup, R. E. Anal. Chem., 1984, 56, 1089.
91. Kucera, P.; Umagat, H. J. Chromatogr., 1983, 255, 563.
92. Simons, S. S.; Johnson, D. F. Anal. Biochem., 1978, 90, 705.
93. Hui, B. S.; Huber, C. O. Anal. Chim. Acta, 1982, 134, 211.
94. Krafil, J. B.; Huber, C. O. Anal. Chim. Acta, 1982, 139, 347.
95. Fleischman, M.; Korinek, K.; Pletcher, D. J. Chem. Soc. Perkin II, 1972, 1396.
96. Loscombe, C. R.; Cox, G. B.; Dalziel, J. A. W. J. Chromatogr., 1978, 166, 403.
97. Alexander, P. W.; Haddad, P. R.; Low, G. K. C.; Maitra, C. J. Chromatogr., 1981, 209, 29.
98. Alexander, P. W.; Maitra, C. Anal. Chem., 1981, 53, 1590.
99. Kok, W. Th.; Hanekamp, H. B.; Bos, P.; Frei, R. W. Anal. Chim. Acta, 1982, 142, 31.
100. Kok, W. Th.; Brinkman, U. A. Th.; Frei, R. W. J. Chromatogr., 1983, 256, 17.

101. Fleet, B.; Little, C. J. J. Chrom. Sci., 1974, 12, 747.
102. Fleet, B., U.S. Patent 4059406, 1977; Chem. Abstr., 1978, 88, 39329f.
103. Goodman, E. L.; Van Gelder, J.; Holmes, R.; Hull, A. A.; Sanford, J. P. Antimicrob. Agents Chemother., 1975, 8, 434.
104. Dahlgren, J. G.; Anderson, E. T.; Hewitt, W. L. Antimicrob. Agents Chemother., 1975, 8, 58.
105. Falco, F. G.; Smith, H. M.; Arcieri, G. M. J. Infect. Dis., 1969, 119, 406.
106. Lerner, S. A.; Sehgoohm, R.; Matz, G. J. Am. J. Med., 1977, 62, 919.
107. Smith, C. R.; Baughman, K. L.; Edwards, C. O.; Logan, J. F.; Lietner, P. S. N. Engl. J. Med., 1977, 296, 349.
108. Jackson, G. G.; Arcieri, G. J. Infect. Dis., 1971, 124, 5130.
109. Black, R. E.; Lan, W. K.; Weinstein, R. J.; Young, L. C.; Hewitt, W. C. Antimicrob. Agents Chemother., 1976, 9, 956.
110. Maitra, S. K.; Yoshikawa, T.; Guze, L. B.; Shotz, M. C. Clin. Chem., 1979, 25, 1361.
111. Edberg, S. C.; Chu, A. Am. J. Med. Technol., 1975, 41, 99.
112. Shanson, D. C.; Hince, C. J.; Daniels, J. V. J. Infect. Dis., 1976, 134, s104.
113. Carlstrom, A.; Dornbusch, K.; Hagelberg, P. Scand. J. Infect. Dis. 1977, 9, 46.
114. Benveniste, R.; Davies, J. Annual Rev. Biochem., 1973, 42, 471.
115. Stevens, P.; Young, L. S.; Hewitt, W. L. Antimicrob. Agents Chemother., 1975, 7, 374.

116. Haas, M. J.; Davies, J. Antimicrob. Agents Chemother., 1973, 4, 497.
117. Holmes, R. K.; Stanford, J. P.; J. Infect. Dis., 1974, 129, 519.
118. Stevens, P.; Young, L. S.; Hewitt, W. L. J. Lab. Clin. Med., 1975, 86, 349.
119. Mahon, W. A.; Ezer, J.; Wilson, T. W. Antimicrob. Agents Chemother., 1973, 3, 583.
120. Lewis, J. E.; Nelson, J. C.; Elder, H. A. Antimicrob. Agents Chemother., 1975, 7, 42.
121. Stevens, P.; Young, L. S.; Hewitt, W. L. Antimicrob. Agents Chemother., 1977, 11, 768.
122. Broughton, A.; Strong, J. E.; Bodey, G. P. Antimicrob. Agents Chemother., 1976, 9, 247.
123. Broughton, A.; Strong, J. E.; Pickering, L. K.; Bodey, G. P. Antimicrob. Agents Chemother., 1976, 10, 652.
124. Ashby, C. D.; Lewis, J. E.; Nelson, J. C. Clin. Chem., 1978, 24, 1734.
125. Chalt, E. M.; Ebersole, R. C. Anal. Chem., 1981, 53, 682A.
126. Esser, L. J. Chromatogr., 1984, 305, 345.
127. Maitra, S. K.; Yoshikawa, T.; Hansen, J. L.; Schotz, M. C.; Guze, L. B. Am. J. Clin. Pathol., 1979, 71, 428.
128. Maitra, S. K.; Yoshikawa, T.; Steyn, C. M.; Guze, L. B.; Schotz, M. C. Antimicrob. Agents Chemother., 1978, 14, 880.
129. Mashimo, I; Yamanchi, S. J. Chromatogr., 1984, 305, 373.
130. Kubo, H.; Kinoshita, T.; Kobayashi, Y.; Tokunaga, K. J. Chromatogr., 1982, 227, 244,

131. Anhalt, J. P. Antimicrob. Agents Chemother., 1977, 11, 651.
132. Mays, D. L.; Van Apeldoorn, R. J.; Lanback, R. G. J. Chromatogr., 1976, 120, 93.
133. Sanger, F. Biochem. J., 1945, 39, 507.
134. Wong, L. T.; Beanbien, A. R.; Pakuts, A. P. J. Chromatogr. 1982, 231, 145.
135. Barends, D. M.; Zwaan, C. L.; Hulshoff, A. J. Chromatogr., 1981, 225, 417.
136. Elrod, L.; White, L. B.; Wong, C. T. J. Chromatogr., 1981, 208, 357.
137. Tsuji, K.; Goetz, W.; Van Meter, W.; Gusciora, K. A. J. Chromatogr., 1979, 175, 141.
138. Hughes, S. Ph.D. Dissertation, Iowa State University, Ames, IA, 1982.
139. Austin, D. S. Ph.D. Dissertation, Iowa State University, Ames, IA, 1984.
140. Pratt, K. Ph.D. Dissertation, Iowa State University, Ames, IA, 1980.
141. Gilroy, D. J. J. Electroanal. Chem., 1976, 71, 257.
142. Smith, R. M.; Martell, A. E. "Critical Stability Constants: Inorganic Complexes", Vol. 4; Neuman Press: New York, 1976.
143. Langmuir, I. J. Am. Chem. Soc., 1918, 40, 1361.
144. Temkin, M. Zh. Fiz. Khim., 1941, 15, 296.
145. Frumpkin, A. Z. Physik. Chem., 1925, 116, 466.
146. Kazarinov, V. E. Elekrokimiya, 1966, 2, 1389.

147. Balashova, N. A.; Kazarinov, V. E. Chapt. 3 in "Electroanalytical Chemistry", Vol. 3, Bard, A. J. (Ed.); Marcel Dekker: New York, 1969.
148. Austin, D. S.; Polta, J. A.; Polta, T. Z.; Tang, A. P. -C.; Cebelka, T. D.; Johnson, D. C. J. Electroanal. Chem., 1984, 168, 227.
149. Koch, K. F.; Merkel, K. E.; O'Connor, S. C.; Occolowitz, J. L.; Paschal, J. W.; Dorman, D. E. J. Org. Chem., 1978, 43, 1430.
150. Schmidt, G. J.; Slavin, W. Chromatogr. Newsletter, 1981, 9, 21.